Universidade de Aveiro
2015

Departamento de Ciências Médicas

Joana Margarida Bispo Serrano

O interactoma da LAP1 e as suas características funcionais durante a espermatogénese

LAP1 interactome and its functional features throughout spermatogenesis

Universidade de Aveiro
2015

Departamento de Ciências Médicas

Joana Margarida Bispo Serrano

O interactoma da LAP1 e as suas características funcionais durante a espermatogénese

LAP1 interactome and its functional features throughout spermatogenesis

Dissertação apresentada à Universidade de Aveiro para cumprimento dos requisitos necessários à obtenção do grau de Mestre em Biomedicina Molecular, realizada sob a orientação científica da Professora Doutora Sandra Rebelo, Professora auxiliar convidada do Departamento de Ciências Médicas da Universidade de Aveiro.

Este trabalho contou com o apoio do grupo de Neurociências e Sinalização Celular do iBiMED, SACS, Universidade de Aveiro e foi financiado por fundos nacionais da FCT no âmbito do projeto PTDC/BEX-BCM/0493/2012.

o júri

presidente

Prof. Doutora Odete Abreu Beirão da Cruz e Silva
Professora Auxiliar com agregação do Departamento de Ciências Médicas da Universidade de Aveiro

Prof. Doutora Maria de Lourdes Gomes Pereira
Professora Associada com agregação do Departamento de Biologia da Universidade de Aveiro

Prof. Doutora Sandra Maria Tavares da Costa Rebelo
Professora Auxiliar Convidada do Departamento de Ciências Médicas da Universidade de Aveiro

agradecimentos

Um agradecimento muito especial à Professora Doutora Sandra Rebelo pela dedicada orientação facultada durante a realização desta dissertação. Um sincero obrigado por toda a boa disposição e por ter contribuído para o desenvolvimento de capacidades científicas e profissionais.

Um obrigado à Professora Doutora Odete da Cruz e Silva por me ter aceite no seu laboratório, tornando possível a realização deste trabalho. Agradeço também as sugestões e oportunidades concedidas.

Ao Professor Doutor João Ramalho-Santos pela colaboração neste projeto.

I would like to thank to Doctor A.M.M. van Pelt PhD, for accepting me in her lab and supporting me throughout the development of this work. It was an absolute pleasure to work under her supervision and mentoring. I am grateful for the exceptional opportunity she conceded me.

A todos os colegas de laboratório do iBiMED, sobretudo aos do Laboratório de Neurociências e Sinalização Celular pelo conhecimento e apoio científico.

Ao CBC e iBiMED, Universidade de Aveiro (UA), por todos os reagentes e equipamentos de base disponibilizados.

I would like to thank the Laboratory for Reproductive Biology, Center for Reproductive Medicine, from the Academisch Medisch Centrum in Amsterdam, for all the laboratory reagents and equipment.

Um sincero e desmedido obrigada à Filipa, ao Roberto e à Soraia por toda a ajuda, contribuição, coordenação, paciência, instrução, supervisão e incansável compreensão, sem as quais nunca teria sido possível concluir este trabalho.

I would like to thank Joana, Ieva, Sabrina, and all the graduate students, research technicians, and collaborators who warmly received me their lab in the AMC and contributed to this research.

A todos os meus amigos, em especial à Carolina, obrigada pela vossa amizade.

Aos meus pais e irmãos, pelo apoio, coragem e suporte, que sem os quais este trabalho não seria possível.

Ao Diogo por toda a paciência, ajuda e carinho.

palavras-chave

Espermatogénese, invólucro nuclear, proteína 1B associada com a lâmina (LAP1B), interações proteína-proteína.

resumo

A proteína 1 associada com a lâmina (LAP1), codificada pelo gene humano *TOR1AIP1*, encontra-se localizada na membrana interna do núcleo. Funcionalmente a LAP1 está associada à manutenção da estrutura do envelope nuclear e ao posicionamento da lâmina e da cromatina. No envelope nuclear a LAP1 forma complexos com várias proteínas, nomeadamente lâminas tipo A e B, torsinas e emerina. A atividade destes complexos sugere a existência de uma função cooperativa entre a LAP1 e as proteínas nomeadas anteriormente, que será essencial, particularmente nos tecidos em que a sua expressão é substancial. Assim, a identificação de novos interactores da LAP1 e das suas respetivas vias de sinalização, será crucial para identificar e compreender as funções biológicas desta proteína. Ao longo deste trabalho foram utilizadas ferramentas bioinformáticas que possibilitaram a descoberta de novas proteínas associadas com a LAP1. Em primeiro lugar, o interactoma da LAP1 foi estabelecido através do acesso a bases de dados públicas, procedendo-se posteriormente à análise manual de cada uma destas interações. De seguida, a integração de múltiplas ferramentas bioinformáticas possibilitou a determinação de novas funções associadas à LAP1, designadamente a resposta a danos no DNA e a interação com os telómeros. Simultaneamente, os resultados bioinformáticos reforçaram a participação da LAP1 no processo de mitose e a intervenção desta proteína na manutenção da morfologia nuclear. Em particular, a função da LAP1 na regulação da mitose e da estrutura do envelope nuclear parece ter semelhanças com processo de espermatogénese. Assim, ao longo deste trabalho foi também estudada a distribuição da LAP1 ao longo deste processo de diferenciação, assim como de alguns dos seus conhecidos interactores, no testículo de ratinho e de humano. Em ratinho, foi possível determinar que a atividade da LAP1 durante a espermatogénese é mais significativa desde a fase VIII até ao fim da espermiogénese, sendo característica do desenvolvimento da manchete. Concomitantemente, alguns dos interactores avaliados possuem uma localização análoga à da LAP1, nomeadamente, as lâminas B1 e A/C, e a proteína serina/treonina fosfatase 1γ2 (PP1γ2). Os resultados obtidos após o estudo da LAP1 ao longo do sistema reprodutor masculino possibilitaram a atribuição de novas e potenciais funções biológicas à LAP1. Assim, este trabalho poderá servir de ponto de partida para estudo futuros da LAP1 e da sua função na regulação de múltiplos processos celulares e doenças.

keywords

Spermatogenesis, nuclear envelope, lamina associated polypeptide 1B (LAP1B), protein-protein interactions.

abstract

The lamina-associated polypeptide 1 (LAP1) is a type II transmembrane protein of the inner nuclear membrane encoded by the human gene TOR1AIP1. LAP1 is involved in maintaining the nuclear envelope structure and appears be involved in the positioning of lamins and chromatin. In the nuclear envelope, LAP1 is suggested to exist as a complex with A-type and B-type lamins, torsins and emerin. The presence of such complexes suggests that LAP1 may cooperate functionally with these proteins in tissues where they play a critical role. Therefore, the identification of LAP1 binding partners and the signalling pathways where LAP1 participates, is crucial for a better understanding of LAP1 functions. The work described in this thesis addresses novel human LAP1 associated proteins found through bioinformatic tools. Public databases allowed for the discovery of the LAP1 interactome, which was manually curated, identifying several functionally relevant proteins. Subsequently, the integration of multiple bioinformatic tools established novel functions to LAP1 such as DNA damage response and telomere association. In conjunction, bioinformatic results also reinforced the association of LAP1 with mitosis, and the already identified role of LAP1 in nuclear morphology. Interestingly, this association of LAP1 with the regulation of the nuclear envelope structure and mitosis progression, shares functional elements with spermatogenesis. Therefore, this work additionally described the localization of LAP1 and some of its interactors throughout the spermatogenic cycle, in mouse and human testis. The results established that the activity of LAP1 during the mouse spermatogenic cycle is most evident from stage VIII until the end of spermiogenesis, which is characteristic of manchette development. Concomitantly, some LAP1 interactors studied in this work share a similar localization, namely, PP1γ2, Lamin B1 and Lamin A/C. The results obtained from the study of LAP1 throughout different periods of the male reproductive system attributed potential new biological functions to LAP1. Thereby, this work can be the foundation of future studies regarding LAP1 and the regulation of multiple cellular processes and disease conditions.

LIST OF CONTENTS

LIST OF ABBREVIATIONS

3D	3-dimensional
AKAP	A kinase anchoring protein
APC/C	Anaphase-promoting complex/cyclosome
ATP	Adenosine triphosphate
BAF	Barrier to autointegration factor
COX IV	Cytochrome c oxidase IV
CTCF	Transcriptional repressor CTCF
DAB	3, 3'-diaminobenzidine
DAG	Directed acyclic graph
DAPI	4',6-diamidino-2-phenylindole
DP	Transcription factor Dp
E2F	Transcription factor E2F
ER	Endoplasmic reticulum
FACE2	Farnesylated proteins-converting enzyme 2
FSH	Follicle-stimulation hormone
FT	Farnesyltransferase
GCL	Germ cell-less protein-like 1
GO	Gene Ontology
HHV-4	Human herpes virus 4 (Epstein-Barr virus (strain AG876))
HIV-1	Human Immunodeficiency Virus 1
HP1	Heterochromatin containing protein 1
HPLC-MS	High-performance liquid chromatography
HRP	Horseradish peroxidase
HRSVA	Human respiratory syncytial virus A (strain A2)
Hs	Homo sapiens
ICMT	Isoprenylcysteine carboxymethyltransferase
IF	Intermediate filament
Ig	Immunoglobulin

IHC	Immunohistochemistry
INM	Inner nuclear membrane
IPA	Ingenuity Pathways Analysis
KASH	Klarsicht/ANC-1/Syne-1 homology
LAP	Lamin associated polypeptide
LBR	Lamin-B receptor
LEM	LEM domain-containing protein
LH	Luteinizing hormone
LINC	Linker of Nucleoskeleton and Cytoskeleton
MAN1	Inner nuclear membrane protein Man1
MCC	Mitotic checkpoint complex
Mm	Mus musculus
MMSET	Histone methyltransferase
MOK2	Zinc finger protein MOK-2
MS	Mass spectrometry
MT	Microtubule
MTOC	Microtubule organising centres
NE	Nuclear envelope
NET	Nuclear envelope transmembrane protein
NLS	Nuclear localization sequence
NPC	Nuclear pore complex
Nup	Nucleoporin
Nurim	Nuclear rim protein
Oct1	Octamer transcription factor 1
ONM	Outer nuclear membrane
PBS	Phosphate-buffered saline solution
PCM	Pericentriolar material
PFA	Paraformaldehyde
PP1	Protein phosphatase 1

PSA-FITC	*Pisum Sativum Agglutinin*-Fluorescein Isothiocynate
RB	Retinoblastoma protein
ROI	Region of interest
rpm	Rotations per minute
R-Smad	Receptor-regulated SMADs
RT	Room temperature
SAC	Spindle assembly checkpoint
SAMP1	Spindle-associated membrane protein 1
sEBSS	Supplemented Earl's balance salt solution
snoRNA	small nuclear RNA
snRNP	small nuclear ribonucleoprotein
SREBP-1	Sterol-response-element binding protein
SUN	Sad1-UNC homology domain-containing protein
TMEM43	Transmembrane protein 43
TOR1AIP1	TorsinA interacting protein 1
UNCL	Unc-50-like
WB	Western blot
WHO	World Health Organization
γ-TuRC	γ-Tubulin ring complex

CHAPTER I - INTRODUCTION

1.1. THE NUCLEAR ENVELOPE

In eukaryotic cells, the nuclear envelope (NE) encloses the genetic material and separates it functionally, constituently and temporally from the cytosol (reviewed in [1]). This specialized barrier is comprised by the inner (INM) and outer (ONM) nuclear membranes, which are continuous with the endoplasmic reticulum (ER)[2]. The perinuclear space, that covers the lumen between the bilayers, spans from 30 to 50 nm in metazoans and it is also contiguous with the lumen of the endoplasmic reticulum (ER)[3]. The two concentric membranes are periodically fused at the nuclear pore complex (NPC), a large supramolecular structure shaping a channel between the cytoplasm and the nucleus[2]. Finally, the nucleoplasmic face of the INM comprises an underlying network of filaments composed of lamina proteins that confer structure and support to the nucleus[4].

Regardless of the lipid continuity between the NE and the ER, the protein content amongst the INM, the ONM and ER membranes is quite diverse (Figure I.1)[5]. Proteomics has revealed the complexity of the NE with the identification of multiple copies of 30 different nucleoporins (Nups) in the NPC, rounding up to roughly 100 proteins per NPC[6]. Adding to this premise, the INM was found to be comprised of 67 unique nuclear envelope transmembrane (NET) proteins[7]. Thus, the INM hosts a unique set of integral and associated proteins that interact directly or indirectly with A-type and B-type lamins, the major components of the nuclear lamina[8]. Alternatively, the ONM has been shown to be physically and constituently associated with the attachment of ribosomes and ER development[9]. In addition to allowing lateral diffusion between the NE and the ER, the ONM is connected to both the actin cytoskeleton network and the centrosome (Figure I.1: Mechanics and nucleoskeleton) [10–13].

Protein association to these membranes is very likely time and tissue specific. Through emerging roles in genome organization, meiosis, mitosis, cell growth, signalling, or differentiation. Thereby, the NE upholds additional purposes besides separating intracellular components (Figure I.1, reviewed in [14]).

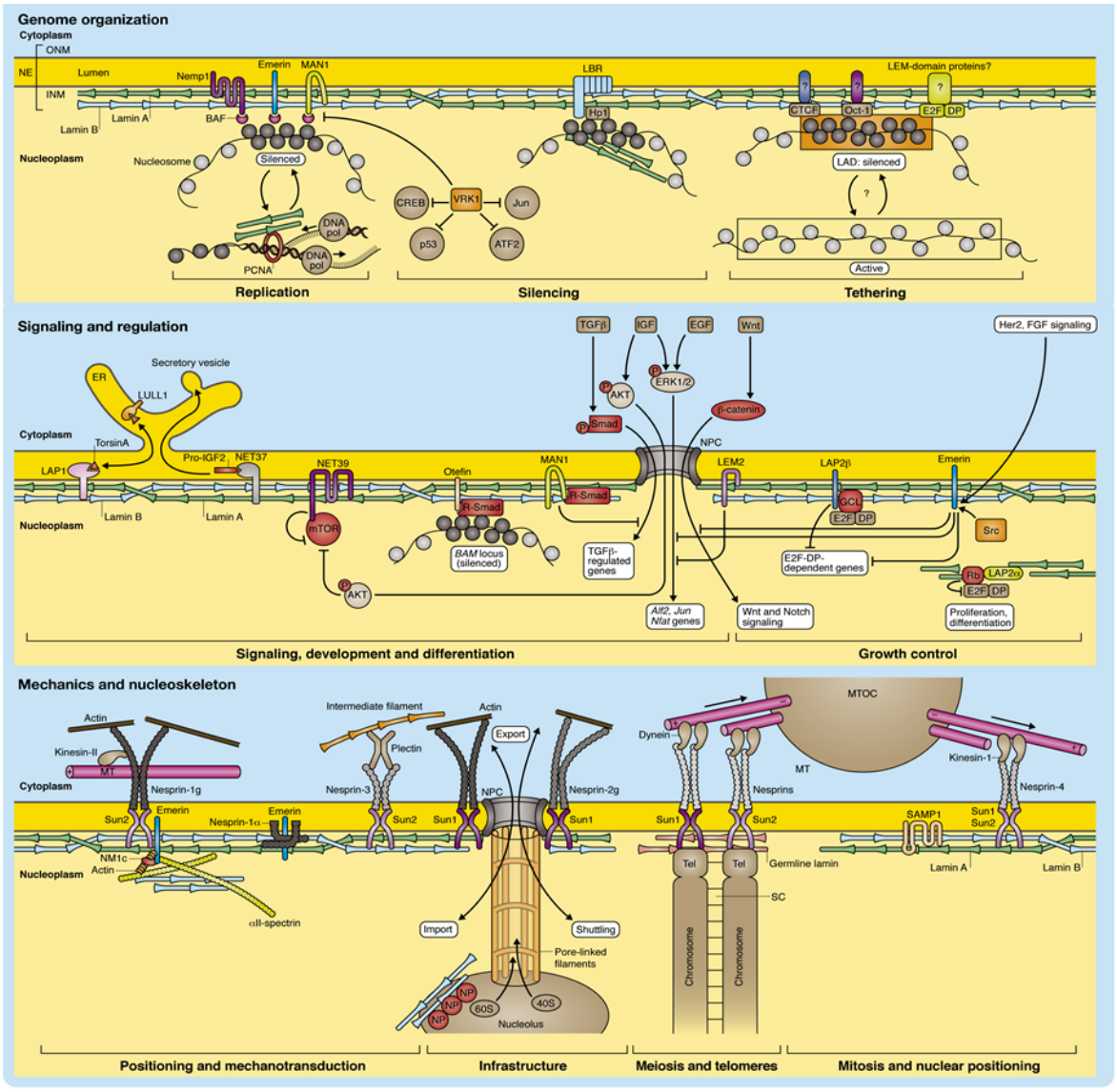

Figure I.1. Biological functions of the NE and its related complexes. Genome organization in the nucleus has been associated to complexes that regulate replication, silencing and chromatin tethering. It has also been described that many proteins of the NE participate in cell signalling, development and differentiation, as well as growth control. Additionally, the nucleoskeleton has been described to associate to cytoskeleton in order to regulate cell positioning and mechanotransduction. Finally, through the interaction with the MTOC and proteins embedded in the NE have been implicated in the processes of meiosis and mitosis. AKT, protein kinase B; ATF2, activating transcription factor 2; BAF, barrier-to-autointegration factor; BAM, bag-of-marbles; CREB, cAMP response element binding; CTCF, CCCTC-binding factor; DNA pol., DNA polymerase; EGF, epidermal growth factor; ER, endoplasmic reticulum; ERK1/2, extracellular signal-regulated kinases 1 and 2; FGF, fibroblast growth factor; GCL, germ cell-less; Her2, human epidermal growth factor; INM, inner nuclear membrane; LAD, lamina-associated domain; LAP1, lamina-associated polypeptide 1; LAP2, lamina-associated polypeptide 2; LBR, lamin B receptor; LEM2, LEM-domain-containing protein 2; LULL1, luminal domain-like LAP1; MT, microtubule; MTOC, microtubule-organizing centre; mTOR, mammalian target of rapamycin; NE, nuclear envelope; NET37, nuclear envelope transmembrane protein 37; NET39, nuclear envelope transmembrane protein 39; NMC1, nuclear myosin 1c; NP, nucleophosmin; NPC, nuclear pore complex; NFAT, nuclear factor of activated T cells; ONM, outer nuclear membrane; P53; protein 53; PCNA, proliferating cell nuclear antigen; pro-IGF2, pro-insulin-like growth factor 2; Rb, retinoblastoma protein; SAMP1, spindle-associated membrane protein 1; SC, synaptonemal complex; Tel, telomere; TGFβ, transforming growth factor β; VRK1, vaccina-related kinase 1. Reproduced from [14].

1.1.1 Nuclear lamins

The nuclear lamina was first described as a thin fibrous meshwork of proteins (approximately 15-20nm in mammals) localized in the nuclear face of the INM (Figure I.1) [15–17]. This scaffold structure is mainly composed of A-type and B-type lamins, a family of type V intermediate filament (IF) proteins[4]. In mammals, the *LMNA* gene encodes A-type lamins which includes the major isoforms lamin A and lamin C, as well as the minor isoforms lamin C2 and lamin AΔ10[18–21]. B-type lamins are comprised by the *LMNB1* gene that encodes for the major isoform lamin B1, and the *LMNB2* gene that originates the major isoform lamin B2 and the minor isoform lamin B3[22–25]. Lamins A, C, AΔ10, B1 and B2 are broadly express in somatic cells[23,25,26], whereas lamins C2 and B3 are testis specific[20,24]. Despite considerable research, determining lamin organization *in vivo* (in somatic cells) has been one of the major challenges in the field, as studies revealed differences between lamin filament assembly *in vitro*[27] and *in vivo*[28].

As predecessors of IF proteins, lamins are structurally comprised by a short N-terminal domain, a central rod domain with four α-helical domains (coils 1A, 1B, 2A and 2B), linker regions (L1, L12 and L2) that separate the N-terminal from the rod domains, and a globular C-terminal domain that contains: the nuclear localization sequence (NLS), an immunoglobulin (Ig) fold motif, and a C-terminal CaaX motif (C, cysteine; a aliphatic amino acid; X, any amino acid) (Figure I.2) [18–25]. The CaaX motif of lamins A, B1 and B2 suffers post-translational modifications (Figure I.2) starting with farnesylation on the Cys residue by a farnesyltransferase (FT), followed by proteolytic cleavage of the aaX residues by farnesylated proteins-converting enzyme 2 (FACE2) on lamins B1 and B2 and by a zinc metallo-endoprotease (ZMPSTE24) in lamin A (reviewed in [29]). Lastly, methylation occurs on the recent C terminus by a isoprenylcysteine carboxymethyltransferase (ICMT), a process that is known to facilitate targeting of newly synthesized lamins to the nuclear envelope membrane, presumably by enhancing the hydrophobic interactions in the INM (reviewed in [29]). However, in the case of lamin A there is an additional step of C-terminal cleavage by ZMPSTE24, which in humans was shown to occur after Tyr646, removing 15 amino acids, including the farnesylated Cys, originating non-farnesylated matured lamin A (reviewed in [29]). Additional post-translational modifications to lamins include phosphorylation[30], ADP-ribosylation[31] and sumoylation[32]. Moreover, it was demonstrated that hyperphosphorylation seems to regulate lamin depolymerisation upon nuclear envelope disassembly on prophase, and dephosphorylation coincides with nuclear envelope reassembly on telophase[30].

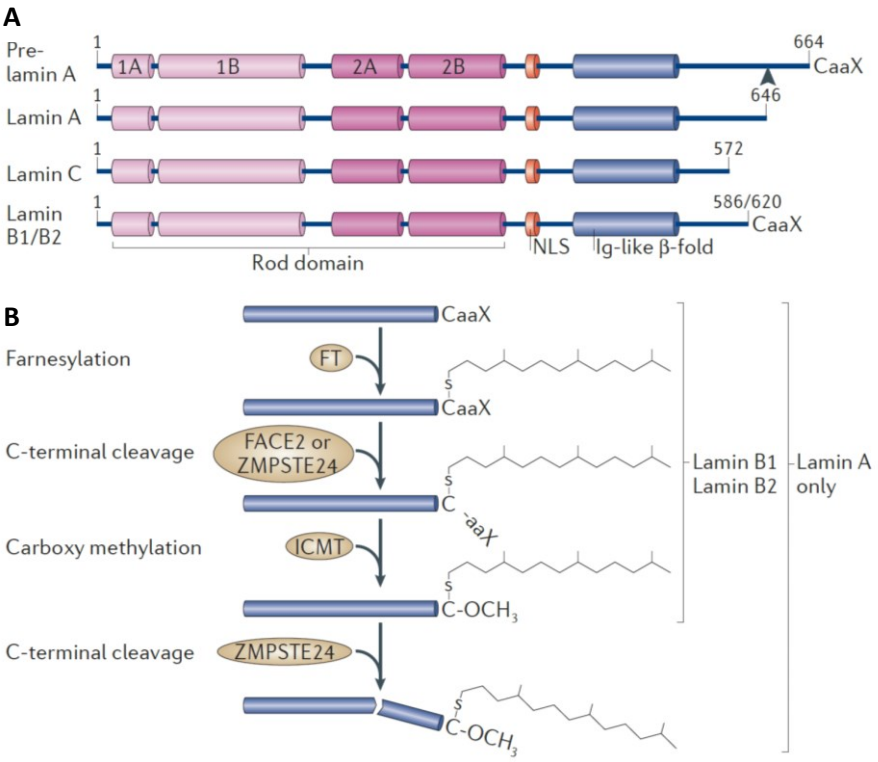

Figure I.2. The CaaX motif of lamins A, B1 and B2 suffers post-translational modifications. (A) Schematic representation of A-type and B-type lamins. **(B)** Post-translational modifications of A-type and B-type lamins. The process starts with farnesylation on the Cys residue by a FT, followed by proteolytic cleavage of the aaX residues by FACE2 on lamins B1 and B2 and by ZMPSTE24 in lamin A. Lastly, methylation occurs on the recent C terminus by ICMT, a process that is known to facilitate targeting of newly synthesized lamins to the nuclear envelope membrane, presumably by enhancing the hydrophobic interactions in the INM. However, in the case of lamin A there is an additional step of C-terminal cleavage by ZMPSTE24, which in humans was shown to occur after Tyr646, removing 15 amino acids, including the farnesylated Cys, originating non-farnesylated matured lamin A. NLS, nuclear localization sequence; Ig, immunoglobulin; CaaX (C, cysteine; a aliphatic amino acid; X, any amino acid); FT, farnesyltransferase; FACE2, farnesylated proteins-converting enzyme 2; ZMPSTE24, zinc metallo-endoprotease; ICMT, isoprenylcysteine carboxymethyltransferase. Reproduced from [29].

1.1.2 NE proteins and nuclear dynamics

Due to localization to the periphery of the nucleus, the nuclear lamina has been associated with multiple functions besides giving structure and support to the nuclear envelope (Figure I.1)[7]. Lamins interact with various proteins in the INM, forming functional complexes that simultaneously enable the attachment of lamin filaments to the INM[7].

Metazoans have been extensively shown to express two different kinds of lamin interacting proteins in the INM (Figure I.1). The first group includes multiple integral INM proteins that interact directly with lamins, such as Nemp1 (nuclear envelope integral membrane protein 1), emerin, MAN1 (inner nuclear membrane protein Man1), LBR (lamin-B receptor), LAP1 (lamin associated polypeptide 1), NETs (nuclear envelope transmembrane proteins 8, 9, 32, 37, 39,51, 56), LEM2 (LEM

domain-containing protein 2), TMEM43 (transmembrane protein 43), LAP2β (lamin associated polypeptide 2β), SUN1 (Sad1-UNC homology domain-containing protein 1), SUN2 (Sad1-UNC homology domain-containing protein 2), Nesprins (1, 2, 2G, 3), SAMP1 (spindle-associated membrane protein 1), Nurim (nuclear rim protein) and UNCL (Unc-50-like) [7] (reviewed in [14,33–35]). The second group is comprised by proteins that are not integral membrane constituents but interact and localize with the nuclear lamina, which include Titin, Nup53 (nucleoporin NUP53), SREBP-1 (sterol-response-element binding protein), c-Fos, GCL (germ cell-less protein-like 1), RB (retinoblastoma protein), Oct1 (octamer transcription factor 1), BAF (barrier to autointegration factor), HP1 (heterochromatin containing protein 1), CTCF (transcriptional repressor CTCF), E2F (transcription factor E2F), DP (transcription factor Dp), R-Smads (receptor-regulated SMADs), LAP2α, MOK2 (zinc finger protein MOK-2), LEM3, LEM4 and LEM5 (LEM domain-containing protein 3-5) (reviewed in [14,33–35]). When complexed with lamins these proteins may contribute to a vast array of functions, including nuclear architecture and mechanotransduction, chromatin organization, gene expression, epigenetic regulation, signalling pathways, replication, transcription regulation, mitosis and meiosis (Figure I.1, reviewed in [14]).

Most INM integral proteins are known to have morphological regulating functions (Figure I.1). For instance, diminished expression of LBR, affects nuclear shape and chromatin organization in blood granulocytes [36]. However, there are exceptions, as additional enzymatic features were designated to this receptor, namely sterol reductase activity that might be essential to regulate cholesterol during human blood and bone development[37]. LBR also binds to B-type lamins and HP1, together they seem to tether and compact chromatin assisting epigenetic gene silencing [38].

Lamina associated polypeptide (LAP), is a term coined to designate a group of INM proteins stably associated with the lamina in the nuclear periphery[39,40]. LAP1 was one of the first lamin binding proteins identified in the INM and comprises 3 isoforms initially described in rat: LAP1A, LAP1B and LAP1C[40]. Structurally, it is a type II membrane protein containing a nucleoplasmic N-terminal domain, a single transmembrane segment and a C-terminal piece that protrudes into the perinuclear space, but in the case of LAP1C this N-terminal domain is truncated[41]. LAP1 remains poorly characterized, yet it has been known to interact with several NE constituents (described in section 1.1.3.2). LAP2 is a polymorphic protein that comprises at least three isotypes (α, β, γ). Isoforms β and γ are type II membrane proteins, consisting of a nucleoplasmic N-terminal piece, a single transmembrane domain and a short C-terminal segment that extends into perinuclear space. LAP2α lacks a transmembrane domain and is localized to the nucleoplasm[42].

The LEM-protein family, in mammalian cells, integrates seven elements that bind directly to lamins: LAP2, emerin, MAN1, LEM2, LEM3, LEM4 and LEM5. This evolutionary conserved group is characterized by the presence of a bi-helical LEM motif which mediates binding to BAF, a conserved chromatin-binding protein. Functionally, lamins, LEM-domain proteins and BAF coordinate NE reassembly after mitosis, aiding lamina structural chromatin organization (Figure I.1) (reviewed in [43]).

Emerin is a single pass transmembrane protein that localizes to the INM and binds lamina A via its nucleoplasmic domain. Mutations in the *EDM* gene causes X-linked Emery-Dreifuss muscular dystrophy[44]. Functionally, emerin associates with A-type lamins, Nesprins and the SUN-domain protein family forming the LINC (Linker of Nucleoskeleton and Cytoskeleton) complex which connects the nuclear envelope to cytoskeletal networks (Figure I.1) [45]. In addition, a fraction of emerin was also detected in the ONM where it can interact directly with microtubules (MTs) and contribute to the positioning of the centrosome near the ONM[46].

SUN and KASH (Klarsicht/ANC-1/Syne-1 homology) domain proteins are large protein families localized in the INM and ONM, respectively, that bind to form LINC complexes in the perinuclear space[12]. Since SUN-domain proteins associate with lamins, and different KASH proteins interact either with actin, IFs or MTs, the LINC complex has multiple regulatory functions, such as mechanotransduction, nuclear positioning, migration, and centrosome association (Figure I.1) (reviewed in [45]). Particular instances of cytoskeletal interactions are provided in Figure I.1, in the mechanics and nucleoskeleton section. The three models displayed include SUN1 and SUN2 interacting with KASH domain proteins, such as Nesprin-1g, emerin, Nesprin-3, Nesprin-2g, and Nesprin-4. As Figure I.1 shows, the regulation of different mechanical features depends on the members of the SUN-dimer/Nesprin complexes.

SAMP1 is a membrane-spanning protein specifically located in the INM (Figure I.1). During mitosis, SAMP1 is dispersed in the ER, as expected. Surprisingly, an additional fraction of SAMP1 concentrates to the polar regions of the mitotic spindle, colocalizing with tubulin and a lipid membrane marker. This distinct membrane subdomain associated with the mitotic spindle, has a unique protein composition, namely SAMP1. This peculiar distribution of SAMP1 occurs in metaphase and anaphase. However, in telophase, SAMP1 is recruited back to the reforming NEs of the daughters' nuclei[47].

1.1.3 LAP1

As previously noted, LAP1 has three isoforms in rodents, despite the fact that only two have been described in human, namely LAP1B and LAP1C. Kondo and colleagues were the first to successfully clone the full-length LAP1B isoform[48]. More recently, our group conducted the identification and analysis of LAP1C as the second human isoform, which is putatively N-terminal truncated[49]. In this particular study, the two human LAP1 RNAs were identified by Northern blot analysis, matching the existence of non-RefSeq mRNAs in GenBank with the putative LAP1C sequence. Therefore, these results suggest that LAP1B and LAP1C are products of different RNAs and thereby their generation is regulated at the transcriptional level. The LAP1 isoforms could arise from alternative splicing or alternative promoter usage and consequently use an alternative transcription initiation site. Database searches for alternative promoters, identified an upstream putative LAP1C translation initiation site, thereby this matter requires additional experiments. It will also be of interest to understand the consequences of the loss of the N-terminal domain of LAP1C regarding protein-protein interactions[49]. In addition, our group studied the resistance of the LAP1 isoforms (in particular LAP1C) to extraction from nuclear membranes, using triton X-100 and increasing salt concentrations (NaCl). It was demonstrated that LAP1C is more easily solubilized than LAP1B, in agreement with the observation that human LAP1C differs from LAP1B in the 5' end region of the first exon located in the nucleoplasmic domain[49]. LAP1B and LAP1C are both localized in the nuclear envelope, though it has been proposed that LAP1C might also be distributed in the nucleus. In fact, the differential localization of the two isoforms might even signify that these two isoforms possible have different cellular functions[49].

The two human LAP1 isoforms seem to have diverse physiological functions. For instance, it was shown that different cell lines display different expressions for human LAP1C in comparison to LAP1B. Additionally, the analysis of human tissue determined that the expression of LAP1B/LAP1C is tissue specific[49]. Furthermore, the expression profile during neuronal differentiation provided a link between LAP1 expression and the state of neuronal differentiation of SH-SY5Y cells and maturation of rat cortical primary cultures, suggesting that LAP1 may play a role in those processes. It was reported that LAP1C is initially highly expressed, stabilizing later on the neuronal differentiation and maturation processes. Conversely, the early expression of LAP1B is almost undetectable but it is increasingly upregulated throughout the differentiation and maturation processes, when compared to LAP1C[49]. Recently, a study found a patient presenting a homozygous mutation in the *TOR1AIP1* gene that causes a frameshift resulting in a premature stop

codon. In the presented case, expression of LAP1B was absent in the patient skeletal muscle fibres, but interestingly, LAP1C was overexpressed. Therefore, a possible explanation is that variation in the level of expression of the different LAP1 isoforms in human tissue might lead to different phenotypes, in the case mentioned above with the loss of function of LAP1B[50].

Protein phosphorylation is a major signalling mechanism in eukaryotic cells that is able to regulate the biological activity of diverse proteins[51]. Our group has additionally reported that LAP1B and LAP1C are both dephosphorylated in vitro by protein phosphatase 1 (PP1)[49,52]. Phosphorylation sites were mapped by high-performance liquid chromatography followed by mass spectrometry (HPLC-MS), identifying five phosphorylated residues for LAP1B and LAP1C (Ser143, Ser216, Thr221, Ser306 and Ser310, the numeration of the residues is relative to the human LAP1B protein sequence). Additionally, PP1 was confirmed to dephosphorylate two of these residues (Ser306 and Ser310)[49].

1.1.3.1 The role of LAP1 in mitosis

Cell division in eukaryotes requires disassembly and reassembly of the NE in the beginning and at the end of mitosis, respectively. This dynamic was termed open mitosis. Initially, MTs that form the mitotic spindle are exclusively cytoplasmic but later have to come into contact with chromosomes for correct chromosome segregation during cell division. Thereby, NE breakdown allows the access of the spindle MTs to chromosomes. The NE breakdown involves disassembly of the nuclear pore complex (NPCs), depolymerisation of lamins, spreading of most NE soluble components to the cytoplasm, and localization of INM proteins to the ER. The NE reassembly at the end of mitosis is characterized by the concentration of INM proteins and lamins to the de-condensing chromatin, by lamin polymerization and NPCs reassembly (reviewed in[53]).

Centrosomes are the main MT organizing centres and are needed to accomplish proper mitotic spindle organization. During the cell cycle, the centrosomes must be duplicated at S phase, separated at G2 phase and correctly positioned near the ONM. Accordingly, NE proteins are proposed to have an extremely relevant role in this process, namely emerin, which interacts directly with MT and anchors the centrosomes at the ONM[46,53]. Interestingly, LAP1 has also been implicated in the regulation of the NE reassembly [41,54] and the organization of the mitotic spindle [55] during mitosis. Besides, it seems that LAP1 is regulated by protein phosphorylation during mitosis, as reported for other nuclear proteins[56,57], which is consistent with the fact that protein phosphorylation represents a crucial regulatory mechanism of cell cycle progression[30,58].

Additionally, it has been proposed that LAP1 may be crucial in the assembly of the mitotic MT spindle and consequently in mitosis progression. Particularly, Neumann and colleagues[55] demonstrated that downregulation of LAP1 led to the formation of deficient mitotic spindles in prometaphase, since the centrosomes form weak mitotic asters and failed to generate a bipolar spindle leading to aberrant mitotic exit and cell death. Indeed, defects in mitotic spindle integrity can affect the stability of MT and therefore the levels of MT acetylation. Posteriorly, in a recent study performed by our group, neuronal-like SH-SY5Y cells were used as a model to study the intracellular levels, localization, and potential role of human LAP1 during the cell cycle[59]. The results revealed that LAP1 is differentially expressed in SH-SY5Y cells during the cell cycle (Figure I.3). For instance, at metaphase, anaphase and the initial stages of telophase, LAP1 was distributed through the cell in speckles, excluding in the chromosomal area. Interestingly, at late telophase, LAP1 was clearly detected encircling the chromosomes, even when they were not completely decondensed. The association of LAP1 with chromosomes in anaphase and late telophase may contribute to the reassembly of the NE, possibly by targeting lamins and membrane vesicles to the chromosomes surface or by anchoring chromatin to the NE[59]. Other INM proteins, for instance, LBR, emerin, and LAP2, were also found to accumulate on the surface of chromatin during anaphase/telophase *in vivo*[39,60]. Thus, the binding of INM proteins to chromatin accompanies NE assembly at the end of mitosis, while dissociation is required for NE breakdown[53].

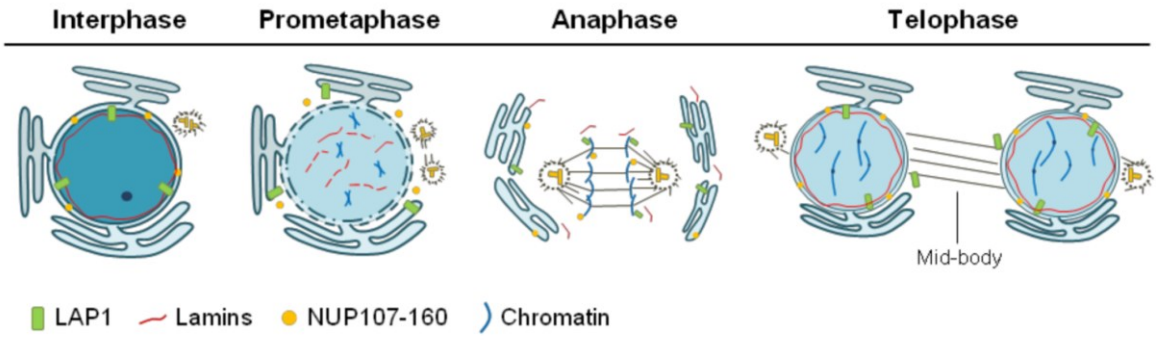

Figure I.3. LAP1 localization during the cell cycle. In interphase cells LAP1 is located in the inner nuclear membrane but at prometaphase LAP1 is distributed through the endoplasmic reticulum. At anaphase LAP1 localizes at chromosomes surface and at telophase LAP1 is redistributed again to the inner nuclear membrane, but is also detected in the mid-body. Nuclear pore complex and nuclear lamina are also disassembled at prometaphase and NUP107-160 are the first nucleoporins recruited by chromatin at anaphase. Reproduced from [61].

Additionally, our previous results also showed that in mitotic cells, specifically at metaphase and telophase, LAP1 colocalizes with acetylated α-tubulin (a marker of MTs stability) in the mitotic spindle and the midbody. Plus, LAP1 colocalizes with γ-tubulin in centrosomes at metaphase and anaphase. The localization of LAP1 in the mitotic spindle, mid-body and centrosomes strongly

suggests a functional association between LAP1 and these cell cycle related components. Moreover, LAP1 expression is reduced in mitosis-arrested cells, whereas it is upregulated in G0/G1-arrested cells after serum deprivation. Additionally, our study concluded that LAP1 knockdown resulted in decreased number of mitotic cells, reduced levels of acetylated α-tubulin and lamin B1, anomalous centrosome positioning near the NE and decreased phosphorylation of histone H3 at Ser10[59]. Histone H3 phosphorylation has been correlated with chromosome condensation during mitosis[62]. Therefore, a decreased number of mitotic cells could be an effect of cell cycle progression impairment.

All together our results indicate that LAP1 is an important protein for centrosome positioning near the NE[59]. Specifically, the altered centrosome positioning after LAP1 depletion may be correlated with the decrease in the number of mitotic cells observed. Interestingly, two other NE proteins, emerin and the novel INM protein SAMP1 are also involved in centrosome positioning and connection to the NE[46,47]. Decreased levels of tubulin acetylation could be the result of MT instability due to the disruption of NE integrity. As mentioned before (section 1.1.2), cytoskeleton elements such as tubulin are connected to the NE through the interaction with Nesprins on the ONM, which in turn associate with SUN-domain proteins in the INM that are lamin binding proteins, resulting in the formation of a LINC complex[12,45]. Depletion of LAP1 from the INM might cause disruption of protein interactions at the NE and subsequent loss of LINC complexes, which in turn can lead to unstable MT dynamics.

Finally, this study also demonstrated that LAP1 is regulated by phosphorylation during both interphase and mitosis but seemed to be highly phosphorylated during mitosis. Therefore, it is proposed that LAP1 could be (de)phosphorylated in a cell cycle-dependent manner at specific residues, as it is the case for lamins (reviewed in[8,63]). Phosphorylation of lamins at different residues might play specific roles throughout the cell cycle. For example, phosphorylation of lamin B2 at Ser17 is specifically involved in lamin depolymerization and NE disassembly[64]. It is accepted that phosphorylation of lamins prompts lamin depolymerization when the NE is disassembled, whereas dephosphorylation leads to lamin polymerization and the end of mitosis (reviewed in[8]). Specifically, the PP1 regulatory subunit A kinase anchoring protein (AKAP)-149 recruits PP1 to the NE upon NE assembly *in vitro* and promotes lamin B dephosphorylation and polymerization[65]. As previously noted LAP1B and LAP1C are both dephosphorylated by PP1[52], a phosphatase that is responsible for the dephosphorylation of several proteins in association with cell cycle events (reviewed in [58]). In fact, PP1 is the major mitotic lamin phosphatase responsible for dephosphorylating lamin B, resulting in nuclear lamina reassemby[63]. Additionally, PP1 mitotic associated functions include:

centrosome duplication, maturation and/or splitting; contribution to anaphase chromosome movements; spindle assembly checkpoint inactivation through dephosphorylation; removal of checkpoint proteins from the kinetochore by dephosphorylating dynein; outer kinetochore disassembly and chromosome segregation, due to dephosphorylation of Aurora B substrates; and targeting of endoplasmic reticulum to chromatin to induce the first step in nuclear envelope re-assembly (reviewed in [58]).

1.1.3.2 LAP1 associated physiopathological functions

LAP1 biological functions remain poorly understood. However throughout the years, some studies have proposed functions associated to proteins that bind LAP1. First and foremost, it was described early on that LAP1 binds directly to lamins and indirectly to chromosomes[39]. Therefore, it is reasonable to deduce that LAP1 may be involved in the positioning and organization of lamina and chromatin, thereby contributing to the maintenance of the NE structure[39,66]. Mutations in several genes that encode proteins of the nuclear envelope such as lamin A/C, lamin B, LBR, Nesprin-1, Nesprin-2 and emerin are known to cause defects of the nuclear envelope. This group of diseases, known as nuclear envelopathies, consist of a wide range of clinical syndromes, including muscular dystrophy, cardiomyopathy, lipodystrophy, mandibuloacral dysplasia, neuropathy, progeria, restrictive dermopathy, arthrogryposis, Pelger-Huet anomaly and leukodystrophy[67,68].

LAP1 gained more attention when it was reported to interact with torsinA in the NE[69,70]. A mutation of a single glutamic acid within torsinA is responsible for most cases of DYT dystonia, a neurological and movement disorder [71]. Thus, LAP1 is also known as torsinA interacting protein 1 (TOR1AIP1) and the gene encoding LAP1 is termed *TOR1AIP1*. More recently, LAP1 was found to interact with the INM protein emerin [72], which is associated with the X-linked Emery-Dreifuss muscular dystrophy disorder [44]. Moreover, LAP1 was found to be required for the normal localization of emerin. Conditional deletion of LAP1 from mouse striated muscle caused muscular dystrophy leading to early lethality, thus arguing that LAP1 plays a crucial role in skeletal muscle maintenance[72]. Recently, the first *TOR1AIP1* mutation identified is a single nucleotide deletion resulting in a frameshift and a putative truncated LAP1B protein (Turkish mutation). This has deleterious effects associated with a specific form of muscular dystrophy. A second point mutation, affecting both human LAP1 isoforms, was also recently described. This mutation involves the replacement of a single glutamic acid to alanine at position 482 (Moroccan Mutation), causing severe dystonia, cerebellar atrophy and cardiomyopathy (reviewed in [73]).

In conclusion, LAP1 is suggested to exist as a complex in the nuclear envelope with A-type lamins, torsins and emerin. The presence of such a complex suggests that LAP1 may cooperate functionally with these proteins in tissues where they play a critical role. The differential expression of the components of this complex in different tissues may lead to changes in the complex's composition and function. For example, torsinA is expressed at relatively higher levels in neuronal tissues whereas torsinB and torsin3 are expressed at higher levels in non-neuronal tissues[74]. Therefore, the identification of LAP1 binding partners and the signalling pathways where LAP1 participates are crucial for a better understanding of LAP1 functions.

1.2 SPERMATOGENESIS

The testes of mammals are paired organs that essentially have two functions, the production of sperm and steroids synthesis. A single testis comprises numerous seminiferous tubules separated by intervening interstitial space, all enclosed by a connective tissue capsule, the tunica albuginea (Figure I.4) (reviewed in [75]). The seminiferous tubules end in a system of narrow straight ducts called tubuli recti. These straight ducts are devoid of spermatogenic germ cells and empty into flattened spaces called the rete testis. The rete testis is located in the thickening of the tunica albuginea, called the mediastinum. Subsequently, the efferent ducts fuse with the head of the epididymis (Figure I.4). The epididymis consists of a highly coiled duct, divided into three distinctive regions: the head, the body, and the tail. Sequentially, sperm are initially produced in the seminiferous tubules and released to the tubuli recti. After passing through the rete testis, the efferent ducts and the head epididymis, sperm mature in the tail of the epididymis and start displaying forward motility[76].

In detail, the seminiferous tubules are formed by coiled structures creating hairpin loops (Figure I.4) with an epithelium composed of germ cells and two different types of somatic cells, the peritubular cells and the Sertoli cells (reviewed in[77]). Essentially, seminiferous tubules are enveloped by a limiting membrane comprised of contractile myoid (peritubular) cells interposed between connective tissue layers of collagen and elastic fibers, which functionally permit movement of mature sperm toward the rete testis (reviewed in [75]). Leydig cells, along with immune cells, blood and lymph vessels, nerves, fibroblasts and loose connective tissue, comprise the interstitial space between the seminiferous tubules. Importantly, Leydig cells produce and secrete the most important male sexual hormone, testosterone (reviewed in [77]).

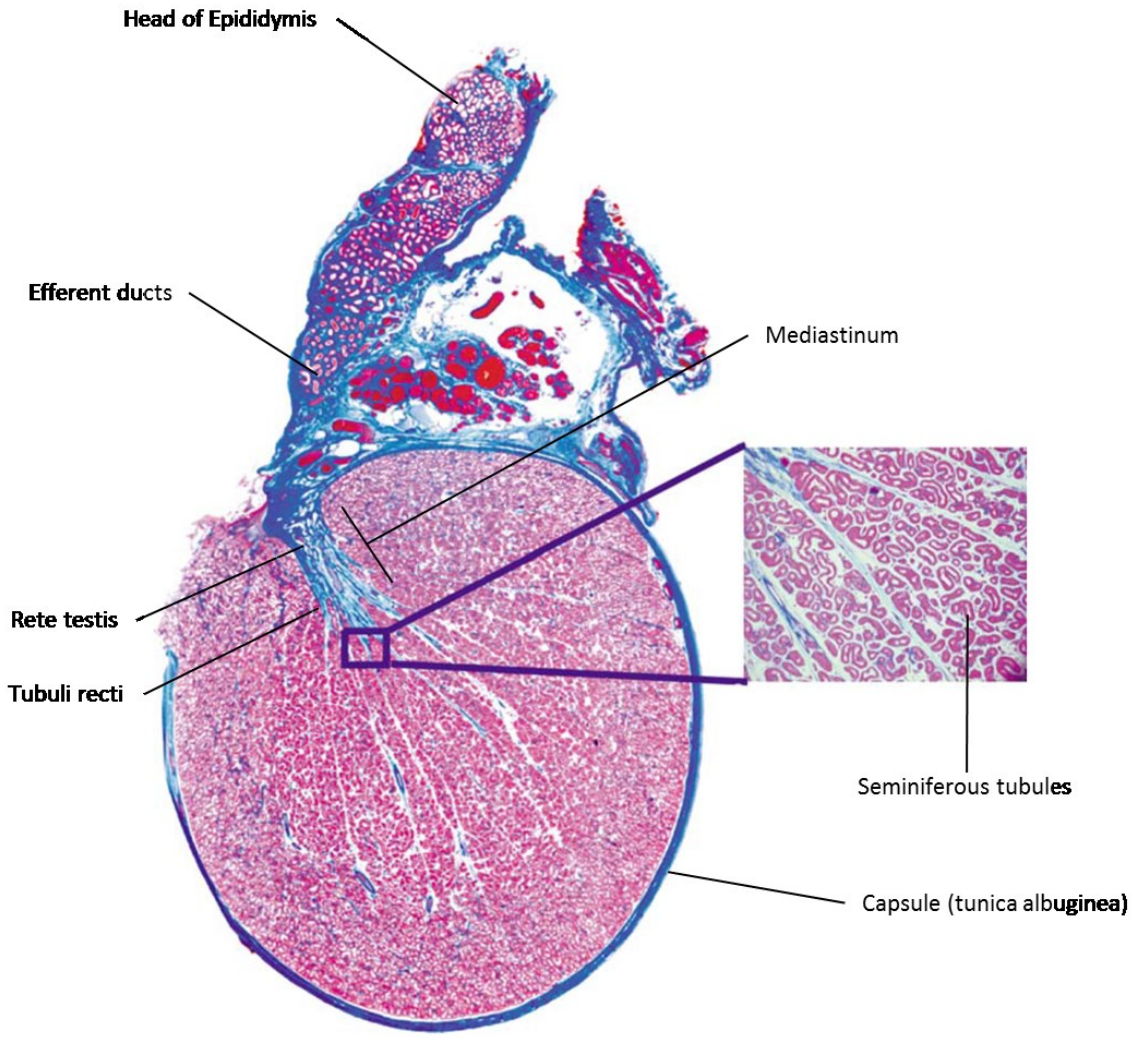

Figure I.4. **Section of an entire human testis cut transversally.** The preparation exhibits the seminiferous tubules which end in a system of narrow straight ducts called tubuli recti that in turn empty into flattened spaces called the rete testis. The rete testis is located in the thickening of the tunica albuginea, called the mediastinum. The preparation also includes parts of the efferent ducts that fuse with the head of the epididymis. Adapted from [77].

In cross sections of testicular seminiferous tubules (Figure I.5), Sertoli and germ cells are intimately associated and together form an epithelium that borders a lumen. Germ cells are organized in a well-defined manner and form concentric layers with immature germ cells, the spermatogonia, residing at the base of the epithelium adjacent to the limiting membrane, and more advanced germ cells generally occupying successive layers (spermatocytes, early and late spermatids) situated closer to the tubular lumen (reviewed in [75,78]).

Sertoli cells are located within the germinal epithelium that extend to the lumen of the seminiferous tubules (Figure I.5) and remain mitotically inactive in adults. Sertoli cells adhere to germ cells to form a highly complex epithelium, in which various tight junctions form the blood-testis barrier and regulate germ cell location and movement toward the lumen, during

differentiation. Additionally, these cells have the function of phagocytosis of degenerating germ cells and residual cytoplasmic bodies left behind by sperm. Interestingly, sperm production is intimately dependent on Sertoli cells since each individual Sertoli cell is in morphological and functional contact with a defined number of sperm. Additionally, Sertoli cells are known to synthesize and secrete a large variety of factors: proteins, cytokines, growth factors, opioids, steroids, prostaglandins, modulators of cell division etc. The Sertoli cell also mediates the actions of follicle-stimulation hormone (FSH) and luteinizing hormone (LH)-stimulated testosterone production in the testis, apparently in a stage-dependent manner. Therefore, it is generally assumed that Sertoli cells coordinate the spermatogenic process topographically and functionally (reviewed in [77,79]).

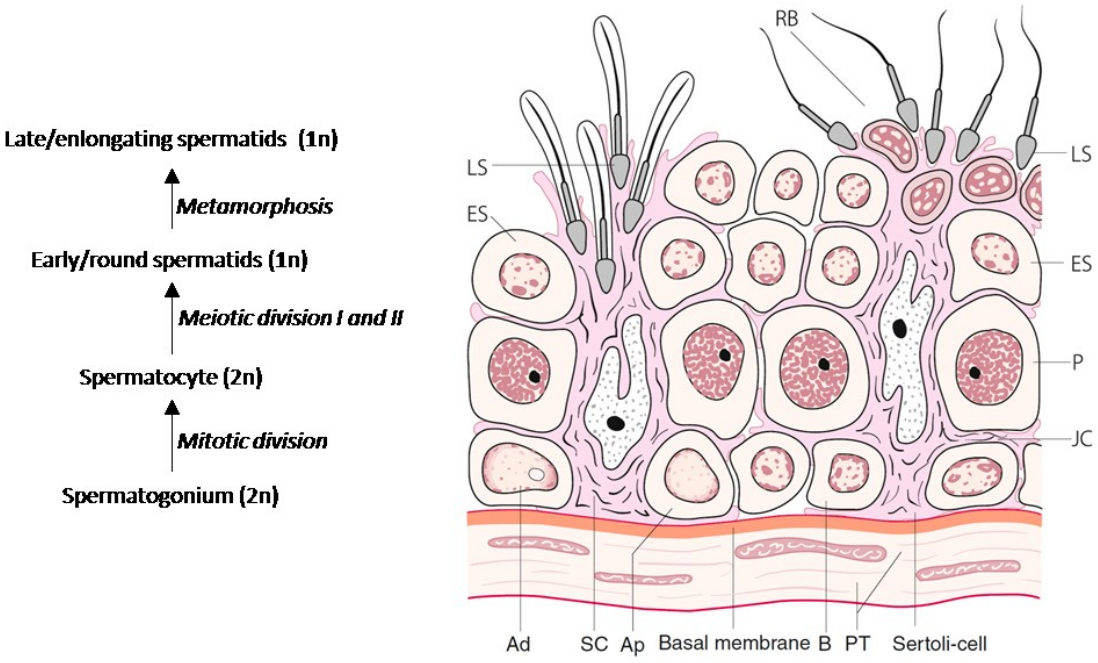

Figure I.5. Schematic representation of the specific functional phases in spermatogenesis (proliferation, meiosis, and metamorphosis) along with the respective architecture of the human seminiferous epithelium. The tubular wall is composed of several layers of peritubular cells (PT) and a basal lamina (BL). RB, Residual Body; LS, Late/elongating and elongated spermatids; ES, Early/round spermatids; P, Spermatocytes; Ad, A-dark spermatogonia (testicular stem cells); Ap; A-pale spermatogonia; B, B spermatogonia; SC, Sertoli cells; JC, junctional complexes constituting the blood-testis barrier built by interconnected Sertoli cells; 1n, haploid cells; 2n, diploid cells. Adapted from [77].

Accordingly, spermatogenesis takes place in the seminiferous tubules. This process is a highly organized and well-defined temporal event whereby undifferentiated spermatogonial germ cells evolve into maturing sperm over a specific time period that varies in mammals. The undifferentiated stem cells produce sperm throughout adult life, thereby transmitting genetic information to future generations, while renewing themselves to maintain a constant supply. Hence, spermatogenesis is characterized by three specific functional phases: proliferation, meiosis, and metamorphosis (Figure I.5). In the proliferation phase, spermatogonia undergo several mitotic divisions to form spermatocytes which undergo two meiotic divisions to form haploid spermatids. The latter develop into sperm as a result of a complicated metamorphosis involving dramatic structural modifications to the shape of their nucleus, compaction of their nuclear chromatin, formation of an acrosome, and establishment of a flagellum permitting eventual motility. The series of modifications occurring to spermatids is referred to as spermiogenesis, a subdivision of spermatogenesis. Spermatogenesis thus constitutes undifferentiated spermatogonial renewal and proliferation, spermatogonial differentiation, meiosis of spermatocytes, and metamorphosis of spermatids (reviewed in [77,78,80]).

1.2.1 Mouse spermatogenesis

Spermatogenesis in humans is different from the process in rodents, or other common mammals. Significant differences include: the 3-dimensional (3D) organization of the seminiferous epithelium; the number of sperm produced daily per gram of testis; and the pattern of spermatogonial renewal and proliferation (reviewed in [80]). Additionally, in mouse, the length of the spermatogenic cycle is quite distinct from humans. In the mouse, the total duration of spermatogenesis, from the stem cell to the mature spermatid, is about 35 days (reviewed in [81]). Moreover, in mice, an entire spermatogenic cycle takes approximately 8.6 days and is divided into stages I to XII, defined by particular combinations of the different stages of spermatogenic cells (Figure I.6). As a result, mouse spermatogenesis exhibits a wave-like progression along the tubule length, which is known as the spermatogenic wave. The precise timing of the cycle in adjacent regions of the epithelium, creates a temporal sequence of stages which is recapitulated in their physical layout within the tubule. This dynamic spatial pattern ensures that fully differentiated sperm are always available for release from a specific proportion of the epithelial surface (reviewed in [75]).

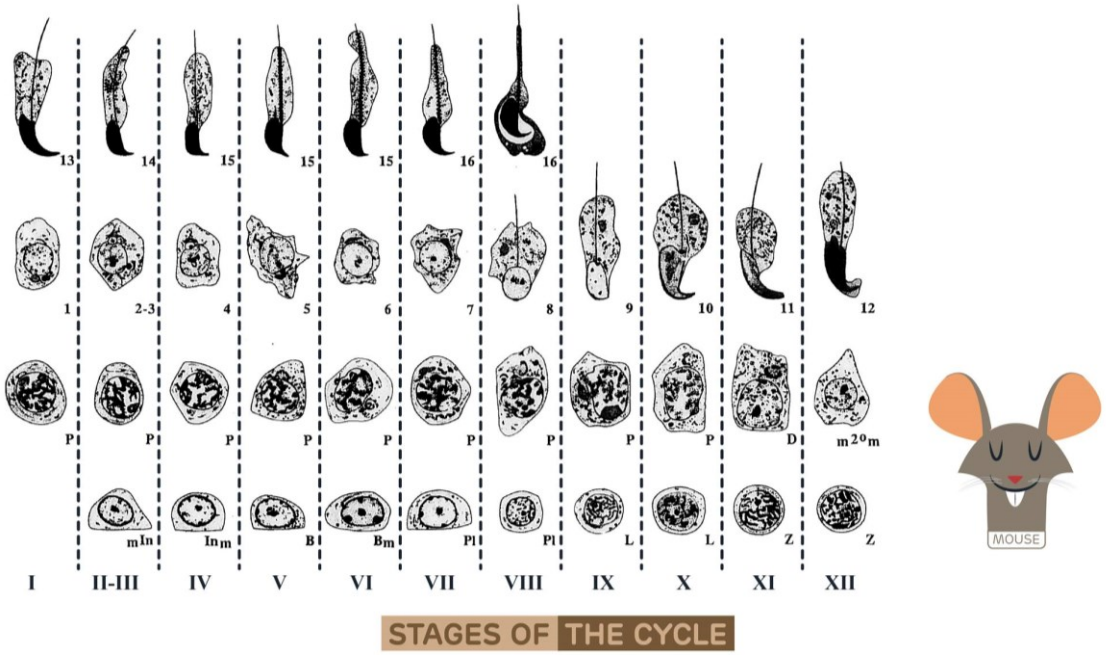

Figure I.6. Cycle of spermatogenesis in the mouse. This schematic representation illustrates the stage-specific morphological alterations during spermatogenesis in mouse testis. There are twelve stages (designated with Roman numerals) in mouse spermatogenic cycle which thoroughly depicted in the scheme. $_{m}$In, intermediate spermatogonium prior to mitosis; In$_{m}$, intermediate spermatogonium after to mitosis; B, B spermatogonium; Bm, B spermatogonium undergoes mitosis; Pl, preleptotene spermatocyte; L, leptotene spermatocyte; Z, zygotene spermatocyte; P, pachytene spermatocyte; D, diplotene spermatocytes; m^{2o}m, two meiotic divisions; 1–16, 16 steps in the development of spermatids. Adapted from [82].

The spermatogenic wave (Figure I.6) is readily apparent in the mouse testis, in which successive stages of the epithelial cycle are arranged as a linear series of cylindrical segments along the seminiferous tubule. Therefore, each tubule will display a specific stage when analysed by immuhistochemical sectioning. In other species, for instance in human, the stages are organised in more complex configurations and hard to identify at first hand[83].

Currently, it is not possible to identify spermatogonial stem cells by routine microscopy, but spermatogonial classes can be characterized by light and transmission electron microscopy according to the presence and distribution of heterochromatin (Figure I.6): undifferentiated A spermatogonia [A single, A paired, A aligned]; differentiated A spermatogonia (A1, A2, A3, A4); intermediate spermatogonia; and B spermatogonia[84,85]. Sequentially, B-spermatogonia divide by mitosis forming two preleptotene spermatocytes, representing the beginning of meiotic prophase[86]. Preleptotene rest on the basement membrane, but the following leptotene, zygotene and pachytene spermatocytes become transit and move through the Sertoli-Sertoli barrier[86]. Preleptotene, leptotene and zygotene spermatocytes are located in specific stages and are identifiable by routine microscopy, although fixation artefacts might wrongfully lead to the observation that these cells are attached to the basement membrane. Spermatocytes are found in

all stages, because meiosis is a prolonged period of spermatogenesis (14 days), thus, any attempt to isolate specific stages of spermatogenesis for molecular analysis will include these cells. Meiotic cell division occurs in stage XII and comprises three phases: meiosis I, the division diplotene (2n); formation of secondary spermatocytes (2n), which are larger than spermatids, but rarely are found as the only spermatocyte in a tubular cross section; and meiosis II, division of secondary spermatocytes (2n) to form haploid (1n) round spermatids (reviewed in [75]).

Spermiogenesis then proceeds with the completion of four phases: Golgi, capping, acrosomal, and maturation (Figure I.7) (reviewed in [79]). Together, these steps are extremely useful for the identification of specific stages in the cycle of the seminiferous epithelium. The Golgi apparatus is very important during the early steps of spermiogenesis as the formation of the acrosome highly dependent on the production of vesicles and granules containing the enzymatic components of the acrosomic system that will cover the developing sperm nucleus. The first three steps of differentiation of round spermatid formation involves a prominent Golgi apparatus. First, spermatids have a small, perinuclear Golgi region without an acrosomic vesicle or granule. Then, proacrosomal vesicles and granules within the Golgi apparatus culminate in the formation of a single, large acrosomal granule within a greater vesicle that will indent the nucleus. Capping in round spermatids, is characterized by the association of the acrosomic granule to the nuclear envelope and by flattening of this vesicle into a small cap over the nuclear surface. Later on, the acrosomic vesicle becomes very thin and the granule flattens. Finally the acrosome flattens completely over approximately 1/3 of the nuclear surface. In late stage VIII, shaping of the nuclei begins. Acrosomal steps include migration of the acrosomal system over the ventral surface of the elongating spermatid nucleus. Conversely, recognition of specific stages of spermatogenesis will typically rely on the acrosomal system observed in the round spermatids, rather than in the elongating cells. These spermatid steps also involve condensation of the chromatin, as the chromosomes are packed more tightly and stain more intensely. Maturation is observed across Stages III-VIII and display fewer changes in nuclear shape and acrosomal migration. The nucleus continues to condense and the acrosome matures into a thin structure that protrudes at the apex but covers nearly all the nucleus, except for the portion connected to the tail. Excess cytoplasm leads to the development of residual bodies in stage VIII, resulting in the formation of prominent cytoplasmic lobes, which contain unused mitochondria, ribosomes, lipids, vesicles and other cytoplasmic components. The residual bodies are excised between steps 14-16 of elongated spermatids noticeable in Figure I.6 (reviewed in [75,79,87]).

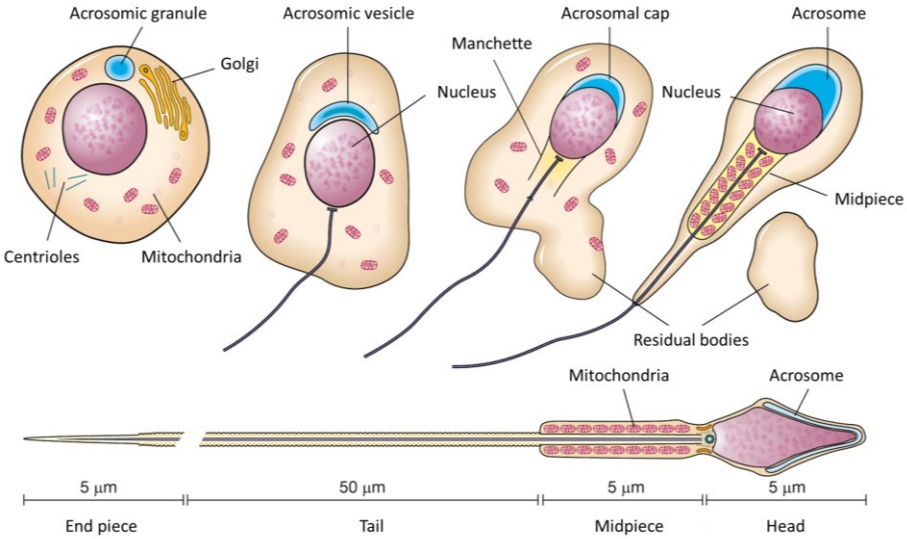

Figure I.7. Process of spermiogenesis involving dramatic structural modifications. Spermiogenesis proceeds with the completion of four phases: Golgi, capping, acrosomal, and maturation. The Golgi apparatus surrounds the condensed nucleus, becoming the acrosomal cap. One of the centrioles of the cell elongates to become the tail of the sperm. A temporary structure called the manchette assists in this elongation. Spermatids orient the tails towards the lumen, away from the epithelium. The excess cytoplasm, known as residual bodies, is excised and later phagocytosed by surrounding Sertoli cells in the testes. Adapted from [88].

1.2.2 Human spermatogenesis

In humans, germ cells have the following terminology: A-dark spermatogonia; A-pale spermatogonia; B-spermatogonia; preleptotene, leptotene, zygotene, pachytene, and diplotene spermatocytes; secondary spermatocytes; spermatids; and spermatoza (Figure I.8). Spermatogonial proliferation and differentiation involve only A pale-spermatogonia, since A dark spermatogonia do not show proliferating activity under normal circumstances and are believed to divide only rarely. Indeed, A pale-spermatogonia divide and differentiate into two B spermatogonia, which in turn, divide to form preleptotene spermatocytes. Meiosis of spermatocytes includes the last synthesis of DNA in preleptotene spermatocytes and 2 meiotic divisions to form spermatids (Figure I.8). Then, spermiogenesis results in the transformation of a round spermatid to an elongated mature spermatid as described previously in Figure I.7. Finally, spermiation occurs when the structures and connections anchoring a mature spermatid to a Sertoli cell disrupt, so that sperm cells are released into the tubule lumen. In humans, the interval between commitment of an A pale-spermatogonium to proliferate and spermiation of resulting sperm averages 74 days (reviewed in[77,80]).

Initially, multiple spermatogonia are connected by intercellular bridges, which provide cytoplasmic continuity among members of a cohort of cells, except when cell death eliminates a

connecting cell. These cohorts of germ cells are layered, with the youngest near the basement membrane. Later on, Sertoli cells systematically move maturing spermatids towards the tubule lumen (Figure I.5). Collectively, the 4–5 cohorts of germ cells theoretically developing concurrently at a circumscribed location in a tubule are termed as stages. Six stages were normally used to describe and study spermatogenesis in humans (designated with Roman numerals) with two to four cellular stages usually evident in a cross-section of a human seminiferous tubule. However, a new stage classification was proposed on the basis of acrosomal development made visible by immunohistochemistry (IHC), distinguishing twelve stages[89]. Overall, the interval between the initial differentiation of A-pale spermatogonia and the spermiation of resulting sperm averages 74 days (reviewed in [80]).

Stage identification can be defined in several ways, but inevitably, this requires recognition of specific cell types (Figure I.8). Nevertheless, the appearance of germ cells is highly dependent on methods of fixation, embedment, staining, and visualization, being extremely difficult to determine by IHC procedures, particularly in cross sections of the human tissue (reviewed in [79,80]).

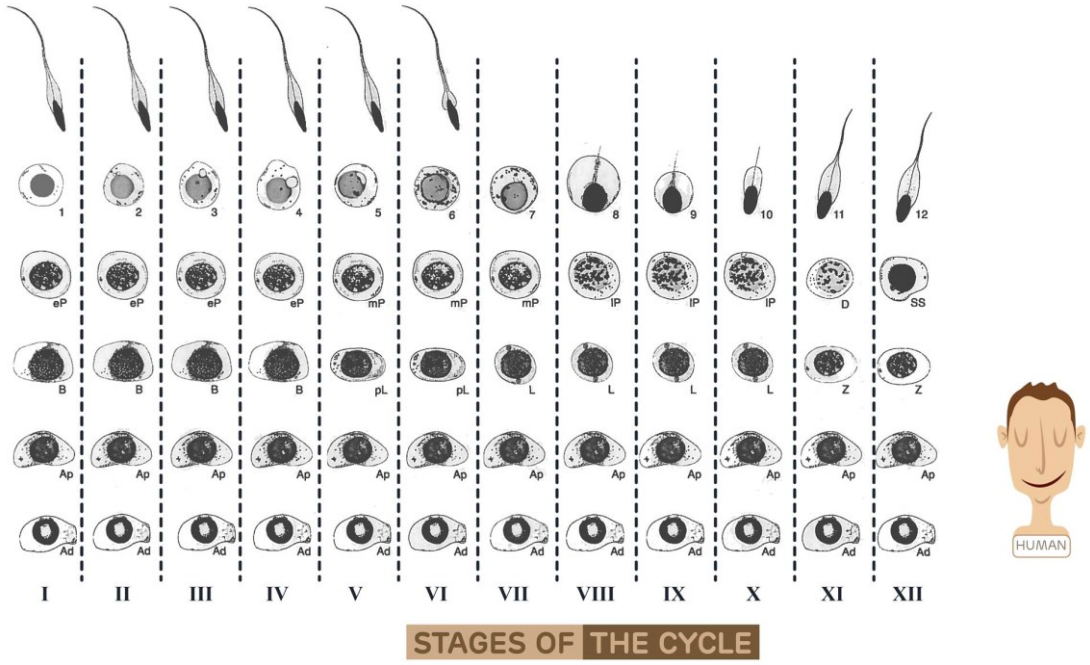

Figure I.8. Cycle of spermatogenesis in human. This schematic representation illustrates the stage-specific morphological alterations during spermatogenesis in human seminiferous tubules. There are twelve stages (designated with Roman numerals) in the human spermatogenic cycle, which are thoroughly depicted in the scheme. Ad, A-dark spermatogonia; Ap; A-pale spermatogonia; B, B spermatogonia; pL, preleptotene spermatocyte; L, leptotene spermatocyte; Z, zygotene spermatocyte; eP, early pachytene spermatocyte; mP, mid-pachytene spermatocyte; lP, late pachytene spermatocyte; D, diplotene spermatocyte; SS, secondary spermatocytes; 1–12, first 12 steps in the development of spermatids. Adapted from [82].

1.2.3 NE shaping during spermatogenesis

The nuclear envelope undergoes evident changes in the course of spermiogenesis (Figure I.7). Throughout the nuclear shaping and condensation process, excess nuclear membrane is eliminated into the posterior cytoplasm in the form of two continuous sheets at either side of the implantation fossa (region where the centrioles connect to the NE). The remaining membrane forms two short extensions at the caudal margin of the nucleus resulting in a redundant nuclear envelope in sperm. In order to reduce the volume of the nucleus and the nuclear envelope, elimination of nuclear excess is concomitant with chromatin condensation. These series of modifications are accompanied by concentration of stacked lamellae along the posterior margin of the NE, nuclear blebbling, and concentration of nuclear pores to the post-acrosomal region. All these morphologic changes seem to be associated with the loss of nuclear contents during the gradual reduction in nuclear volume (reviewed in [81,90]).

A curious "organelle" worth mentioning when referring to the NE dynamics in spermatogenesis is the chromatoid body. This granular component localizes to cytoplasm and is mainly responsible for regulating RNA processing through the differentiation process. The chromatoid body moves in relation to the NE in two different ways: either along the NE on a wide area surrounding the Golgi apparatus, developing frequent transient associations with this organelle; or perpendicular to the nuclear envelope. Additionally, it has been observed to be located very transiently at the top of prominent outpocketing of the nuclear envelope with apparent material continuities through nuclear pore complexes with intranuclear particles (reviewed in [81,90]).

1.2.4 NE proteins throughout spermatogenesis

The role of nuclear envelope components has been investigated in relation to the various phases of spermatogenesis. Importantly, lamins, LAP2, LBR, and elements of the LINC complex are amongst nuclear envelope proteins with more prominent associations to multiple functions in the spermatogenic cycle[91–97].

As part of a differentiation process, spermatogenic cells suffer major structural and morphological alterations throughout the cycle. When compared with somatic cells, the nuclear envelope of mammalian spermatogenic cells shows a series of peculiarities. For instance, among somatic lamins, lamin A, C, and B1 are expressed during spermatogenesis. Lamin B2 is not present

in any phase of this differentiation process[98,99]. Instead, two short gametogenesis-specific lamins appear at different stages to become part of a reformed lamina. These are the A-type lamin C2 that is selectively expressed during meiotic prophase I[100], and lamin B3, a short lamin B2 isoform whose expression is restricted to postmeiotic stages[101]. Compared to their somatic counterparts, both gametogenesis-specific lamins are N-terminally truncated versions, lacking the complete N-terminal head including a significant part of the rod domain. These domains are replaced by short unique sequences [102]. Interestingly, from the investigations on somatic lamins it is known that the domains that are absent in lamins C2 and B3 seem to be involved in the dimerization as well as the formation of more complex structures. According to this, it has been proposed that lamins C2 and B3 would supply a flexible setting to the NE[100].

Interactions between the chromosomes and the nuclear envelope might be important for meiotic pairing. Particularly, in early meiotic prophase, chromosomes become attached to the nuclear envelope via their telomeres. This attachment is highly dynamic as it allows telomeres to move within the nuclear envelope and to congregate at one of its poles in order to form a so-called bouquet and to move apart later during pachytene spermatocytes. Telomere movements at the plane of the nuclear envelope are suggested to allow chromosome recognition as well as the stable pairing of the homologues (reviewed in [102]). Lamin C2, in particular, presents a series of peculiarities that are consistent to the notion that it fulfils specific functions, different from that of other A-type isoforms. This isoform is selectively expressed during the first meiotic prophase. Later in meiosis, it is no longer detectable by IHC and biochemical methods[100]. Remarkably, lamin C2 is highly enriched at the attachment sites of the telomeres. In light of this specific localization pattern and on basis of the proposed influence of the N-terminal truncation on the polymerization properties of lamin C2, this isoform might lead to a local flexibility of the nuclear envelope at the attachment sites that in turn enables the movement of telomeres and therefore supports pairing, recombination, and synapsis[92]. Additionally, it is proposed that the C2-containing domains might also function as local reinforcements of the NE that would give to the subjacent membrane a higher mechanical stability that would be required for the proper attachment to the synaptonemal complex (Figure I.1)[92].

Furthermore, examination of the testes of *Lmna*-/- mice revealed that spermatogenesis is dramatically affected, as almost no post-meiotic stages appeared within the seminiferous tubules[103]. Correspondingly, virtually no sperm was found in the epididymis. Recently, investigation of *C2*-/- mice that show normal expression of all other A-type lamins, recapitulates the meiotic failure seen in *Lmna*-/- mice, where spermatogenesis was disrupted and defects in meiosis-specific processes were observed. In addition, it was observed that chromosomes frequently fail to synapse

and they engage in heterologous associations or show aberrant telomere-telomere interactions, representing defects that are rare in wild-type spermatocytes. Lastly, as a result of extensive apoptosis and failure of sperm maturation, males are completely infertile[104]. Conversely, lamin A/C was shown to be expressed in the mouse testis not only in the different stages of spermatogenesis but also in mature sperm[99].

Alternatively, the nuclear lamina of spermatids is mainly composed of lamin B1 and the spermiogenesis-specific lamin B3. In contrast to meiotic stages, no A-type lamins are detectable at any time[101]. An additional major difference deals with lamin distribution. In round spermatids, lamin B3 was detected at the nuclear periphery as well as diffusely distributed in the nucleoplasm. Later, lamin B3 of the nuclear envelope and the nucleoplasm progressively polarize at the posterior pole of elongating spermatid nuclei where they accumulate before becoming undetectable at the end of spermiogenesis[101]. As mentioned above regarding lamin C2, Lamin B3 has peculiar polymerization properties that would possibly provide the nuclear periphery of spermatids with a flexible condition, which in turn would be required for nuclear reshaping. Lamin B3 becomes polarized as spermiogenesis progresses. Interestingly, a similar polarization could be observed for lamin B1 and the inner nuclear membrane proteins LAP2 and LBR [91,96,101]. Currently, the molecular basis and functional significance of this redistribution is unclear. However, due to chromatin-binding associated functions of most of the nuclear envelope proteins involved, it can be speculated that nuclear envelope remodelling would contribute to the process of sperm-specific chromatin reorganization [91,96].

Adding to the interest of lamin function in this differentiation process, the role of two lamin interacting proteins (LAP2 and LBR) was ascertained during spermatogenesis. Interestingly, LAP2 and lamin B1 seem to be involved with changes in chromatin organization that occur during spermiogenesis. During spermiogenesis the nuclear envelope undergoes a profound reorganization that leads to the formation of a domain in the posterior pole, which differs in morphology from other regions of the spermatid nuclear periphery. LAP2 and lamin B1 both progressively localize to the posterior pole (centrioles) of elongating rat spermatid nuclei. By moving to the posterior pole, the chromatin binding sites at the nuclear envelope would possibly contribute to the achievement of the non-random, sperm specific chromatin distribution. Also, as mentioned earlier (chapter 1.1.1), nuclear envelope proteins, in particular the lamins, play an important role in chromatin dynamics and function. According to this evidence, it was purposed that the progressive disappearance of lamin B1 and LAP2 observed in elongating spermatids may signify the process of chromatin condensation and inactivation that normally takes place during spermiogenesis[91].

Similarly, in elongating spermatids, another lamin-binding protein, LBR, temporarily associates with P1 protamine. During mammalian spermiogenesis, histones are replaced by protamines P1 and P2. As a result of this exchange, the chromatin is compacted into a volume of about 5% of that of a somatic cell nucleus, through a phosphorylation regulated process[96].

Equally relevant for the associative study of nuclear envelope proteins throughout spermatogenesis are LINC complexes. As previously mentioned (section 1.1.2), LINC complexes are nuclear envelope bridging protein structures formed by interaction of SUN and KASH proteins. They physically connect the nucleus with the peripheral cytoskeleton and are critically involved in a variety of dynamic processes, not only nuclear anchorage, movement, positioning and shaping, as well as meiotic chromosome dynamics[95,97].

One example is the attachment of meiotic telomeres to the NE which is mediated by SUN-KASH protein complexes (Figure I.1)[105]. For instance, SUN1 is essential for the efficient attachment of telomeres to the NE, and SUN2 also appears to be involved in the tethering of meiotic telomeres to the NE. In the absence of SUN1, an unexpectedly large proportion of telomeres are still able to attach to the NE and, beyond this, are also able to move within the NE, forming bouquet-like clustered telomere patterns. This suggests that in the SUN1 deficient background some of the telomeres not only succeed to establish a tight connection to the NE, but even become linked to the cytoskeletal motor system. Consistent with this observation, is that in *Sun1*$^{-/-}$ mice the NE-attached telomeres colocalize with SUN2 and KASH5, suggesting that telomere attachment is mediated by SUN2/ KASH5-LINC complexes in SUN1 deficient meiocytes[95].

During mouse sperm development, particularly spermiogenesis, two novel distinctive LINC complexes were discovered, namely, SUN3-Nesprin1 and SUN1g-Nesprin3. These two LINC complexes specifically polarize to opposite spermatid poles of the nucleus, connecting sperm-specific cytoskeletal structures. So, formation of the mammalian sperm head seems to involve assembly and different polarization of these two novel spermiogenesis-specific LINC complexes. Therefore, these LINC complexes connect the differentiating spermatid nucleus to surrounding cytoskeletal structures to enable its directed shaping and elongation, which in turn is a critical parameter for male fertility[97].

OBJECTIVES

When compared to proteins discovered contemporaneously, strikingly, the biological functions of LAP1 remain unknown. Therefore, the study of this INM protein interactors' using bioinformatic tools might shed some light into its associated cellular pathways and functions.

In the past, mutations in LAP1 and its interactors have been vastly associated to several envelopathies. Given the major role of the NE in the differentiation process, LAP1 most prominent interacting proteins have been systematically studied through the course of spermatogenesis. However, LAP1 expression or localization have never been investigated during this differentiation process nor it has been analysed in sperm. Therefore, it was our objective to reveal the main function of LAP1 throughout spermatogenesis and its possible association to infertility.

Thus, the specific aims of this dissertation are the following:

- To determine LAP1 interactors using bioinformatics tools;
- To establish the main cellular pathways and functions associated with LAP1, based on the bioinformatic study of its interactors;
- To determine the localization of LAP1 and some of its interactors in the testis;
- To evaluate if LAP1 and its interactors might potentially be relevant to the differentiation process in spermatogenesis.

CHAPTER II – BIOINFORMATIC ANALYSIS OF LAP1 INTERACTORS

LAP1 is suggested to exist as a complex in the nuclear envelope with A-type and B-type lamins, torsins and emerin[39,66,67,69,70]. The presence of such complexes suggests that LAP1 may cooperate functionally with these proteins in tissues where they play a critical role[74]. Therefore, the identification of LAP1 binding partners and the signalling pathways where LAP1 participates are crucial for a better understanding of LAP1 functions. Therefore, the work described in the chapter II addresses the novel human LAP1 associated proteins found through bioinformatic tools. This work was included in the manuscript entitled: "Lamina Associated polypeptide 1 (LAP1) interactome and its functional features", published in the journal *Membranes*.

“Lamina Associated polypeptide 1 (LAP1) Interactome and its Functional Features”

Joana B. Serrano, Odete A. B. da Cruz e Silva, and Sandra Rebelo

Laboratório de Neurociências e Sinalização, iBiMED, DCM, Universidade de Aveiro, Campus Universitário de Santiago, Agra do Crasto, 3810-193 Aveiro, Portugal

Abstract

Lamina-associated polypeptide 1 (LAP1) is a type II transmembrane protein of the inner nuclear membrane encoded by the human gene *TOR1AIP1*. LAP1 is involved in maintaining the nuclear envelope structure and appears be involved in the positioning of lamins and chromatin. To date, the precise LAP1 function is not fully elucidated but analysis of its interacting proteins will permit unravelling putative associations to specific cellular pathways and cellular functions. Public databases allowed the identification of the LAP1 interactome, which was curated. In total, 41 interactions were identified. Several functionally relevant proteins, such as TRF2, TERF2IP, RIF1, ATM, MAD2L1 and MAD2L1BP were identified and might support putative functions proposed for LAP1. Furthermore, by making use of the Ingenuity Pathways Analysis tool and submitting the LAP1 interactors, the top two canonical pathways include “Telomerase signalling” and “Telomere Extension by Telomerase” and top functions include “Cell Morphology”, “Cellular Assembly and Organization” and “DNA Replication, Recombination, and Repair”. Once again, putative LAP1 functions are reinforced but novel functions are emerging.

2.1 INTRODUCTION

The eukaryotic nucleus is a complex organelle enclosed by a highly organized double membrane, the nuclear envelope (NE). The NE separates the nucleus from the cytoplasm and is essentially composed by inner nuclear membrane (INM), the outer nuclear membrane (ONM), the nuclear pore complexes (NPCs) and nuclear lamina. The INM and ONM are separated by the perinuclear space of 40-50nm of diameter and are crossed and therefore connected at the NPCs. The perinuclear space is continuous with the lumen of the endoplasmic reticulum (ER) and the ONM is continuous with the rough endoplasmic reticulum membrane that comprises the ribosomes. The nuclear lamina is composed by lamins which are type V intermediate filament proteins exclusively found in the nucleus and are associated with INM proteins. The NE and NE proteins have received more attention in the last few years and there is increasing evidence that the NE is responsible for integration of many cellular functions, including chromatin organization, signalling pathways, transcription regulation and cytoskeletal organization[106–108].

The nuclear membranes are considered an interconnected membrane system associated with the ER that comprises a specific group of proteins that are specifically enriched in the INM and ONM, but not in the ER. Of these, approximately 80 transmembrane proteins are concentrated in the INM[7] and a significantly lower number is concentrated in the ONM. Regarding the INM proteins some remain uncharacterized, but other were found to interact with lamins and/or chromatin. One of the first lamina associated proteins identified was lamina-associated polypeptide 1 (LAP1)[40] which is a type II transmembrane protein of the inner nuclear membrane encoded by the human gene *TOR1AIP1*. In rats, three LAP1 isoforms were described and are derived by alternative RNA splicing, being designated as LAP1A, LAP1B and LAP1C with molecular weights of 75, 68 and 55 KDa, respectively[40,41]. In humans, the LAP1B isoform was previously identified by Kondo *et al.*[48] and we recently identify a novel human isoform, the LAP1C. This new isoform is N-terminally truncated, with a molecular weight of approximately 55 KDa contrasting with the 68 KDa of the LAP1B[49]. The function of LAP1 remains poorly understood. However, several LAP1 binding partners have been identified as is the case of lamins (directly binding) and chromosomes (indirectly binding)[39]. Therefore it is believed that LAP1 might be involved in the positioning of lamins and chromatin in close proximity with the NE, thereby contributing to the maintenance of NE structure[41,109]. Another important LAP1 binding protein identified was torsinA, which is the central protein in DYT1 dystonia[69]. A mutation of a single glutamic acid within torsinA (ΔE-torsinA) is responsible for DYT1 dystonia, a dominantly inherited neurological and movement disorder characterized by prolonged involuntary twisting movements[71]. Interestingly, while the wild type torsinA is localized in both ER

and the perinuclear space, the mutated torsinA (ΔE-torsinA; pathogenic variant) preferentially concentrates in the perinuclear space[110,111]. Of note, torsinA variants with decreased ATPase activity bind more efficiently to LAP1. More recently, LAP1 was found to interact with another INM protein named emerin[70] that is associated with the X-linked Emery-Dreifuss muscular dystrophy[44]. The interaction of these two INM proteins is mediated by their nucleoplasmic domain, particularly emerin binds to LAP1 residues 1-330[70]. We recently reported that the human LAP1B binds to protein phosphatase 1 (PP1) in the nucleoplasm domain and that it is dephosphorylated by this phosphatase[52]. Furthermore, by mass spectrometry we identified 5 different LAP1 phosphorylated residues: Ser143, Ser216, Thr221, Ser306 and Ser310. From these, it was possible to establish that only Ser306 and Ser310 are dephosphorylated by PP1[49].

Recently, two mutations were identified of *TOR1AIP1* gene were directly associated with disease conditions. The first *TOR1AIP1* mutation ('Turkish' mutation) was reported and it affects three members of a Turkish family with an autosomal recessive limb-girdle muscular dystrophy with joint contractures. It was predicted that this c.186delG mutation, truncates the 584 amino acid LAP1B protein to an apparently non-functional protein, only 83 amino acids long[112]. Consequently, expression of LAP1B was absent in the skeletal muscle fibres of these patients. The authors also showed, by ultrastructural examination of the muscle fibres, that patients had intact sarcomeric organization but clearly evident alterations of the nuclear envelope including nuclear fragmentation. Of note, this study places LAP1B as a pivotal protein associated with striatal muscle function and increases the number of genes associated with nuclear envelopathies. A second *TOR1AIP1* mutation ('Maroccan' mutation) was reported in a boy, born from consanguineous healthy parents, who developed rapidly progressing dystonia, progressive cerebellar atrophy, and dilated cardiomyopathy. Upon whole exome sequencing a homozygous missense mutation in *TOR1AIP1* was identified, resulting in a highly conserved glutamic acid change to alanine at amino acid 482[113]. The in vivo studies performed by the authors indicated that the patients revealed reduced expression levels of LAP1 and its misallocation and aggregation in the endoplasmic reticulum[113]. Of note, both LAP1 human isoforms (LAP1B and C) are affected by this mutation. These two mutations strengthen functional association of LAP1 with DYT1 dystonia (in neurons) and muscular dystrophy (skeletal muscle)[73].

To date the precise function of LAP1 is not fully elucidated. However a significant amount of work has been associated with the identification and functional characterization of LAP1 interactions, particularly with lamins, torsinA, emerin and PP1. The identification of additional LAP1 binding proteins and their association to specific cellular pathways and cellular functions are

therefore crucial to the understanding of the precise physiological roles of LAP1. The work here described proposes novel LAP1 functions through the bioinformatic study of its interactors.

2.2 EXPERIMENTAL SECTION

2.2.1 Collection of associated interactions of LAP1

In order to develop a comprehensive computational analysis of LAP1 interactome, experimentally detected protein-protein and protein-nucleic acid interactions were extracted from the following public databases: BioGRID[114] (version 3.4.129, consulted Oct 12th 2015), IntAct[115] (version 4.1.8, consulted Oct 13th 2015), mentha[116] (version of Oct 13th 2015), I2D[117] (version of Oct 13th 2015), APID[118] (version of Oct 13th 2015), HIPPIE[119] (version of Oct 13th 2015), NCBI[120] (version of Oct 13th 2015) and PSICQUIC[121] (version 1.4.5, consulted Oct 14th 2015).

The resulting set of 180 binary interactions includes high and low-throughput data that was later manually curated by consulting the corresponding articles. Despite the worth and accessibility of protein interaction data from online databases, it comes with limitations. Numerous databases (including the ones used in this analysis) contain interactions based on indirect evidence, for instance, data mining, genetic interactions, metabolic evidence and colocalization data. The output from these eight online databases resulted in the identification of 49 LAP1 interactors. However, after analysing the respective publications, 10 interactions were excluded resulting in the confirmation of 39 LAP1 interactors (Table II.1 and Figure II.2).

2.2.2 Gene Ontology term enrichment analysis

Gene Ontology (GO) provides a system of terms to consistently describe and annotate gene products[122]. GO term enrichment analysis (supported by Panther 10.0, released May 15th 2015; analysed Oct 15th 2015)[123] was performed online using the *Search GO data* tool (available at http://geneontology.org/)[124] to enquire for GO terms that are over-represented using the annotations regarding *biological process* and *cellular component*. The list of genes was pasted into the corresponding box to be analysed, choosing *Homo sapiens* as the species of genes integrated in the gene set. GO analysis of LAP1 the interactome was only possible by extrapolating the mouse and rat interactions to human. The output retrieved a table that lists significant shared GO terms (or parents of GO terms) used to describe the set of genes that users entered on the previous page,

the background frequency, the sample frequency, expected p-value, an indication of over/underrepresentation for each term, and p-value. The statistical analysis included Bonferroni's correction for multiple testing and a term was reported as enriched if the adjusted p-value is below a significance threshold of 0.05. All the input genes were mapped, however two were unclassified: TOR3A for biological process ontology and HPDL for cellular component. The p-values were corrected for multiple testing using the Bonferroni procedure and transformed by taking the -log10 for easier visualization. The online GO term enrichment service, retrieved from the online platform was stored and analysed as Excel spreadsheet files (Figure II.4).

2.2.3 Software platforms and plugins

Data obtained from the online databases already described were stored and analysed as Excel spreadsheet files. The network of LAP1 interactors was built using Cytoscape (3.2.1, freely available online at http://www.cytoscape.org/)[125]. Cytoscape is one of the most popular tools for visualizing, integrating, modelling, and analysing molecular and genetic interaction networks[125].

The GeneMANIA plugin (version 3.4.0) was installed using the Cytoscape App Manager (Cytopscape plugin can be download at http://apps.cytoscape.org/apps/genemania)[126]. GeneMANIA is a particularly convenient and user-friendly metasearch platform that generates a highly correlated signalling network centred on the proteins of interest[127]. To determine the interactions between the LAP1 interactors inside the network, the gene set was introduced into GeneMANIA on Cytoscape. Different results can be produced from the same gene list when using GeneMANIA. In this case, by only selecting *physical interactions* data, the network will only show genes linked if the proteins in question share a binary interaction established through physical experiments[127]. The integrated network obtained after using GeneMANIA was subsequently manually curated with the respective publications to confirm the binary interactions. With the editing tools offered by Cytoscape this network was designed to obtain the final result presented on Figure II.3.

BiNGO is a tool used to determine which GO categories are statistically overrepresented in a set of genes and outputs a network that allows interactive visualization of results mapped by the GO hierarchy[128]. The BiNGO plugin (version 3.0.3) was installed using the Cytoscape App Manager (freely available to download at http://apps.cytoscape.org/apps/bingo)[128]. In Cytoscape, BiNGO outputs a network of the significant GO terms using p-values that were corrected for multiple testing using the Bonferroni correction. Each term is size and colour-coded, so that larger nodes

have more genes and darker nodes are more significantly enriched. Intermediate terms that are not significant are present as small white nodes[128]. GO terms are organized in a tree-like structure, starting from more general terms at the root (for example, biological regulation) to the most specific at the leaves (for example, the regulation of mitotic cell cycle) distributed across the two main semantic domains — *biological process* and *cellular location*. As GO terms might have more than one parent, they are technically structured as a network called a DAG (Figures S1 and S2).

Ingenuity® Pathway Analysis (IPA®, QIAGEN Redwood City, www.qiagen.com/ingenuity) is a commercially available software program that helps model, analyse and understand complex biological and chemical systems. The Ingenuity Knowledge Base is a repository of expertly curated biological information. Gene identifications of the previously described interactors were imported into the Ingenuity Pathways Analysis (IPA) tool, once more extrapolating the mouse and rat interactions to human and excluding viral connections. Function classifications, signal pathways and interacting networks were constructed and analysed based on the underlying biological evidence from the IPA's database. The core analysis performed in IPA retrieved seven distinctive functional sets: canonical pathways, upstream regulators, diseases and disorders, molecular and cellular functions, physiological system development and functions, associated network functions and toxicological lists. The output generated through the use of QIAGEN's Ingenuity Pathway Analysis (IPA®, QIAGEN Redwood City, www.qiagen.com/ingenuity) is depicted in Tables II.2-II.5 and Figures II.5, S3-S6. Right-tailed Fisher's exact test was used to calculate the significance of each biological function and/or disease assigned, which was reported if the adjusted p-value was below a significance threshold of 0.05.

2.3 RESULTS AND DISCUSSION

In order to determine LAP1 interacting proteins a specific approach was adopted, as summarized in Figure II.1. Briefly, binary interactions with LAP1 were collected and manually curated to obtain the working dataset of LAP1 interactors of (step 2.1, Figure II.1). Subsequent integration of the interactions among the listed interactors was performed with GeneMANIA, resulting in a more complete prospective network (step 2.2, Figure II.1). GO and BiNGO enrichment analysis assisted in ascertaining the most prevalent biological processes and the cellular distribution of the interactors (step 2.3, Figure II.1). Finally, by resorting to Ingenuity Pathway Analysis the physiological and functional relevance of the selected proteins were explored (step 2.4, Figure II.1).

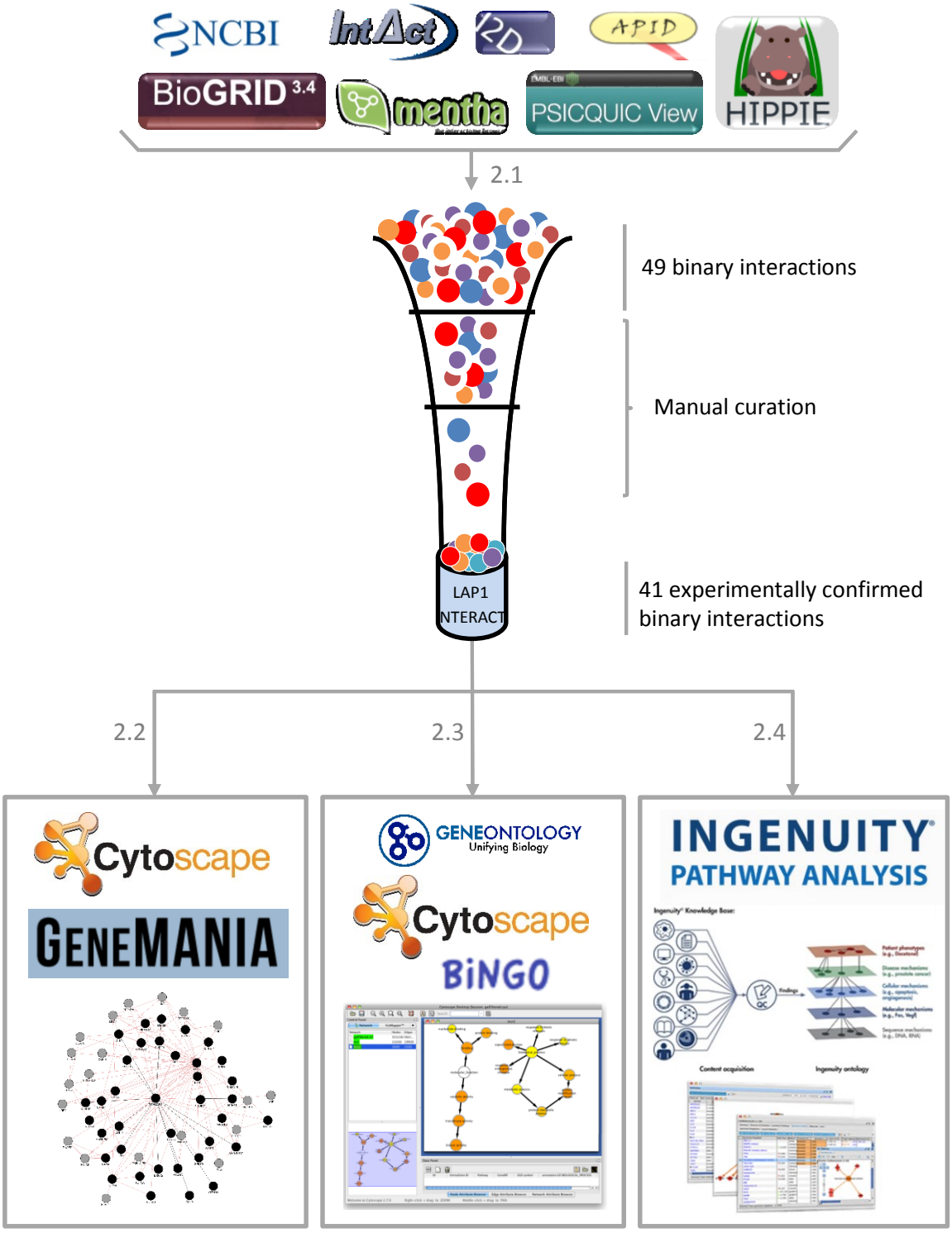

Figure II.1. Methods overview. Schematic representation of the workflow, the steps necessary to integrate the Network of LAP1 integrators are depicted.

2.3.1 LAP1 interactor's network

Having curated information retrieved from the set of online databases, all the experimentally tested interactions (Table 1) were loaded into Cytoscape 3.2.1[125] in order to manually build the network of LAP1 interactors (Figure II.2). Of these interactions, 36 were verified in human (grey), 1 in mouse and rat (blue), 1 only in rat (green) and 3 between human LAP1 and viral proteins (pink for HIV-1, red for HRSVA and orange for HHV-4). All the white nodes represent proteins, while RNA is denoted with yellow filling. Grey edges signify protein-protein interaction, while protein-RNA or RNA-RNA interactions are coloured in black (Figure II.2).

The bioinformatic analysis retrieved two RNA integrating interactions with LAP1. Of these, ELAVL1 is a RNA-binding protein that regulates the stability and translation of numerous mRNAs encoding proteins that respond to stress or proliferation[129]. ELAV-like protein 1 physically interacts with *TOR1AIP1* mRNA (Figure II.2), possibly promoting stability or influencing translation, in response to environmental changes[129]. Another identified RNA interaction was described for WHSC1, which is a histone methyltransferase (MMSET) that has a sequence for ACA11 within an intron of its gene[130]. ACA11 is an orphan box H/ACA class small nuclear RNA (snoRNA) that is localized to the nucleoli and integrates a new small nuclear ribonucleoprotein (snRNP) complex that is involved in post-splicing intron complexes[130]. This snRNP is proposed to target other snoRNAs intermediates, in particular, snoRNAs hosted within ribosomal protein genes and to bind various nucleolar proteins associated with the regulation of RNA processing[130]. Functionally, ACA11 was found to suppress oxidative stress, confer resistance to chemotherapy and increase the proliferation in multiple myeloma cells. In the work of Chu and colleagues[130], LAP1 was found to bind this snoRNA, both sharing binary interactions with HNRNPM, VIM, LMNA and LMNB1 (Figure II.2)[130]. Given the absence of additional functional studies on ACA11, the meaning of its associations with LAP1 and its interactors remains unclear. However, the emerging hypothesis is that LAP1 might be associated with transcription regulation through the interaction with ACA11 and HNRNPM (Figure II.2).

Moreover, a subset of viral proteins that integrates the LAP1 network, namely tat, 1C and LMP2 (Figure II.2) was also identified. Tat is a nuclear regulatory protein crucial for HIV-1 replication that also coordinates HIV-1 provirus transcriptional regulation[131]. Alternatively, RNA viruses like HRSV have limited coding capacity, and their proteins often possess multiple functional domains with the ability to interact either with viral or cellular proteins[132]. This is the case for 1C, which binds various human proteins that are associated with transcriptional and cell cycle regulation[132].

Lastly, Epstein–Barr virus LMP2B isoform colocalizes with LMP2A in perinuclear regions in transiently transfected cells[133], however LMP2 function in the NE remains unclear.

Due to the significant role of the NE as a cellular barrier, multiple viral organisms have developed the capability to modulate their permeability in order to infect the host cell (reviewed in [134]). Viruses can modulate NE permeability for different reasons. Some viruses disrupt NE in order to transport the viral genome into the nucleus for replication (HIV), while others cause NE disruption during nuclear egress of newly assembled capsids (HHV-4) (reviewed in [134]). In addition, many viruses modulate NE permeability either to destabilize compartmentalization of host proteins or to inhibit the nuclear transport of host antiviral response proteins (reviewed in [134]).

Table 1. LAP1 interactors obtained from online databases after manual curation of respective publications.

Gene	Protein	Uniprot Accession Number	Species	Interaction detection method	References
1C	Non-structural protein 1	P04544	*TOR1AIP1 Hs – 1C HRSVA*	Affinity Capture-MS	[132]
AIFM1	Apoptosis-inducing factor 1, mitochondrial	O95831	*Homo sapiens*	Affinity Capture-MS	[135]
ATM	Serine-protein kinase ATM	Q13315	*Homo sapiens*	Affinity Capture-MS	[136]
Atp1b4	Protein ATP1B4	Q99ME6	*Mus musculus*	Two-hybrid	[137]
		Q9R193	*Rattus norvegicus*	Affinity Capture-WB	
CA10	Carbonic anhydrase-related protein 10	Q9NS85	*Homo sapiens*	Affinity Capture-MS	[138]
CANX	Calnexin	P35564	*Tor1aip1 Mm - CANX Hs*	Affinity Capture-MS	[139]
CCDC8	Coiled-coil domain-containing protein 8	Q9H0W5	*Homo sapiens*	Affinity Capture-MS	[140]
EGFR	Epidermal growth factor receptor	P00533	*Homo sapiens*	Affinity Capture-MS	[141]
ELAVL1*	ELAV-like protein 1	Q15717	*Homo sapiens*	Affinity Capture-RNA	[129]
HNRNPM	Heterogeneous nuclear ribonucleoprotein M	P52272	*Homo sapiens*	Co-fractionation	[142]
HPDL	4-hydroxyphenylpyruvate dioxygenase-like protein	Q96IR7	*Homo sapiens*	Co-fractionation	[142]
KLHL15	Kelch-like protein 15	Q96M94	*Homo sapiens*	Affinity Capture-MS	[135]
LMNA	Prelamin-A/C	P48678	*Mus musculus*	Affinity Capture-MS	[143]
		P02545	*Homo sapiens*	Two-hybrid	[144]
			Homo sapiens	Reconstituted Complex	[39]

Gene	Protein	Uniprot Accession Number	Species	Interaction detection method	References
			Homo sapiens	Proximity Label-MS	[145]
Lmnb1	Lamin-B1	P70615	*Rattus norvegicus*	Affinity Capture-WB	[66]
LMP2	Latent membrane protein 2	Q1HVJ2	*TOR1AIP1 Hs - LMP2 HHV-4*	Affinity Capture-MS	[146]
LRRK2	Leucine-rich repeat serine/threonine-protein kinase 2	Q5S007	*Homo sapiens*	Affinity Capture-MS	[147]
Mad2l1	MAD2 mitotic arrest deficient-like 1	Q9Z1B5	*TOR1AIP1 Hs - Mad2l1 Mm*	Affinity Capture-MS	[139]
MAD2L1BP	MAD2 mitotic arrest deficient-like 1	Q15013	*Homo sapiens*	Affinity Capture-MS	[135]
MDM2	E3 ubiquitin-protein ligase Mdm2	Q00987	*Homo sapiens*	Affinity Capture-MS	[148]
NDUFV1	NADH dehydrogenase [ubiquinone] flavoprotein 1, mitochondrial	P49821	*Homo sapiens*	Co-fractionation	[142]
NIT2	Omega-amidase NIT2	Q9NQR4	*Homo sapiens*	Co-fractionation	[142]
NTRK1	High affinity nerve growth factor receptor	P04629	*Homo sapiens*	Affinity Capture-MS	[149]
NUP50	Nuclear pore complex protein Nup50	Q9UKX7	*Homo sapiens*	Co-fractionation	[142]
OXCT1	Succinyl-CoA:3-ketoacid coenzyme A transferase 1, mitochondrial	P55809	*Homo sapiens*	Co-fractionation	[142]
PPP1CA	Serine/threonine-protein phosphatase PP1-alpha catalytic subunit	P62136	*Homo sapiens*	Affinity Capture-WB	[150]
				Two-hybrid	[151]
PPP1CC	Serine/threonine-protein phosphatase PP1-γ catalytic subunit	P36873	*Homo sapiens*	Affinity Capture-WB	[150]
				Two-hybrid	[152]
PTCH1	Protein patched homolog 1	Q13635	*Homo sapiens*	Affinity Capture-MS	[138]
RIF1	Telomere-associated protein RIF1	Q5UIP0	*Homo sapiens*	Co-fractionation	[142]
SCARNA22*	small Cajal body-specific RNA 22	Gene ID: 677770	*Homo sapiens*	Affinity Capture-RNA	[130]
S100A16	Protein S100-A16	Q96FQ6	*Homo sapiens*	Co-fractionation	[142]
SEPT9	Septin-9	Q9UHD8	*Homo sapiens*	Co-fractionation	[142]
tat	Protein Tat	P04608	*TOR1AIP1 Hs - tat HIV- 1*	Affinity Capture-MS	[131]
TERF2	Telomeric repeat-binding factor 2	Q15554	*Homo sapiens*	Two-hybrid	[153]
TERF2IP	Telomeric repeat-binding factor 2-interacting protein 1	Q9NYB0	*Homo sapiens*	Two-hybrid	[153]

Gene	Protein	Uniprot Accession Number	Species	Interaction detection method	References
TOR1A	Torsin-1A	O14656	*Homo sapiens*	Affinity Capture-MS/WB	154 155 69 156 157
				Reconstituted Complex	157 156 157
				Affinity Capture-MS	67
TOR1AIP1	Lamina-associated polypeptide 1B	Q5JTV8	*Tor1aip1 Mm - TOR1AIP1 Hs*	Affinity Capture-MS	139
TOR1B	Torsin-1B	O14657	*Homo sapiens*	Affinity Capture-WB	67
TOR2A	Torsin-2A	Q5JU69	*Homo sapiens*	Affinity Capture-WB	67
TOR3A	Torsin-3A	Q9H497	*Homo sapiens*	Affinity Capture-WB	67
UBC	Polyubiquitin-C	P0CG48	*Homo sapiens*	Affinity Capture-MS	158 159 160 161 162 163
VIM	Vimentin	P08670	*Homo sapiens*	Affinity Capture-WB	164

* signify protein-RNA and ** represents RNA-RNA interactions. *Hs, Homo sapiens; Mm, Mus musculus; HRSVA, Human respiratory syncytial virus A (strain A2); HHV-4, Human herpes virus 4 (Epstein-Barr virus (strain AG876)); HIV-1, Human Immunodeficiency Virus 1;* MS, mass spectrometry; WB, western blot.

Figure II.2. LAP1 interactome built using Cytoscape 3.2.1[125]. Of these interactions, 36 were verified in human (grey), 1 in mouse and rat (blue), 1 only in rat (green) and 3 between human LAP1 and viral proteins (pink for HIV-1, red for HRSVA and orange for HHV-4). All the white nodes represent proteins, while RNA is denoted with yellow filling. Grey edges signify protein-protein interaction, while protein-RNA or RNA-RNA interactions are coloured with black edges. LAP1 is also able to form dimers, which is represented by a self-binding edge.

The mammalian proteins interactions were analysed in the next section with the support of GeneMANIA.

2.3.2 Network construction with GeneMANIA

In order to generate an extended protein-protein interaction network compiled by the set of proteins that were obtained previously, excluding RNA interactions and viral proteins, all the remaining binary interactions were imported to GeneMANIA[126]. Network mapping of LAP1 protein interactors was only possible by extrapolating the mouse and rat interactions to human. The version 3.4.0 of GeneMANIA[126] was installed into Cytoscape 3.2.1[125] enabling network editing and manipulation after output.

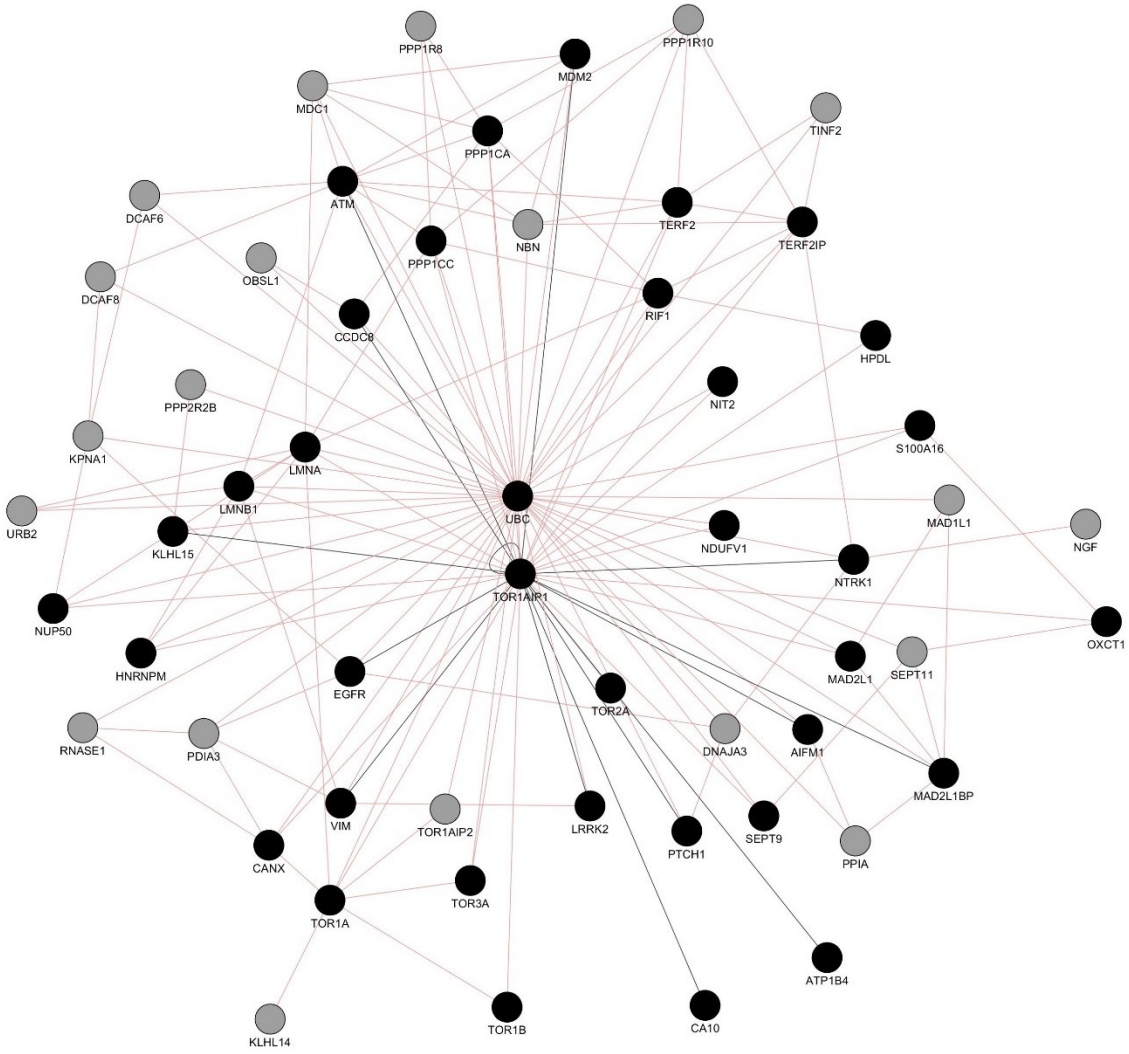

Figure II.3. LAP1 (*TOR1AIP1*) interactor's network complemented by the GeneMANIA plugin in cytoscape. Missing binary interactions to *TOR1AIP1* were added to the GeneMANIA output and are represented in black, while the remaining are in pink. Black nodes signify the interactors inserted into the plugin and grey nodes denote GeneMANIA's additional input. LAP1 is also able to form dimers, which is represented by a self-binding edge.

The set of gene IDs was introduced and the functional associative network was set to include only physical interactions between proteins. The output includes probable protein participants in the interactome of LAP1, extending the network based on a guilt-by-association approach that derives predictions from a combination of potentially heterogeneous data sources[126]. The resulting network represents a prospective LAP1 interactome (Figure II.3) that we propose to have functional relevance regarding its probable integrative role as a complex assembly or stabilization protein. For instance, LAP1 association with itself could be important to form dimers that provide a structural link between the nucleoskeleton (lamina) and cytoskeleton across the NE, as previously described for SUN domain proteins in the NE (reviewed in [34]).

The association between MAD2L1 and MAD2L1BP occurs in the mitotic checkpoint complex (MCC)[165], and both proteins have been proposed to physically bind LAP1 and MAD1L1[139] (Figure II.3). The MCC inhibits the anaphase-promoting complex/cyclosome (APC/C), which is an E3 ubiquitin ligase that initiates chromosome segregation[166]. This inhibition regulates the spindle assembly checkpoint (SAC) which is responsible for delaying chromosome segregation until all sister chromatids achieve bipolar attachment to the mitotic spindle, ensuring genome stability[166]. The experimental evidence of LAP1 direct interactions with MAD2L1 and MAD2L1BP reinforces the early preposition that LAP1 is a key regulator of mitosis[39,59], and strengthens the upcoming perspective that LAP1 might be functionally associated to the MCC.

Human LAP1B was previously described to be phosphorylated on Ser143, in a proline-directed manner similar to CDKs substrates[167], and on Ser164 within the ATM/ATR recognition sequence motifs[56]. Furthermore, rat LAP1B Ser142 (homologous to human LAP1B Ser143) was found to be phosphorylated by CDK1-cyclin B[168]. Indeed, LAP1 seems to be functionally associated with several signalling proteins that activate, inhibit and mediate signalling cascades. Among the most relevant regulators are protein kinases, in this case comprising EGFR, NTRK1, LRRK2 and ATM (Figure II.3). DNA damage events, such as ultraviolet irradiation, result in the nuclear translocation of EGFR, in a ligand-independent pathway[169]. Similarly, LAP1 phosphorylation by ATM on S133, S145, S169 and S164 was associated to DNA damage, consolidating the hypothesis that LAP1 might be phosphorylated as a cellular response to genotoxic stress[136].

Alternatively, protein phosphatases PP1α (*PPP1CA*) and PP1γ (*PPP1CC*) were shown to regulate LAP1 by dephosphorylation, forming a complex that was validated in rat brain and cultured cells[52]. This instance reveals the potential role of LAP1 bridging complexes for protein regulation through phosphorylation. Moreover, the PP1 regulatory protein CCDC8 (alternatively termed PPP1R20) is a core component of the 3-M complex. This complex is required to regulate MT dynamics and genome integrity[140]. Correspondingly, CCDC8 associates to the mRNA splicing machinery, in particular to the HNRNP family, which is highly represented in the 3-M interactome[140]. The above mentioned LAP1 mediated events illustrate the potential dynamic role of LAP1 in the regulation of transcription and cytoskeleton mechanisms through the interaction with CCDC8 (Figure II.3).

LAP1 might communicate to the shelterin complex, which is an emerging protein complex with DNA remodelling activity that coordinates with DNA repair factors to change the structure of the telomeric DNA, thereby protecting chromosome ends (reviewed in [170]). This complex is composed by TRF1 and TRF2 as double-stranded DNA binding proteins that recognize TTAGGG

repeats[153]. TRF2 in particular is associated to TERF2IP which is then regulated by RIF1 (reviewed in [170]). RIF1 is required for checkpoint mediated arrest in response to DNA damage during the S-phase (the intra-S-phase checkpoint)[171]. This checkpoint can be activated at least by 2 parallel pathways involving the ATM kinase[171]. LAP1 might have a role in assembly or stabilizing this particular subset of proteins of the shelterin complex, as it binds to TRF2, TERF2IP, RIF1 and ATM (Figure II.3). Telomere associated functions have been previously described for various INM proteins such as LMNA, SUN1, LAP1 and BAF (reviewed in [35]).

The relevance of LAP1 interactions regarding biological processes and cellular localizations were analysed in the next section with the support of GO enrichment analysis[124] and BiNGO[128].

2.3.3 GO term enrichment analysis

The online GO Consortium term enrichment service, supported by Panther (available at http://geneontology.org/)[123,124], was used to conduct a GO term enrichment analysis for the 38 LAP1 interactors described in table 1, excluding viral connections (tat, 1C and LMP2). In this instance, *biological process* and *cellular component* GO terms that were enriched among these target proteins were sought (Figure II.4). All the IDs of the interactors were mapped with one exception, SCARNA22.

BiNGO[128] was alternatively used to build a directed acyclic graph (DAG) network that conveys visualization of the enriched terms organized in a tree-like structure, starting from more general terms at the root (for example, biological regulation) to the most specific at the leaves (for example, the regulation of mitotic cell cycle)[128]. Each term is coded by size and colour, so that larger nodes contain more genes and darker nodes are more significantly enriched. Insignificant intermediate terms are denoted as small white nodes[128] (Figures S1 and S2).

Examining the biological processes of the proteins found in the filtered list of interactions (Figure II.4A and S1), significant enrichment was observed in the processes of regulation of response to DNA damage stimulus, nuclear membrane organization, nuclear envelope organization, cell cycle, chaperone mediated protein folding requiring cofactor, chaperone-mediated protein folding, nucleus organization, telomere maintenance, cellular component organization, telomere organization and cellular component disassembly involved in execution phase of apoptosis. Analysing the cellular component that the protein interactors might integrate (Figure II.4B and S2), significant and relevant enrichment was found in the nuclear envelope, chromosomal region, endoplasmic reticulum lumen, chromosome and telomeric region and lamin filament.

This output reinforces the idea that LAP1 might function as a stabilizing element upon the formation of multiple complexes as noted before. In particular, integrating a response to DNA damage by ATM activation and subsequently participating in telomere regulation as a result, through the interaction with RIF1, TERF2IP and TRF2[171]. Furthermore, there are strong evidences that LAP1 intervenes in mitotic regulation via association to MCC complex proteins, as previously studied[39]. The vastly documented relationship with the Torsin family[172], resident in the endoplasmic reticulum, conveys the chaperone related annotations observed in the enrichment analysis. Finally, LAP1 collaboration with the NE cytoskeleton[39,172] outputs nuclear membrane organization, nuclear envelope organization, cellular component organization and nucleus organization, as some of the most prominent biological processes attributed to LAP1.

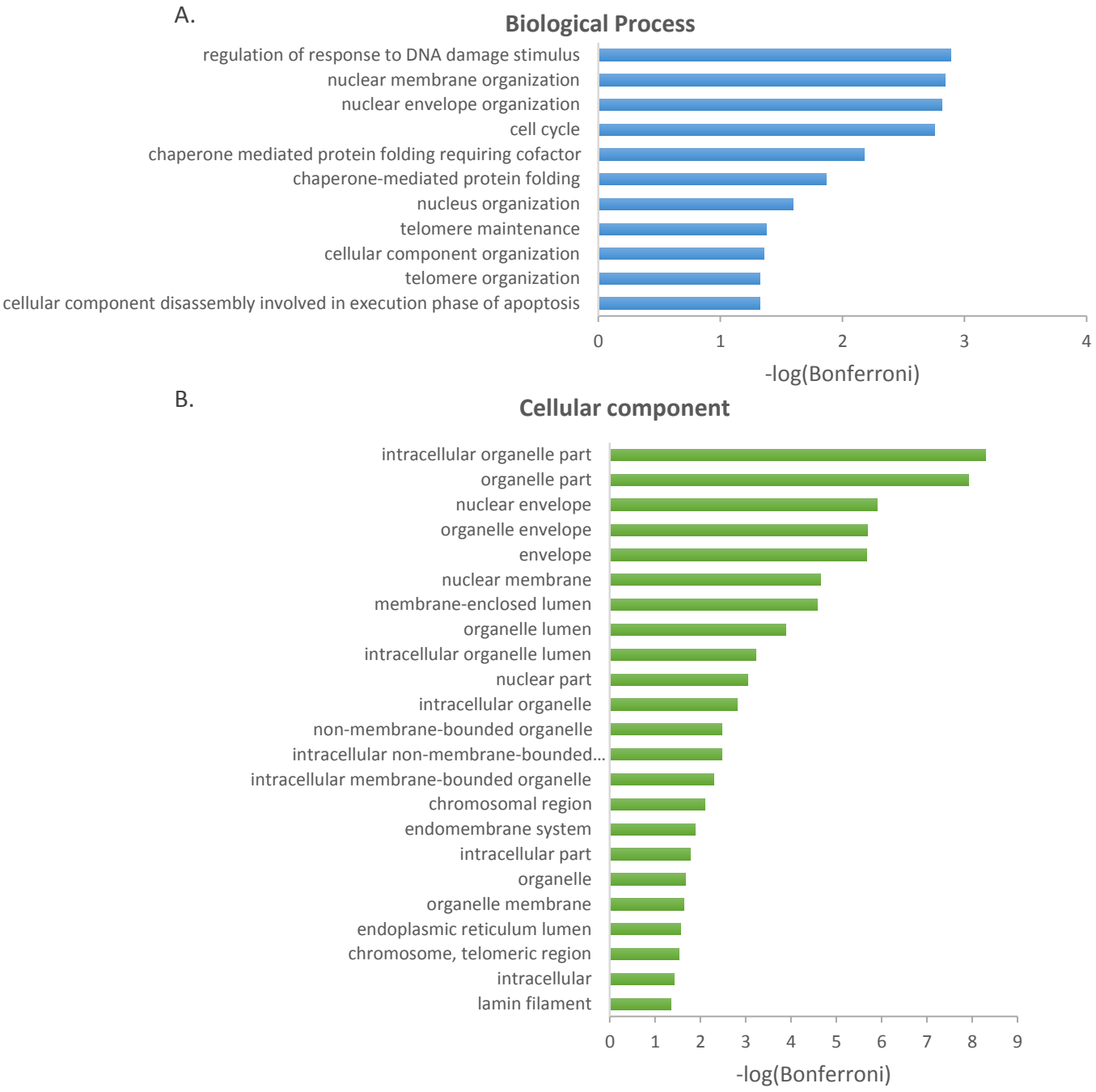

Figure II.4. Significantly enriched Gene Ontology terms from LAP1 interaction network. (A) Biological process and **(B)** Cellular Component. Bonferroni corrected p-values ($\alpha = 0.05$) were transformed by -log10.

Physiological and functional analysis of the pathways which LAP1's interactome integrates is discussed in the next section resorting to Ingenuity Pathway Analysis.

2.3.4 IPA physiological and functional analysis

Gene identifications of the previously described interactors were imported into the IPA software, once more extrapolating the mouse and rat interactions to human and excluding viral connections. Function classifications, signal pathways and interacting networks were constructed and analysed based on the underlying biological evidence from the IPA's database. The core analysis performed in IPA retrieved seven distinctive functional sets: canonical pathways, upstream regulators, diseases and disorders, molecular and cellular functions, physiological system development and functions, associated network functions and toxicological lists that are depicted in Tables II.2-II.6 and Figures II.5, S3-S6. Right-tailed Fisher's exact test was used to calculate the significance of each biological function and/or disease assigned, which was reported if the adjusted p-value was below a significance threshold of 0.05.

IPA reinforced the idea that LAP1 might be communicating with the shelterin complex, as it is evident in Table 2, where the top two canonical pathways include "Telomerase signalling" and "Telomere Extension by Telomerase". Furthermore, IPA analysis of physiological system development and function identified "Skeletal and Muscular System Development and Function" as the most relevant (Table 3). This result is in accordance with the previous described functions of LAP1 regarding its association with the Torsin family[172].

Regarding the rank for associated networks in table 4, the analysis is not strict to molecular interactions. The result delivered the most pertinent functions of LAP1 interactors, which is attributed to "Cell Morphology, Cellular Assembly and Organization, DNA Replication, Recombination, and Repair" (Figure II.5).

Additionally, IPA retrieved BRAC1 as the most probable upstream regulators of LAP1's interactome (Figure S3). This inference is in accordance with the regulation of important intervenients of the proposed network for LAP1 interactors (Figure S3), namely EGRF and ATM concerning DNA damage events and MAD2L1 which might be activated for mitosis regulation with the MCC. Furthermore, table 5 confirms this hypothesis with the identification of "Cell Cycle: G2/M DNA Damage Checkpoint Regulation" and "Cell Cycle: G1/S Checkpoint Regulation" as top toxicological attributes.

Lastly, IPA's analysis of molecular and cellular functions attributed to LAP1's interactome (Table 6) acknowledges "Cell Morphology" and "Cellular Assembly and Organization" as the most pertinent, followed by "DNA Replication, Recombination, and Repair", "Cell Cycle" and "Cell Death and Survival". The networks describing and integrating these functions are available in the supplementary figures S4 and S5. By studying these interactions it is possible to deduce the

interconnected pathways in which LAP1 might participate, unfolding its crucial role regulating nuclear morphology, cell cycle progression and cell survival.

Table 2. Top canonical pathways for LAP1 interactors' dataset.

Name	p-value	Overlap %	Overlap
Telomerase Signalling	2.99E-05	4.00%	4/99
Telomere Extension by Telomerase	3.28E-04	13.30%	2/15
HER-2 Signalling in Breast Cancer	3.47E-04	3.90%	3/76
Glioma Signalling	6.68E-04	3.20%	3/95
Huntington's Disease Signalling	7.49E-04	1.70%	4/229

* Overlap represents the percentage of LAP1 interactors integrated in the total number of proteins associated to each specific pathway on the IPA Knowledge Base.

Table 3. Physiological System Development and Function for LAP1 interactors dataset.

Name	p-value	#Molecules
Skeletal and Muscular System Development and Function	3.61E-03 - 1.82E-06	7
Tissue Development	3.61E-03 - 1.82E-06	13
Nervous System Development and Function	3.61E-03 - 3.93E-06	13
Organ Morphology	3.61E-03 - 3.93E-06	9
Tissue Morphology	3.61E-03 - 3.93E-06	16

Table 4. Top Associated Networks for LAP1 interactors dataset.

ID	Associated Network Functions	Score
1	Cell Morphology, Cellular Assembly and Organization, DNA Replication, Recombination, and Repair	47
2	Cancer, Organismal Injury and Abnormalities, Respiratory Disease	32
3	RNA Post-Transcriptional Modification, Protein Synthesis, Gene Expression	3
4	Developmental Disorder, Neurological Disease, Behaviour	2

* Score attributes a numerical value used to rank networks according to how relevant they are to the genes in the input dataset.

Table 5. Top Toxicological Lists for LAP1 interactors dataset.

Name	p-value	Overlap %
Hypoxia-Inducible Factor Signalling	2.72E-04	4.3 % 3/70
Mitochondrial Dysfunction	3.90E-03	1.7 % 3/176
Cell Cycle: G2/M DNA Damage Checkpoint Regulation	3.97E-03	3.8 % 2/52
Cell Cycle: G1/S Checkpoint Regulation	6.32E-03	3.0 % 2/66
TR/RXR Activation	1.03E-02	2.4 % 2/85

* Overlap represents the percentage of LAP1 interactors integrated in the total number of proteins associated to each specific pathway on the IPA Knowledge Base.

Table 6. Molecular and cellular functions for LAP1 interactors dataset.

Name	p-value	#Molecules
Cell Morphology	3.61E-03 - 3.18E-11	18
Cellular Assembly and Organization	3.61E-03 - 3.18E-11	20
DNA Replication, Recombination, and Repair	3.61E-03 - 1.34E-10	15
Cell Cycle	3.61E-03 - 9.17E-09	17
Cell Death and Survival	3.61E-03 - 4.21E-07	20

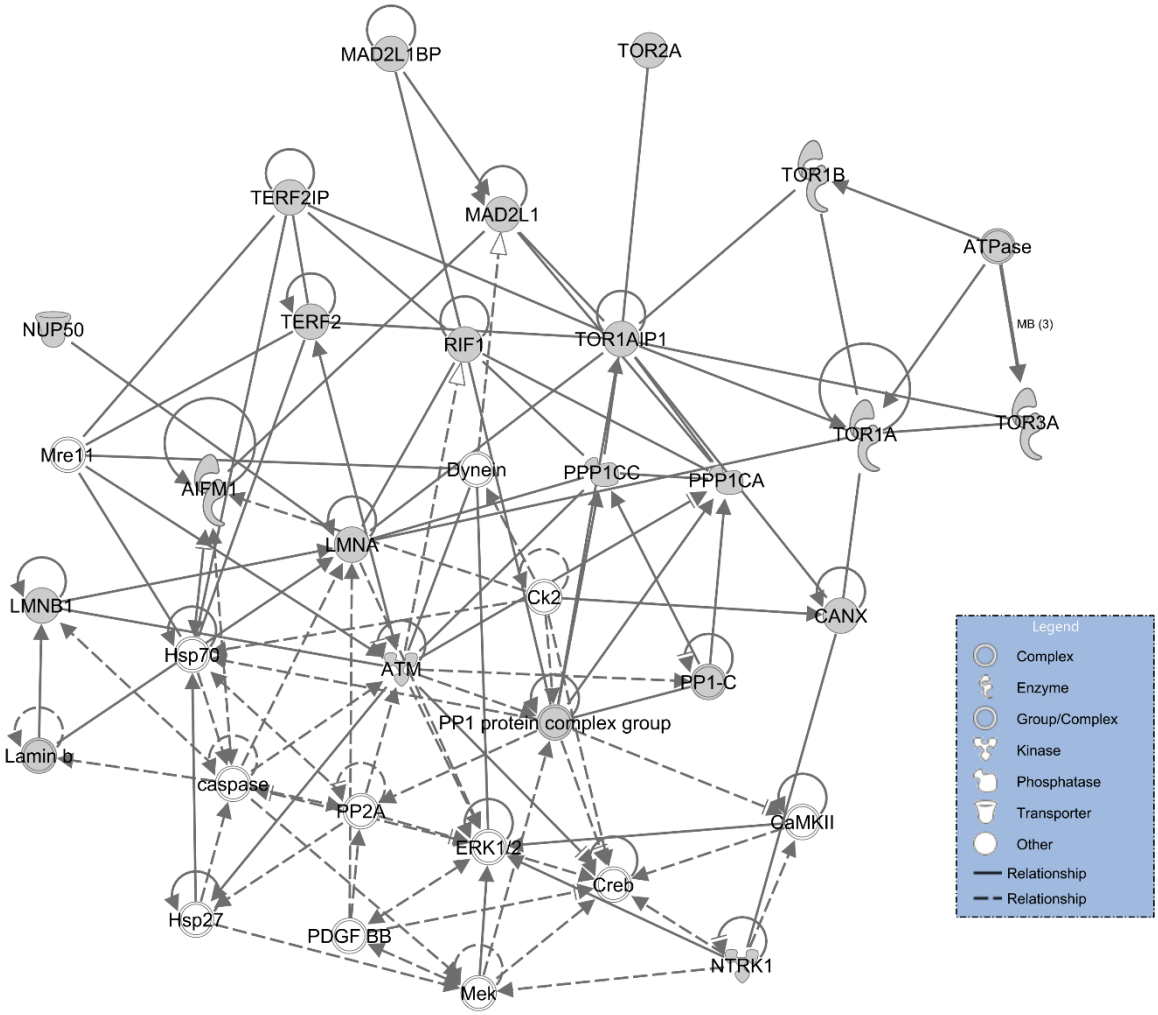

Figure II.1. Network ID 1. IPA Associated Network Functions: Cell Morphology, Cellular Assembly and Organization, DNA Replication, Recombination, and Repair. Grey nodes represent proteins that are integrated in the initial dataset, while white nodes convey IPA's supplementary missing proteins.

Ingenuity pathway analysis confirmed the hypothesis that LAP1, besides the functional associations with lamins and nuclear morphology, might be a crucial intervenient in cell cycle progression and DNA damage responses. These conclusions are in accordance with our prior analysis performed with GO and GeneMANIA.

2.4 CONCLUSIONS

The integration of multiple bioinformatic tools allowed the development of an intricate study of LAP1 interactors. These analyses attribute functions to LAP1 that have not been previously described. For instance, various DNA damage response proteins that incorporate or regulate the shelterin complex were shown to directly interact with LAP1. This function has been previously associated with INM proteins such as LMNA, SUN1, LAP1 and BAF. Additionally, the previously described association of LAP1 with mitosis was confirmed through the interaction with MCC. Therefore, these and other prospective functions of LAP1 convey the significant role of INM proteins in the regulation of multiple cellular processes and disease conditions.

2.5 SUPPLEMENTARY DATA

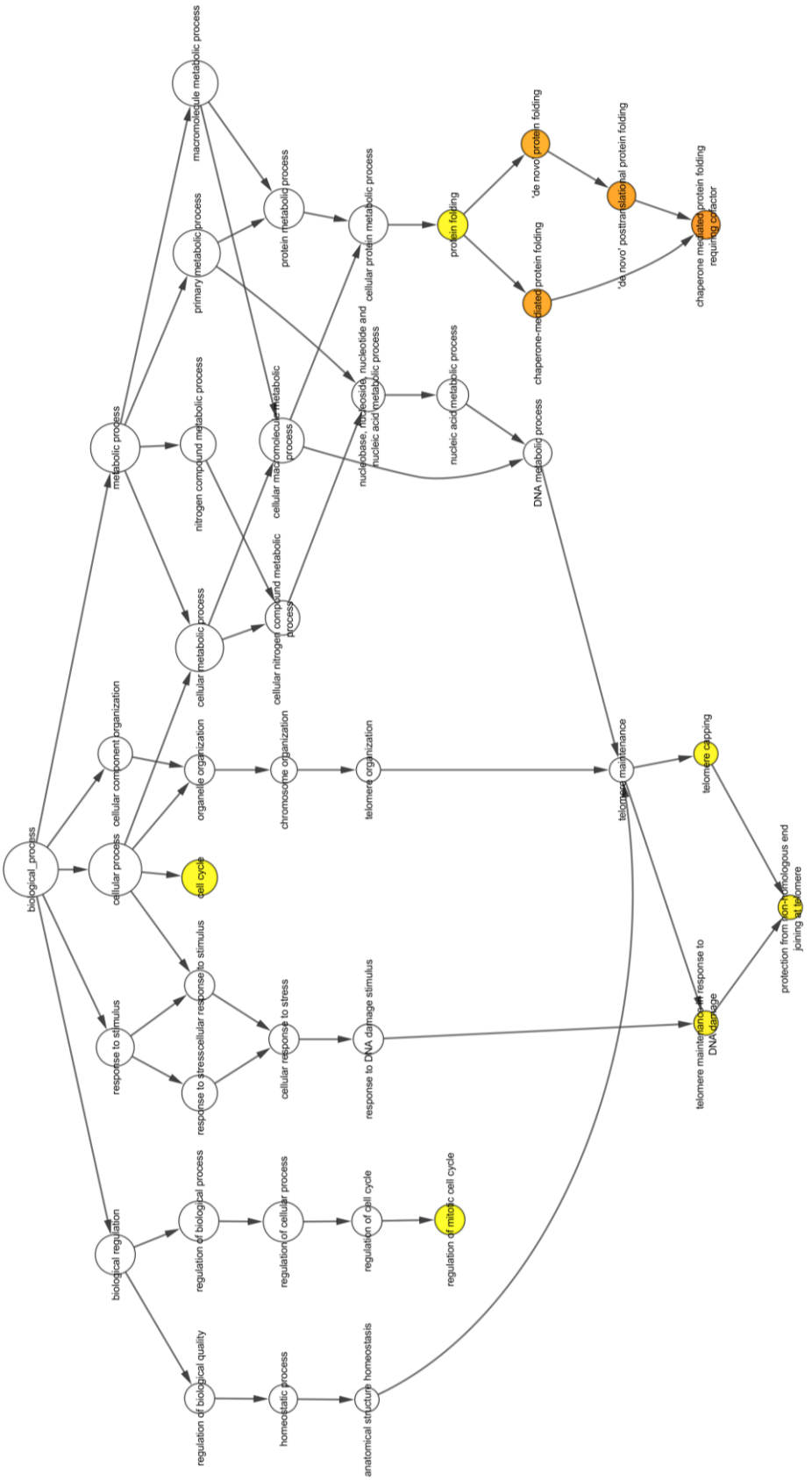

Figure S1: Significantly enriched Gene Ontology terms from LAP1 interaction network concerning Biological Processes. Directed acyclic graph (DAG) network of the enriched terms organized in a tree-like structure, starting from more general terms at the root (for example, biological regulation) to the most specific at the leaves (for example, the regulation of mitotic cell cycle) [72]. Each term is coded by size and colour, so that larger nodes contain more genes and darker nodes are more significantly enriched. Insignificant intermediate terms are denoted as small white nodes [72]. Bonferroni corrected p-values ($\alpha = 0.05$).

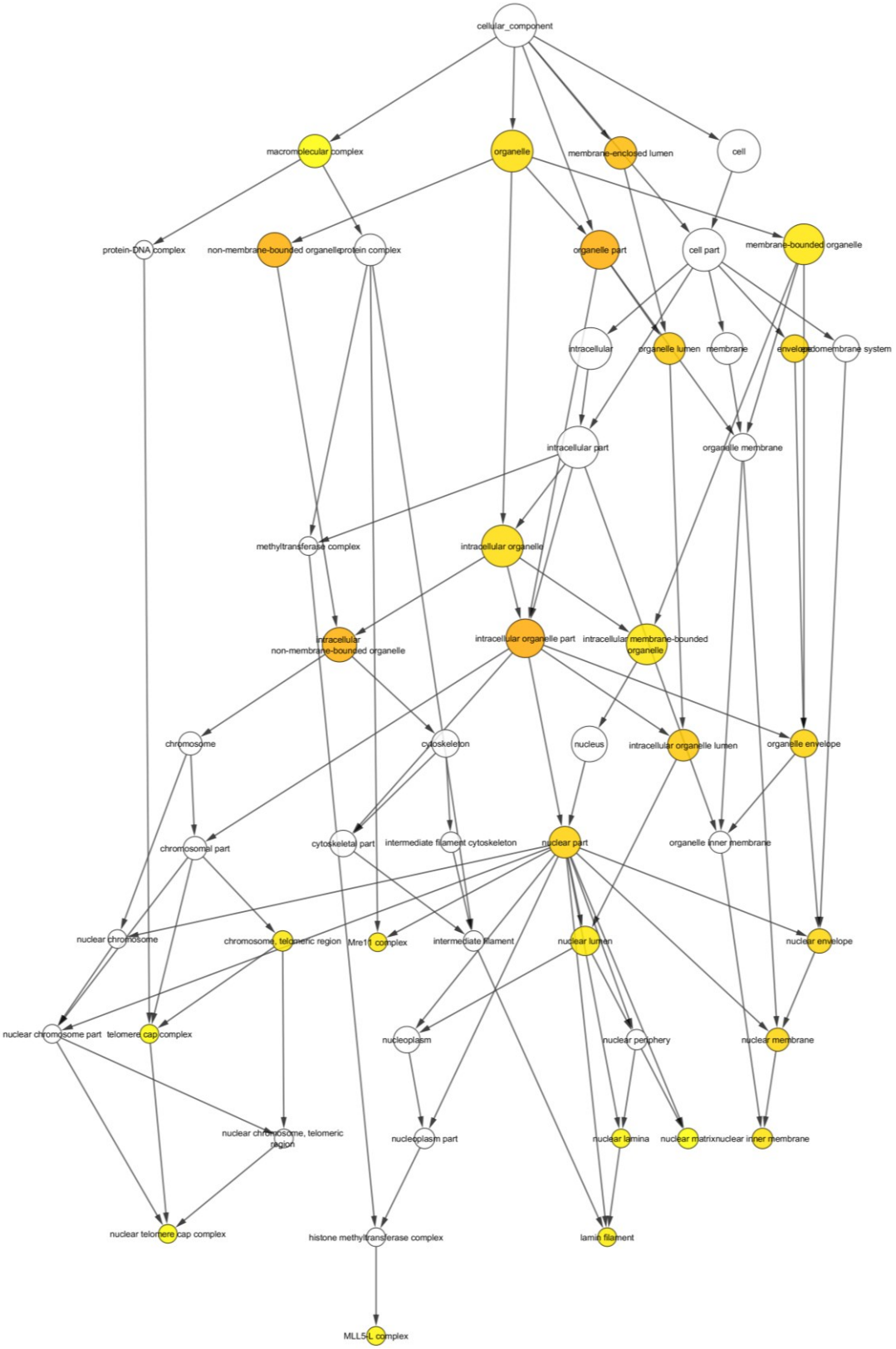

Figure S2. Significantly enriched Gene Ontology terms from LAP1 interaction network concerning Cell Components. Directed acyclic graph (DAG) network of the enriched terms organized in a tree-like structure, starting from more general terms at the root (for example, macromolecular complex) to the most specific at the leaves (for example, nuclear telomere cap complex) [72]. Each term is coded by size and colour, so that larger nodes contain more genes and darker nodes are more significantly enriched. Insignificant intermediate terms are denoted as small white nodes [72]. Bonferroni corrected p-values ($\alpha = 0.05$).

A.

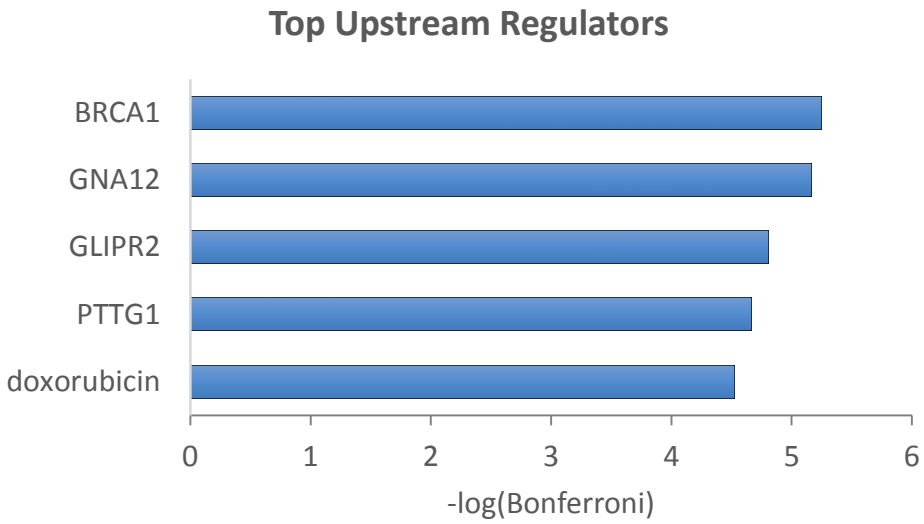

B.

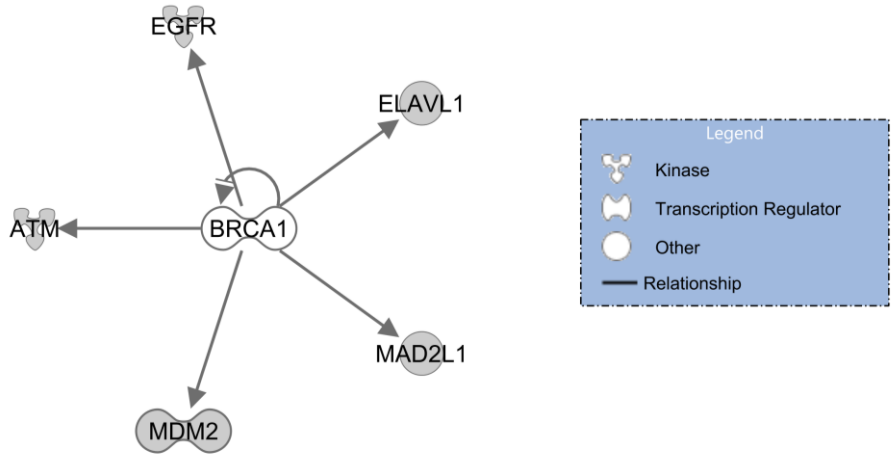

C.

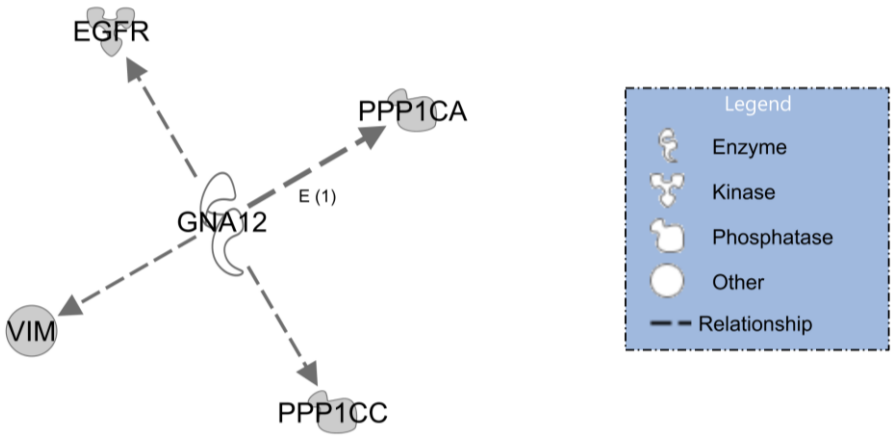

Figure S3. Top Upstream Regulators of LAP1 interactome. IPA retrieved BRAC1 as the most probable upstream regulators of LAP1's interactome, followed by GNA12, GLIPR2, PTTG1 and doxorubicin. Networks for BRAC1 (B) and GNA12 (C) are represented.

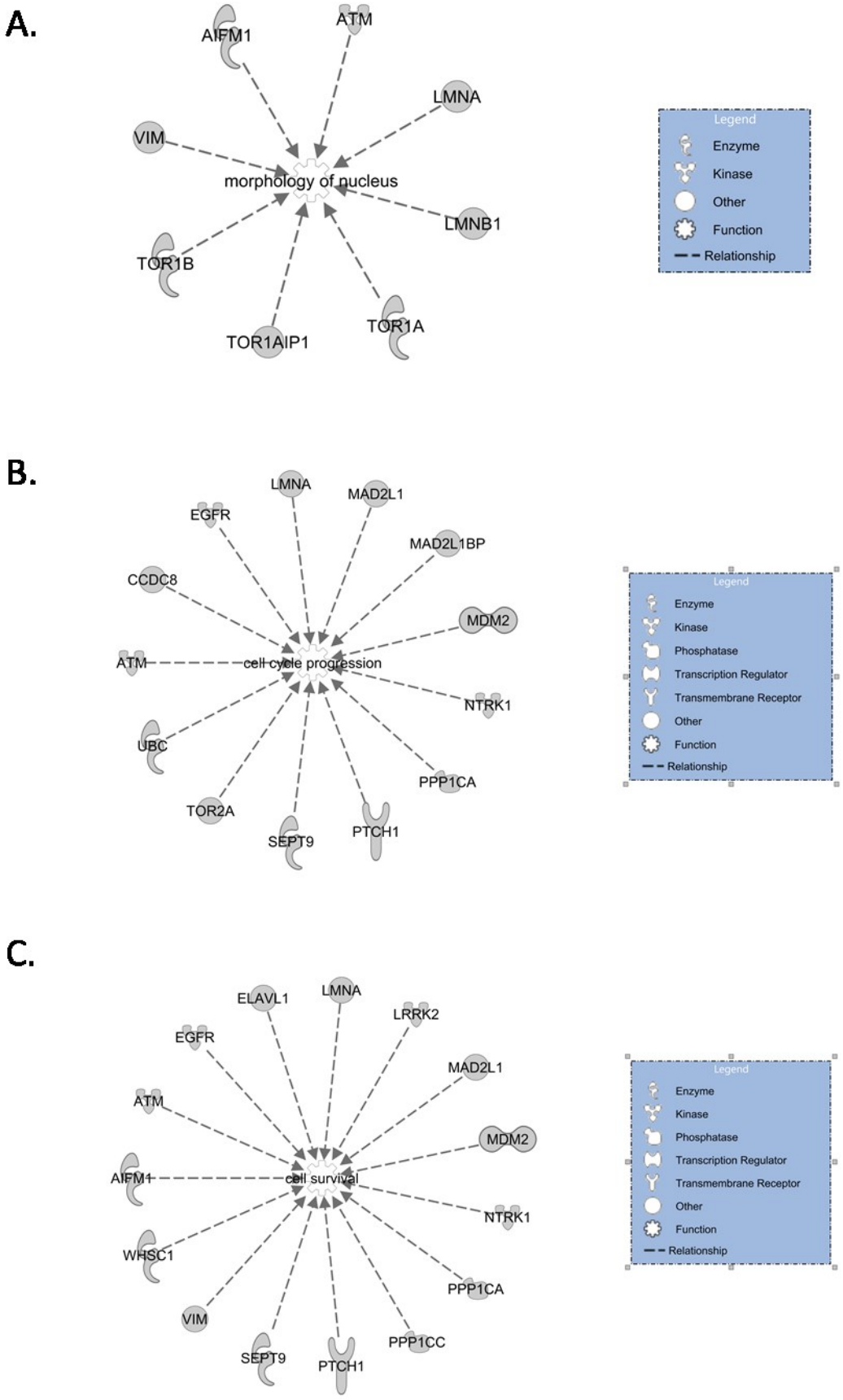

Figure S4. Molecular and cellular functions associated with LAP1 interactors. Singular networks relating morphology of the nucleus (A), cell cycle progression (B), and cell survival (C) to each associated member of LAP1 interactome.

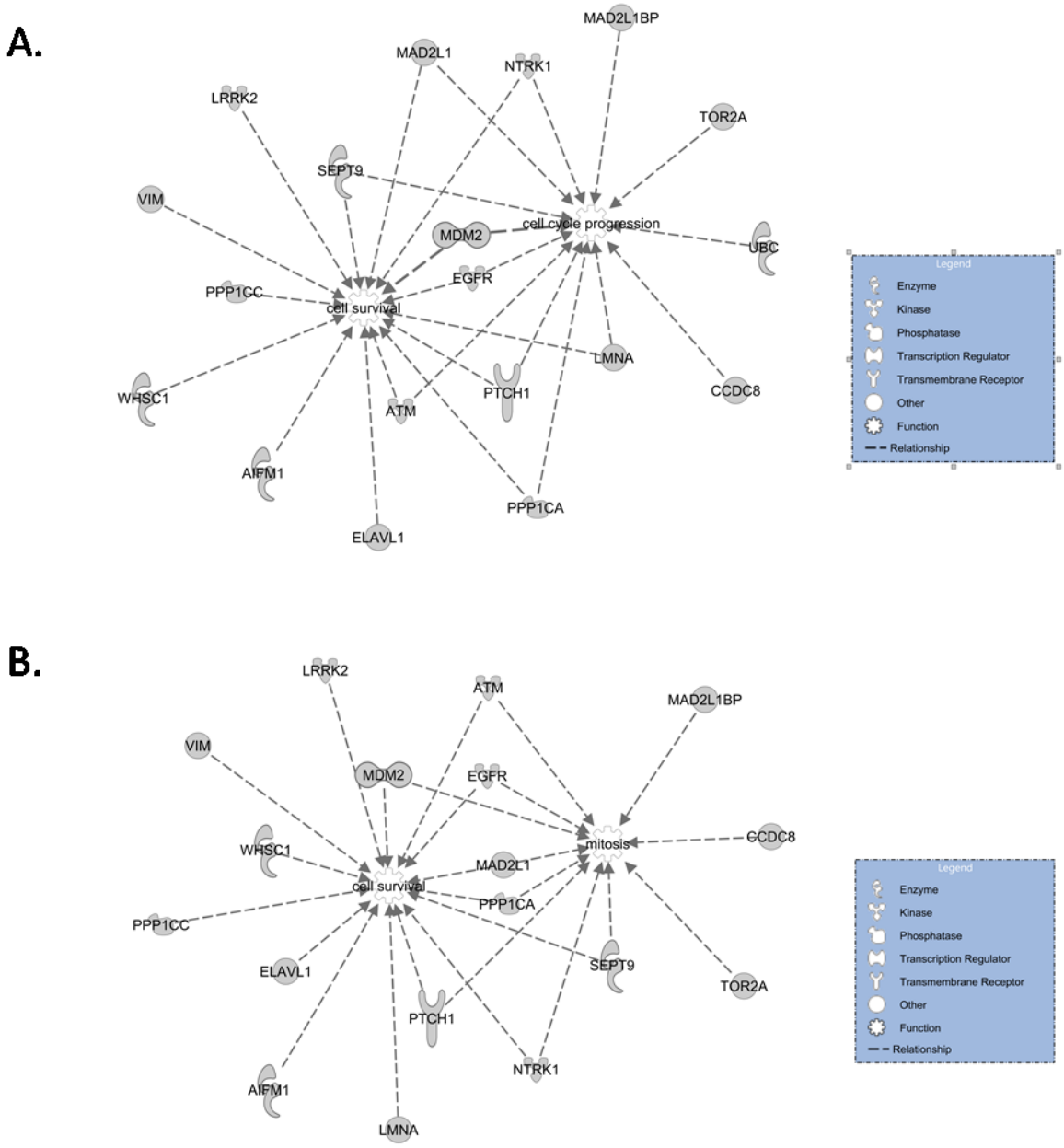

Figure S5. Merged molecular and cellular functions associated with LAP1 interactors. Integrated networks relating cell cycle progression and cell survival (A) or cell survival and mitosis (B) to each associated member of LAP1's interactome.

CHAPTER III – LAP1 AND ITS INTERACTORS IN THE MALE REPRODUCTIVE SYSTEM

LAP1 was one of the first lamin associated proteins identified[40], however its physiological function remains poorly understood. Interestingly, LAP1 is probably involved in the regulation of the NE structure and mitosis progression, processes that share functional elements with spermatogenesis. Therefore the work described in chapter III provides particular insights with respect to the localization of LAP1 and some of its interactors during the spermatogenic cycle. The results presented in this chapter provide a basis for future studies and will be submitted for publication in a manuscript entitled: “Analysis of LAP1 and its interactors throughout spermatogenesis”.

3.1 INTRODUCTION

Spermatogenesis is a highly complex and particular process of differentiation, which implicates germ-cell proliferation and renewal, meiosis, and spermiogenesis under the regulation of Sertoli cells. Through this process of differentiation, cells undergo complex morphological and biochemical transformations that lead to the formation of highly specialized cells, the haploid sperm[81]. In the proliferation phase, spermatogonia undergo several mitotic divisions to form spermatocytes which undergo two meiotic divisions to form haploid spermatids. The latter develop into sperm as a result of a complicated metamorphosis involving dramatic structural modifications to the shape of their nucleus, compaction of their nuclear chromatin, formation of an acrosome, and establishment of a flagellum permitting eventual motility (reviewed in [77,78,80]). After leaving the seminiferous tubules, sperm is stored along the epididymis and go through maturation. Ejaculation follows with sudden activation of their motility. Then, in the female genital tract, especially during the ascension towards the ovary through the uterus and fallopian tube, the sperm experience capacitation. Finally, acrosome reaction occurs in the immediate vicinity of the oocyte[173].

In mice, germ spermatogenic cells are characterized according to the presence and distribution of heterochromatin: undifferentiated type A spermatogonia; differentiated type A spermatogonia; intermediate spermatogonia; and type B spermatogonia[84,85]. Sequentially, B-spermatogonia divide by mitosis forming two preleptotene spermatocytes, representing the beginning of meiotic prophase[86]. Preleptotene rest on the basement membrane, but the following leptotene, zygotene and pachytene spermatocytes become transit and move through the Sertoli-Sertoli barrier[86]. Preleptotene, leptotene and zygotene spermatocytes are located in specific stages and are identifiable by routine microscopy, although fixation artefacts might wrongfully lead to the observation of these cells attached to the basement membrane. Meiotic cell division occurs in stage XII and comprises three phases: meiosis I, the division of diplotene (2n); formation of secondary spermatocytes (2n), which are larger than spermatids, but rarely are found as the only spermatocyte in a tubular cross section; and meiosis II, the division of secondary spermatocytes (2n) to form haploid (1n) round spermatids (reviewed in [75]). The total duration of spermatogenesis, from the stem cell to the mature spermatid, is approximately 35 days (reviewed in [81]).

Differently, in human, germ cells have a rather different terminology, namely: type A-dark spermatogonia; type A-pale spermatogonia; B-spermatogonia; preleptotene, leptotene, zygotene, pachytene, and diplotene spermatocytes; secondary spermatocytes; spermatids; and sperm. Spermatogonial proliferation and differentiation involve only A pale-spermatogonia, since A dark

spermatogonia do not show proliferating activity under normal circumstances and are believed to divide only rarely. Indeed, A pale-spermatogonia divide and differentiate into two B spermatogonia, which in turn, divide to form preleptotene spermatocytes. Meiosis of spermatocytes includes the last synthesis of DNA in preleptotene spermatocytes and 2 meiotic divisions to form spermatids. Then, spermiogenesis results in the transformation of a round spermatid to an elongated mature spermatid. Finally, spermiation occurs when the structures and connections anchoring a mature spermatid to a Sertoli cell disrupt, so that sperm is released into the tubule lumen. In humans, the interval between commitment of an A pale-spermatogonium to proliferate and spermiation of resulting maturated spermatid averages 74 days (reviewed in[77,80]).

Interestingly to this study are morphological changes that occur in spermiogenesis. This process includes four crucial phases: Golgi, capping, acrosomal, and maturation (reviewed in [79]). Together, these highly heterogeneous phases enable the identification of specific stages in the cycle of the seminiferous epithelium. Firstly, spermatids have a small, perinuclear Golgi region without an acrosomic vesicle or granule. Then, proacrosomal vesicles and granules within the Golgi apparatus culminate in the formation of a single, large acrosomal granule within a greater vesicle that will indent the nucleus. Capping in round spermatids is characterized by the association of the acrosomic granule to the nuclear envelope and by flattening of this vesicle into a small cap over the nuclear surface. Later on, the acrosomic vesicle becomes very thin and the granule flattens. Finally the acrosome flattens completely over approximately 1/3 of the nuclear surface, and shaping of the nuclei begins. Acrosomal steps include migration of the acrosomal system over the ventral surface of the elongating spermatid nucleus. The morphological changes in spermatids also involve condensation of the chromatin, as the chromosomes are packed more tightly and stain more intensely. Maturation displays fewer changes in nuclear shape and acrosomal migration. The nucleus continues to condense and the acrosome matures into a thin structure that protrudes at the apex but covers nearly all the nucleus, except for the portion connected to the tail. Excess cytoplasm is then removed, resulting in the formation of prominent cytoplasmic lobes and residual bodies, which contain unused mitochondria, ribosomes, lipids, vesicles and other cytoplasmic components (reviewed in [75,79,87]).

Relevant to this study are evident changes that the nuclear envelope undergoes in the course of spermiogenesis. Throughout the nuclear shaping and condensation processes, excess nuclear membrane is eliminated into the posterior cytoplasm in the form of two continuous sheets at either side of the implantation fossa (region where the centrioles connect to the NE). These modifications are accompanied by concentration of stacked lamellae along the posterior margin of the NE,

nuclear blebbling, and concentration of nuclear pores to the post-acrosomal region. All these morphologic changes seem to be associated with the loss of nuclear contents during the gradual reduction in nuclear volume (reviewed in [81,90]).

The role of nuclear envelope components has been investigated in relation to the various phases of spermatogenesis. Importantly, lamins, LAP2, LBR, and elements of the LINC complex are amongst nuclear envelope proteins with more prominent associations to multiple functions in the spermatogenic cycle[91–97]. In spite of being one of the first lamin associated proteins identified[40], the physiological functions of LAP1 remain poorly understood. Interestingly, LAP1 has been described to be involved in the regulation of the NE structure and mitosis progression[59], both processes that share functional elements with spermatogenesis. A previous study of the expression of LAP1 in various human tissues concluded that this protein is differentially present. In fact, testis appeared to have a quite equivalent amount of LAP1B and LAP1C isoforms when compared to other tissues[49].

LAP1 interactors analysed in this work include lamin A/C, Lamin B1, PP1, and torsinA. Most of these proteins have been previously studied throughout spermatogenesis except for torsinA. Lamins have been associated with meiotic chromosome dynamics and with morphological flexibility of the nucleus which would be required for nuclear reshaping after meiosis[93,104]. PP1 is a ubiquitous serine/threonine phosphatase, estimated to dephosphorylate about a third of all proteins in eukaryotic cells. In mammals there are four PP1 isoforms: PP1α, PP1β/δ and the splice variants PP1γ1 and PP1γ2. They possess specific distinct tissue and subcellular distributions: PP1α, PP1β/δ and PP1γ1 are widely expressed across mammalian tissues, particularly in brain and PP1γ2 is testis enriched[174]. PP1 isoforms expression profiles in spermatogenesis varies between cell types of the adult mice testis. In detail, PP1γ2 is the only isoform present in abundance in secondary spermatocytes, round spermatids, and elongating spermatids, whereas for the most part, PP1γ1 and PP1α expressions are restricted to spermatogonia, pachytene spermatocytes, and somatic cells[175,176]. TorsinA is a member of the AAA+ superfamily of adenosine triphosphatases (ATPases associated with a variety of cellular activities). AAA+ proteins participate in numerous functions, including vesicle fusion, cytoskeleton dynamics, intracellular trafficking, protein folding and degradation and organelle biogenesis[177]. Mutations in the *DYT1* gene are associated with dystonia and with the colocalization of torsinA with LAP1 in the NE[69].

Interestingly, the localization of LAP1 in the mitotic spindle, mid-body and centrosomes strongly suggests a functional association between LAP1 and these cell cycle related components. Specifically, LAP1 colocalizes with γ-tubulin in centrosomes at metaphase and anaphase during mitosis. Furthermore, LAP1 depletion seems to be correlated with the altered centrosome

positioning and a decrease in the number of mitotic cells[59]. Therefore, due the functional association of LAP1 in the organization of the mitotic spindle during mitosis[55,59] the distribution of γ-tubulin in the spermatogenic cycle was also analysed. So, we proposed to examine the localization of LAP1 and some of its interactors during the spermatogenic cycle, in order to investigate the feasible role of this NE protein in the differentiation of germ cells into sperm.

3.2 EXPERIMENTAL SECTION

3.2.1 Patient Material and Ethical Approval

For IHC, testicular material was donated after oral informed consent by four patients undergoing bilateral orchidectomy as part of prostate cancer treatment (patients URO0179, URO0368, URO0059 and URO0126). According to Dutch law, approval of the ethics committee was not required, because anonymized tissue samples were used. None of the patients had previously received chemotherapy or radiotherapy, and the morphology of the testes showed normal spermatogenesis in all cases. Testis biopsies were fixated in 4% paraformaldehyde (PFA) or dilluted Bouin solution and embedded in paraffin. All the biopsies and following procedures were performed according to regulations from the Academic Medical Centre, in Amsterdam.

Fresh sperm samples were obtained from patients undergoing routine semen analysis or fertility treatments in the Human Reproduction Service at University Hospitals of Coimbra. Patients signed informed consent forms and the samples were used in accordance with the appropriate Ethical and Internal Review Board of the participating institution. Sperm samples were obtained by masturbation after 3-5 days of sexual abstinence and routine seminal samples analysis was performed according to the World Health Organization guidelines (WHO)[178]. All the samples used in this study had no detectable leukocytes (or any other round cells). After liquefaction, sperm cells were prepared by direct swim-up and allowed to capacitate in a supplemented Earl's balance salt solution (sEBSS) for at least 3 hours at 37°C under 5% CO_2/95% air before starting the experiments. Acrosome reaction (AR) was induced by incubating capacitated sperm with 1mM calcium ionophore A23187 (Sigma-Aldrich) for 1 hour at 37°C.

3.2.2 Animals

Previously obtained paraffin-embedded surplus testes of 8 to 10 weeks old Balb/c mice were used for IHC. The animals were used and maintained according to regulations provided by the animal ethical committee of the Academic Medical Center, Amsterdam.

3.2.3 Cell culture

An immortalized cell line was used to study the localization of LAP1 in spermatogonia. Namely, the CG-1 spg (ATCC® CRL 2053™) cell line derived from postnatal day 10 mouse testis. This cell line has been described as an intermediate spermatogenic cell type between type B spermatogonia and primary spermatocytes. GC-1 cells were maintained in Dulbeco's Minimum Essential Media (DMEM; Gibco) supplemented with 10% fetal bovine serum (FBS) (Gibco) and 100 U/mL penicillin and 100 mg/mL streptomycin (Gibco). Cultures were maintained at 37°C under 5% CO_2. Cells were subcultured whenever 80-90% confluence was reached.

3.2.4 Antibodies

Several primary antibodies were used to detect multiple proteins analysed in the experimental procedures of the dissertation, namely anti-LAP1, anti-lamin A/C, anti-lamin B1, anti-PP1α, anti-PP1γ, anti-PP1γ2, anti-γ-tubulin, and lastly, anti-torsinA (Table III.1). Additionally, as a negative control for IHC, isotypes mouse and rabbit IgGs (Vector Laboratories) were used instead of the primary antibody in the corresponding concentrations.

Table III.1. Primary antibodies used in order to detect the multiple proteins analysed in ICC and IHC.

Antibody	Antibody type	Target	Dilution	Blocking solution
Anti-LAP1[69]	Rabbit, polyclonal	LAP1	ICC: 1:4000	3% BSA
			IHC: 1:2000	5% BSA + 0.01% BSA-C
Anti-Lamin A/C (#2023) (Cell Signalling)	Rabbit polyclonal	Lamin A/C	IHC: 1:50	3% BSA
Anti-Lamin B1 (H-90): sc-20682 (Santa Cruz Biotechnology, Inc.)	Rabbit polyclonal	Lamin B1	IHC: 1:100	5% BSA
Anti-PP1α (CBC2C)[179]	Rabbit polyclonal	PP1α	IHC: 1:250	5% BSA + 0.01% BSA-C
Anti-PP1γ (CBC3C)[179]	Rabbit polyclonal	PP1γ	ICC: 1:500	3% BSA
			IHC: 1:500	5% BSA + 0.01% BSA-C
Anti-PP1γ2 (CBC502)[180]	Rabbit polyclonal	PP1γ2	IHC: 1:500	3% BSA
Anti-acetylated α-tubulin	Mouse Monoclonal	Acetylated α-tubulin	ICC: 1:250	3% BSA
Anti-γ-tubulin (GTU-88) (Sigma)	Mouse Monoclonal	γ-tubulin	IHC: 1:2000	5% BSA + 0.01% BSA-C
Anti-TorsinA (MAB5550) (Millipore)	Mouse Monoclonal	TorsinA	IHC: 1:100	3% BSA
Anti-COX IV (Thermo Fisher)	Mouse Monoclonal	COX IV	ICC: 1:100	3% BSA

BSA, bovine serum albumin; BSA-C, acetylated bovine serum albumin; ICC, immunocytochemistry; IHC, immunohistochemistry; COX IV, Complex IV Subunit IV.

Specific secondary antibodies were used in accordance to the particular technique performed (Figure III.1) alternating between IHC (Table III.2), and immunocytochemistry (ICC) (Table III.3) protocols.

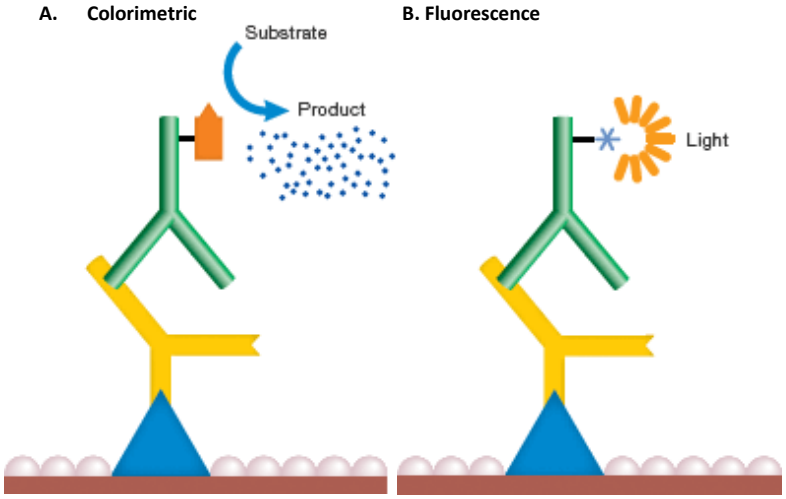

Figure III.1. Detection methods using indirect antibody labelling. In each detection method, a visible signal is generated following binding of a secondary antibody to a primary antibody, specific for the protein of interest. **(A)** In colorimetric detection, the signal is a coloured precipitate. (B) In fluorescence detection, the antibody is labelled with a fluorophore. Adapted from[181].

The secondary antibodies used in IHC follow the colorimetric principal (Figure III.1.A). The secondary antibody is directly polymerized with horseradish peroxidase (HRP), into compact polymers bearing a high ratio of enzymes to antibodies. These polymers demonstrated drastically improved detection sensitivity, efficiency and reliability compared to conventional secondary antibody conjugates. Direct polymerization also avoids an endogenous biotin reaction. HRP is an enzyme that converts the substrate, 3, 3'-diaminobenzidine (DAB), into a brown precipitate that is insoluble in alcohol and xylene. As the precipitate accumulates on the sample a coloured signal develops and is readily visible by eye. The enzymatic reaction can be monitored and stopped when the desired signal over background is reached[182]. In IHC, the indirect immunofluorescence method was applied (Figure III.1.B). In this technique, the secondary antibody carries the fluorophore, and recognises the primary antibody which binds the protein of interest[183].

Table III.2. Secondary antibodies used in IHC analysis

Antibody	Target
Powervision™ Poly-HRP Anti Ms/Rb/Rt IgG Biotin free, one component (Leica Biosystems)	Anti-mouse/rabbit/rat primary antibodies
Powervision™ Poly-HRP Anti Ms IgG Biotin free, one component (Leica Biosystems)	Anti-mouse primary antibodies

Table III.3. Secondary antibodies used in ICC analysis

Antibody	Excitation maximum (nm)	Emission maximum (nm)	Observed colour
Alexa Fluor 594 goat anti-mouse IgG (Invitrogen)	590	617	Red
Alexa Fluor 488 goat anti-rabbit IgG (Invitrogen)	495	519	Green

ICC, immunocytochemistry.

3.2.5 Immunohistochemistry

The IHC analysis of human and mouse samples were performed in the Center for Reproductive Medicine, Academic Medical Center in Amsterdam, under the supervision of Dr. A.M.M. van Pelt PhD.

Tissue samples from both human and mouse were previously fixated in Bouin´s solution or 4% PFA and dehydrated using graded ethanol solutions. These graded solutions progressively expose the sample to changes in hydrophobicity, minimizing damage to cells. Leica ASP200S (Leica Biosystems), an automated device for tissue dehydration and wax penetration, was used for the procedure. Finally, tissue embedding with paraffin had been previously performed, resulting in the available paraffin blocks (stored at 4°C) that were used in the following steps.

3.2.5.1 Tissue fixation

An essential part of all histological and cytological techniques is the preservation of cells and tissues as they naturally occur. To accomplish this, tissue blocks are usually immersed in a fixative fluid. The fixatives employed prevent autolysis by inactivating lysosomal enzymes, and stabilize the fine structure, both inside and between cells, by making macromolecules resistant to dissolution by water and other liquids. Fixatives also inhibit the growth of bacteria and molds that give rise to putrefactive changes[184].

In this work, two fixatives, Bouin and 4% PFA, were tested in order to optimize the staining process for each of the primary antibodies used in IHC. Bouin's solution contains formaldehyde, glacial acetic acid and picric acid, in water. The formaldehyde reaction results in the formation of cross-linking methylene bridges. Picric acid penetrates tissues rather slowly, coagulating proteins and causing some shrinkage, simultaneously dying the tissue yellow. The acetic acid coagulates nuclear chromatin and opposes the shrinkage caused by picric acid. The coagulation of nucleic acids

is often used in cases where preservation of chromosomes is required. This makes it particularly useful in the fixation of the testis if visualization of the meiotic chromosomes is sought. The complementary effects of the three ingredients of Bouin's solution work well together to maintain morphology[185]. Alternatively, 4% PFA, a compound that is obtained through the condensation product of formaldehyde, was used as a fixative. As mentioned previously, formaldehyde acts as a fixative due to formation of cross-links between proteins known as methylene bridges. Fixation in 4% PFA results in obvious tissue shrinkage artefacts, especially between seminiferous epithelium cells. Shrinkage artefacts are also observed in the central area of the testes fixed in Bouin. Additionally, clarity of nuclear detail in testes fixed in Bouin is better compared to 4% PFA[184,185]. Due to the formation of the protein cross-links during fixation from the two fixatives, antigenic sites can be masked which can prevent recognition of the antigen by the antibody. This can be overcome by adding an antigen retrieval step before IHC protocols. This process can be performed via a heat or chemical induced protocols. Both methods break the methylene bridges exposing antigenic sites to the antibodies[185].

During the present work, the testis biopsies were fixated 16-18 h in Bouin at 4°C, on a roller mixer. Washes were performed three times for 30 min each, with 70% EtOH on a roller mixer at 4°C, until the solution becomes clear. Alternatively, the testis biopsies were fixated 16-18 h in 4% PFA at 4°C, on a roller mixer. First testis were washed in phosphate-buffered saline solution (PBS) for 30 min on a roller mixer at 4°C, subsequent washes were performed three times for 30 min each, with 70% EtOH on a roller mixer at 4°C.

3.2.5.2 Slicing and mounting paraffin sections on microscope slide

Tissue samples which are embedded into paraffin can be sliced using a microtome. The tissue sections can then be mounted on a microscope slide, stained, and examined. The microtome was initially adjusted to a thickness of 5 µm per slice. First, it is necessary to securely clasp the paraffin block into the block holder. Subsequently, the sections are cut and placed in a water bath (37°C) until the section is completely uniform in the water surface. Using adhesive microscope slides (KP-Silan adhesive slides grounded-90, Klinipath BV) the sections were fished out of the water bath. The microscope slides were then placed on the heating plate at 42°C in order to stretch the tissue homogeneously. Lastly, the slides are incubated overnight at 37°C in order to dry the tissue completely.

3.2.5.3 Histological staining

IHC staining was performed on the 5 µm mouse and human testis sections, previously fixed, in Bouin's solution or 4%PFA, and embedded in paraffin. The tissue sections were then deparaffinized in Xylene I and Xylene II, for 3 min each. Hydration followed with sequential immersion in 100% EtOH-absolute (2x), 96% EtOH (1x) and 70% EtOH (1x), each for 2 min. After, sections were placed in tap water and antigen retrieval was performed in order to uncover hidden antigenic sites by breaking the protein cross-links formed by fixation, improving IHC results. Thereby, sections were immersed in sodium citrate, pH 6.0, at microwave oven irradiation for 2 min at maximum Watt, followed by heating for 10 min at minimum Watt, without boiling. As this procedure depends on the specific protein that is being analysed, all the primary antibodies were tested in three conditions: no antigen retrieval; one time antigen retrieval; or three times antigen retrieval. After optimization, the best staining methods were determined for each primary antibody based on the background and specificity when compared between the three conditions mentioned above and the IgG staining. Finally, sections were allowed to cool down for 10 min and washed in PBS afterwards.

As the staining protocol relies in the enzymatic activity of HRP (Figure III.1) the endogenous peroxidase was blocked, preventing false positive signals. H_2O_2 blocks endogenous peroxidase, therefore tissue sections were incubated with freshly made 0.3% H_2O_2/PBS for 10 min at room temperature (RT), with agitation in the dark. After, samples were washed 3 times for 5 min with PBS, slowly shaking. Nonspecific adhesion sites were blocked for 1h at RT, in a humidified chamber. The blocking solutions for each antibody were optimized in this work, as it was the first time that all the described antibodies were used for colorimetric IHC in the lab (Table III.1). Sections were subsequently incubated with the primary antibody or IgG (Vector Laboratories) as negative control, for 2h at RT. After washing with PBS, 3 times for 10 min, slowly shaking, the sections were incubated in the Poly-HRP secondary antibody. Tissue samples were washed 3 times for 5 min with PBS, slowly shaking. Posteriorly, sections were incubated with Bright-DAB (Immunologic) which in the presence of peroxidase enzyme, produces a brown precipitate that is insoluble in alcohol and xylene. This incubation period varied between 1-4 min depending on the primary antibody used. After staining the sections were placed in PBS to stop the reaction and rinsed in demineralised water two times.

Finally, sections were counterstained 12 sec with freshly filtrated haematoxylin in order to visualize the nucleus dark blue or violet. Dehydration of the sections started with immersion in 70% EtOH (1x), 96% EtOH (1x), 100% EtOH (2x), Xylene I (1x) and Xylene II (1x), each for 2 min. Sections

were then mounted by embedding in Entellan. The slides were examined and pictures were taken using an Olympus BX41 bright-field microscope with an Olympus DP20 colour camera.

3.2.6 Immunocytochemistry

In the present work, cell culture was performed as described in section 3.2.3 in 6-well plates (Corning) with coverslips. Cells were then washed with PBS and 4% PFA was added for 20 min. Following fixation, cells were washed trice with PBS and 0.2% Triton-X in PBS was added for 10 min to achieve permeabilization. Then, unspecific binding of the primary antibodies was blocked for 1 h with 3% BSA/PBS. Cells were then incubated for 2 h with the specific primary antibodies depicted in Table III.1. Then followed incubation for 1 h with the appropriate fluorescent secondary antibodies (Table III.3). Cells were washed thrice with PBS following permeabilization, between antibody incubation periods and after incubation with the secondary antibodies. Coverslips were then mounted on a microscope slide with VECTASHIELD® Mounting Media with 4',6-diamidino-2-phenylindole (DAPI) (Vector Laboratories) and visualized by epifluorescence microscopy, using the Olympus IX-81 (Olympus, Optical Co. GmbH) motorized inverted microscope equipped with a PlanApo 100x/1.40 oil immersion objective lens. Photographs were taken with a Digital CCD monochrome camera F-View II (Soft Imaging System).

Acrosome-reacted sperm cells were fixed with 2% formaldehyde in PBS for 40 min, washed with PBS and permeabilized with 1% Triton X-100 in PBS for 20 min. After washing, sperm cells were blocked with 1% BSA and 100 mmol/L glycine in PBS for 30 min. After blocking, 100 µl of sperm cells was incubated for 2 h at 37^{o}C with the respective primary antibody (Table III.1). Followed this period of incubation, sperm cells were washed with 0.1% Triton X-100 in PBS for 30 min. Sperm cells were then incubated 1 h at 37^{o}C with the respective secondary antibody (Table III.3) and acrosome reacted sperm cells were incubated with PSA-FITC (*Pisum Sativum Agglutinin*-Fluorescein Isothiocynate, 1:200). Sperm cells were then washed with 0.1% Triton X-100 in PBS for 15 min. Between washing steps, sperm cells were centrifuged at 1800 rpm during 5 min. Samples were mounted on a microscope slide with VECTASHIELD® Mounting Media with DAPI (Vector Laboratories) and visualized by epifluorescence microscopy, using the Olympus IX-81 (Olympus, Optical Co. GmbH) motorized inverted microscope equipped with a PlanApo 100x/1.40 oil immersion objective lens. Photographs were taken with a Digital CCD monochrome camera F-View II (Soft Imaging System). Additionally, samples were visualized using a LSM510-Meta confocal

microscope (Zeiss) and a 100x/1.4 oil immersion objective. The argon laser lines of 405 nm, 488 nm, and a 561 nm DPSS laser were used. Sperm with negative staining with PSA-FITC were considered acrosome reacted, as this is an acrosome content marker.

3.3 RESULTS AND DISCUSSION

IHC analysis was performed to investigate the localization of LAP1 and its interactors between the different cell types present in sections of mouse and human testis biopsies. Afterwards, ICC analysis provided grounds to: the localization of LAP1 in a spermatogonial cell line; the characterization of LAP1 distribution in sperm, through the colocalization with COX IV; and the investigation of PP1γ and LAP1 interacting profile, by colocalization in sperm.

3.3.1 LAP1 and interacting proteins in the testis

3.3.1.1 LAP1 localization in the testis

After examination of seminiferous tubules representative of all the stages of the seminiferous epithelium in mouse, it was possible to observe a differential cellular localization of LAP1 between stages of the spermatogenic cycle. For instance, Figure III.2.B clearly shows that the subcellular distribution of LAP1 between stages I, VI, VIII and XII is extremely distinct. As the negative control (Figure III.2.A) shows only staining in the interstitial space between Leydig cells, it is safe to propose that there is positive staining in the NE of peritubular and Sertoli cells. Similarly, in germ cells, LAP1 is localized exclusively in the NE of type A spermatogonia, all intermediate spermatogonia, B spermatogonia and spermatocytes. However, at the beginning of stage VIII of the differentiation process (Figure III.3.A), LAP1 is homogeneously distributed not only in the NE but also in the cytoplasm of round spermatids. Interestingly, later in stage VIII (Figure III.3.B) LAP1 polarizes to one half of the NE of round spermatids, maintaining cytoplasmic presence that is characteristic with the beginning of spermiogenesis. Afterwards, in early stage IX (Figure III.4.A), the previous indications of a polarization of the signal to one half of the nuclear periphery became more evident, with a distinctive increase in LAP1 staining. In Figure III.4.B, this polarization coincides with nuclear reshaping and the shifting in directionality of round spermatids, characteristic in the progression of spermiogenesis.

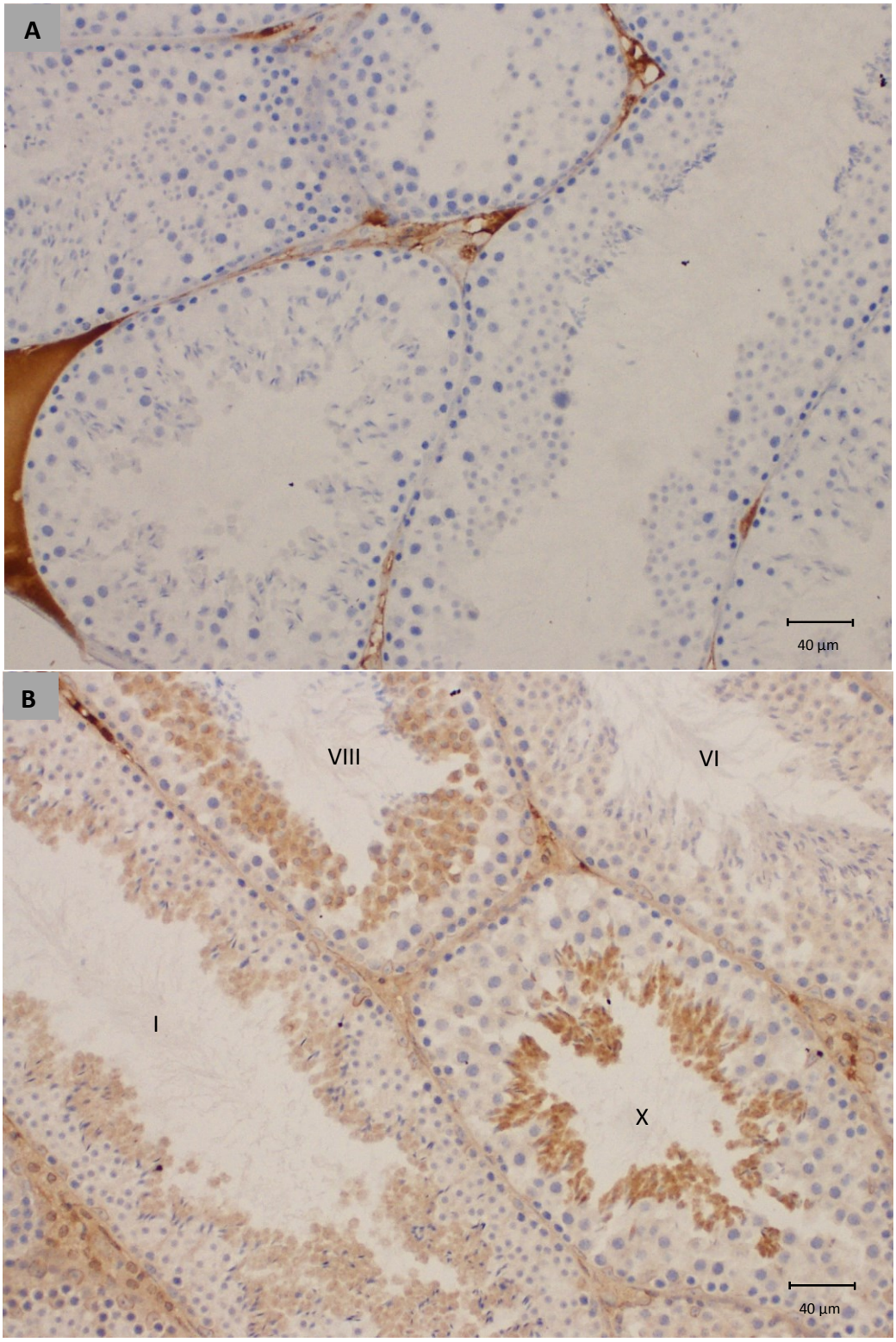

Figure III.2. Immunohistochemical localization of LAP1 in mouse testis sections fixated in Bouin. Positive immunostaining in brown colour, counterstaining with haematoxylin. **(A)** Negative controls showed staining in the interstitial tissue. **(B)** LAP1 is present in the NE of peritubular, Leydig, Sertoli cells, type A spermatogonia, all intermediate spermatogonia, B spermatogonia and spermatocytes. Between round and elongated spermatids LAP1 shows a shift in nuclear distribution and an increasing presence in the cytoplasm, concomitant with cellular reshaping. All epithelial stages were examined, depicted are stages I, VI, VIII and X. LAP1 polarizes in round spermatids at stage VIII, then presents high positive staining in the cytoplasm of stage X, which later decreases staining on stage I. Stages are indicated with Roman numerals.

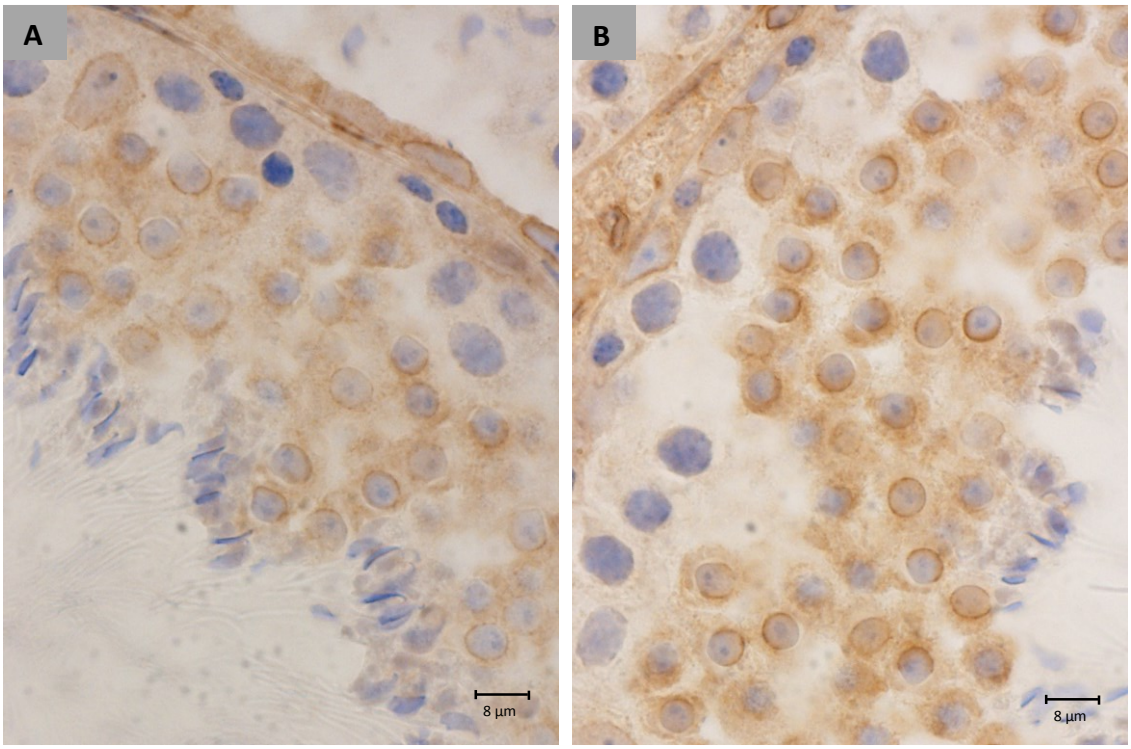

Figure III.3. Immunohistochemical localization of LAP1 in mouse testis sections fixated in Bouin. Positive immunostaining in brown colour, counterstaining with haematoxylin. **(A)** Depicted is early stage VIII with LAP1 present in the NE of all germ cells but most prominently distributed around the nucleus of round spermatids. **(B)** Image of late stage VIII where LAP1 concentrates in one half of the NE.

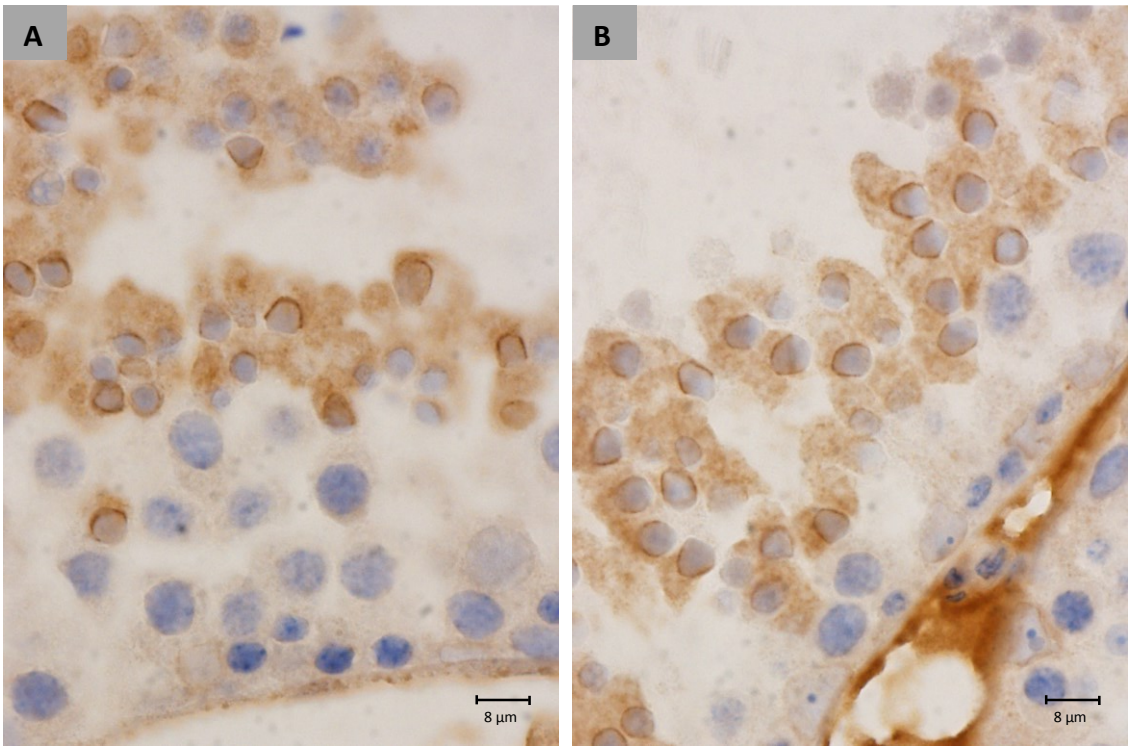

Figure III.4. Immunohistochemical localization of LAP1 in mouse testis sections fixated in Bouin. Positive immunostaining in brown colour, counterstaining with haematoxylin. **(A)** In early stage IX, elongating spermatids display LAP1 distributed in highly concentrated on side of nucleus, starting nuclear reshaping in form of a U-shape. **(B)** In stage IX, spermatids start displaying a shift in the nuclear direction, pointing to the tubule lumen; simultaneously LAP1 increases in the cytoplasm as it expands its volume.

These IHC results (Figures III.2-4) provide evidence that LAP1 undergoes dramatic changes in its distribution pattern during the initial stages of mouse spermiogenesis. Namely, in stage VIII, where round spermatids begin the elongation process, LAP1 becomes highly expressed and most importantly, relocates to the centriolar pole of the NE. In addition, LAP1 appears dispersed in the cytoplasm, which is quite unusual regarding the typical localization of this INM protein in the NE. In early stage IX, nuclear reshaping and simultaneous redirection of round spermatids towards the centre of the lumen is concomitant with increasing LAP1 expression both in the NE centriolar pole and the cytoplasm. The behaviour of LAP1 is partially comparable to that of LBR, LAP2, Lamins B1 and B3. In round and elongating spermatids, these NE proteins shift to the nuclear centriolar pole but remain only in the nuclear periphery[91,96,101]. As in the case of LAP1, the significance of the redistribution of these NE proteins is presently unknown. However, it is tempting to speculate that all of them, including LAP1, might be involved in chromatin reorganization that occurs during spermiogenesis. By moving to the posterior pole, the chromatin binding sites at the nuclear envelope would contribute to the achievement of the non-random, sperm-specific chromatin distribution. Furthermore, previous reports extensively describe that NE proteins, in particular lamins and its interactors, play an important role in chromatin dynamics and function (reviewed in [14]).

Alternatively, it is tempting to speculate that LAP1 might be associated with cytoskeleton regulation, as it is described for LINC complexes in spermiogenesis. In fact, Sun3 can participate in LINC complex formation through its interaction with Nesprin1. This LINC complex polarizes to the posterior pole of the spermatid NE, which is maintained throughout spermatid elongation process. There is strong indication that Sun3 and Nesprin1 assemble a spermiogenesis-specific LINC complex which polarizes to the posterior pole, thereby facing sites where cytoplasmic manchette MTs contact the NE[97]. The manchette is a transient microtubular structure in the posterior half of the nucleus that forms during nuclear elongation. The perinuclear ring of the manchette surrounds the base of the elongating nucleus and plays a key role in shaping the nucleus and the spermatid head[186]. LAP1 expression in the nucleus of elongating spermatids seems to coincide with manchette formation and function. Taking these facts into account, it is extremely interesting to inquire how LAP1 might be regulating or communicating with these cytoskeletal elements and how is it connected to the elongating nucleus.

In Figure III.5.A, the nucleus of elongating spermatids in late stage IX becomes progressively thinner at the centriolar pole, where staining of LAP1 in NE remains highly distinguished. In addition, the cytoplasm of elongating spermatids extends into the tubular lumen, which is characteristic of residual body development. Concomitantly, the signal of cytoplasmic LAP1 increases exponentially, with homogenous distribution through the cytoplasm (Figure III.5.B). The significance of this quite unusual distribution of LAP1 is currently undisclosed. However, it is tempting to explore the possibility that dispersion of LAP1 in the cytoplasm might be a behaviourally translated from its distribution in mitosis. Interestingly, LAP1 is distributed throughout the cytoplasm of cell in a punctuate pattern throughout mitosis, colocalizing with α-tubulin in the mitotic spindle and with γ-tubulin in centrosomes. Additionally, it was shown that not only is LAP1 important for centrosome positioning near the NE, but also that LAP1 depletion results in a decrease of mitotic cells and of the levels of acetylated α-tubulin and lamin B1. These attribute a crucial role to LAP1 in the maintenance of the NE structure and progression of the cell cycle[59]. This functional association might be reproduced during spermiogenesis, as dynamic MTs are essential for the assembly of various MT-based structures that participate in spermatid remodelling, such as manchette formation and nuclear reshaping[187].

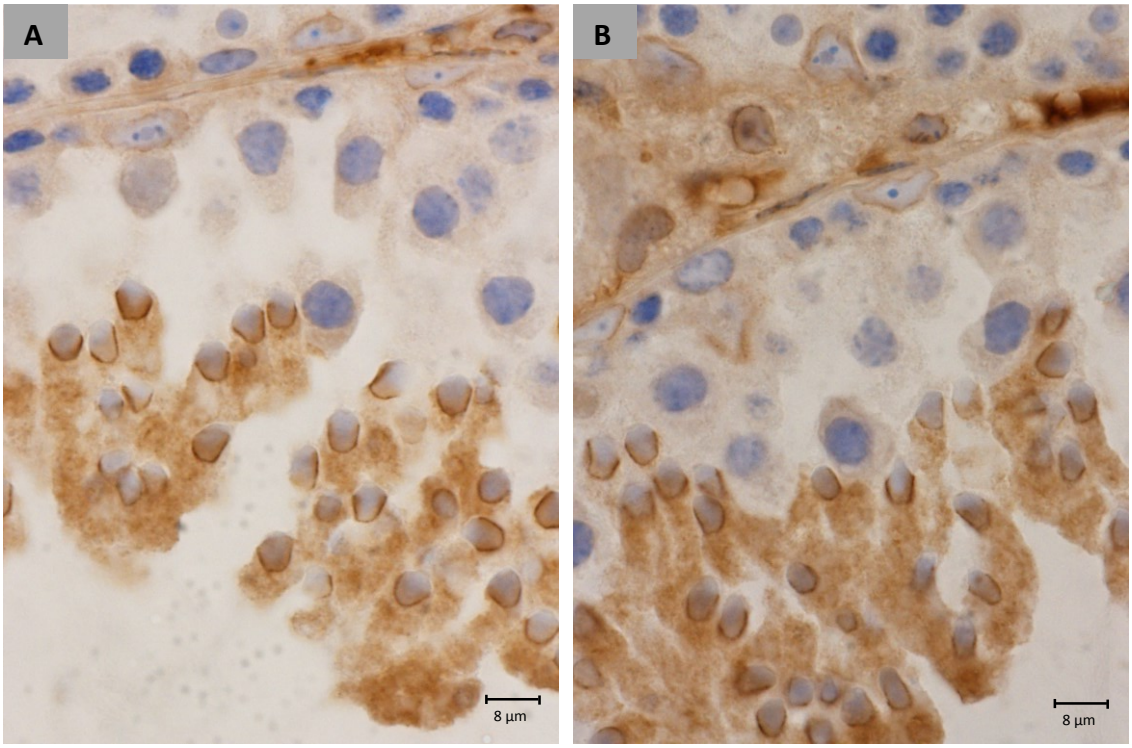

Figure III.5. Immunohistochemical localization of LAP1 in mouse testis sections fixated in Bouin. Positive immunostaining in brown colour, counterstaining with haematoxylin. Elongating spermatids in late stage IX show **(A)** an increasing in nuclear narrowing in the centriolar pole and **(B)** cytoplasmic elongation of spermatids is associated with LAP1 increased colouration in the extended cytoplasm.

With the beginning of stage X (Figure III.6.A), dramatic nuclear reshaping ensues, with progressive narrowing of the nucleus. In this stage, LAP1 is distributed along the nucleus periphery, when its reshaping into a needle-like structure begins. Finally, in stage XI (Figure III.6.B), the spermatid head forms a distinct protrusion with a sharp angle and the spermatid nuclei become thinner, more elongated and begin to stain more intensely, indicating chromatin condensation. During stage XI, LAP1 is still circumscribed to one half of the nuclear periphery but its presence decreases drastically when compared to the previous stages. This observation could be associated with chromatin condensation that occurs at this late stage. As previously proposed, lamin binding proteins and lamins themselves have been extensively reported to regulate chromatin tethering and reorganization. Once again, in stage XI, the clear presence of LAP1 through the cytoplasm of elongating spermatids during the nuclear reshaping process might be related to residual body development.

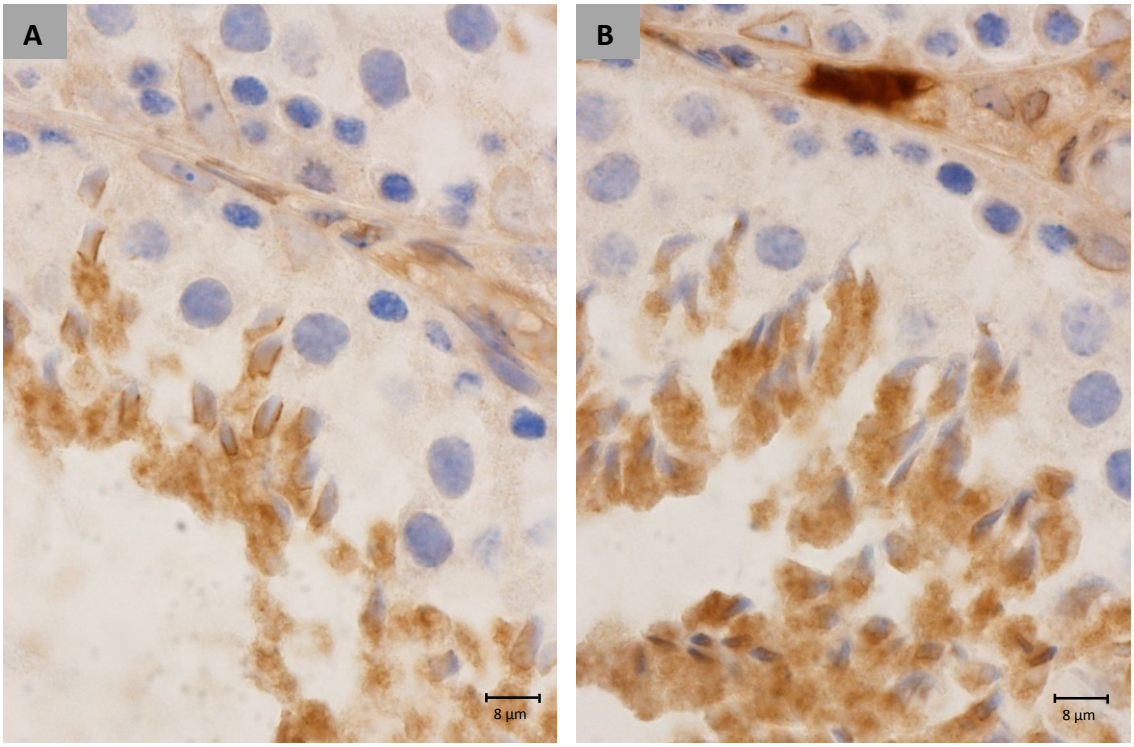

Figure III.6. Immunohistochemical localization of LAP1 in mouse testis sections fixated in Bouin. Positive immunostaining in brown colour, counterstaining with haematoxylin. **(A)** Early stage X tubules show LAP1 distributed along the nucleus, when its reshaping into a needle-like structure begins. **(B)** In stage XI, LAP1 circumscription along the NE decreases when compared to the previous stages but cytoplasmic staining remains.

In stage XII (Figure III.7), meiosis ensues and spermatid elongation continues. LAP1 staining that is observed in previous stages around the nucleus is no longer verified. Additionally, there is a decrease in cytoplasmic staining.

Overall, in mouse spermatogenesis, LAP1 presents a peculiar distribution in elongating spermatids, from stage VIII onwards. First, it shifts progressively to the centriolar pole of spermatid nuclei, then it stains the elongating cytoplasm homogenously before it becomes progressively undetectable in fully differentiated mature spermatids (stage VI, Figure III.2). According to these evidences, we propose that the progressive disappearance of LAP1 observed in fully elongated spermatids may be a consequence of the ending process of chromatin condensation. Moreover, LAP1 cytoplasmic staining might be associated with residual body formation which coincides with normal cytoplasm outspreading that takes place during spermiogenesis.

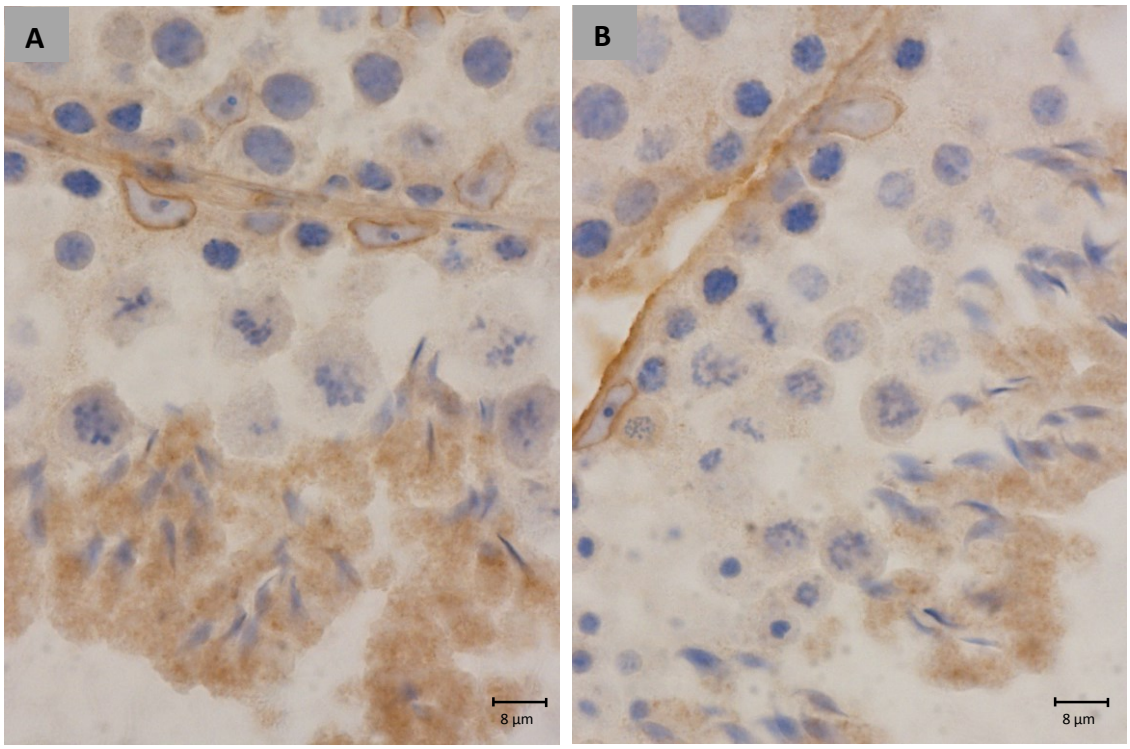

Figure III.7. Immunohistochemical localization of LAP1 in mouse testis sections fixated in Bouin. Positive immunostaining in brown colour, counterstaining with haematoxylin. **(A, B)** In stage XII tubules with representative meiotic cells, LAP1 is present in the cytoplasm of elongated spermatids but with less staining than the previous stages.

In human spermatogenesis the seminiferous tubules do not clearly present stage specific differentiation. This fact leads to increased difficulties in the distinction of cell types throughout spermatogenesis. Moreover, stage identification can be defined in several ways, but inevitably, this requires recognition of specific cell types. The appearance of germ cells is highly dependent on methods of fixation, embedment, staining, and visualization, being extremely difficult to determine by IHC procedures, particularly in cross sections of the human tissue (reviewed in [79,80]). Two different fixatives (Bouin, 4% PFA) were tested for IHC analysis of each antibody. The results were presented after considering tissue and cellular morphology, background staining and comparison to the negative control.

Previously presented IHC analysis for LAP1 distribution throughout mouse spermatogenesis (Figures III.2-7) was performed in testis fixated in Bouin. Despite the fact that Bouin's fixation leads to better conserved tissue morphology, in the case of LAP1 analysis in human testis, fixation with 4% PFA delivered better staining. In Figure III.8.A, negative controls show very light staining when compared to sections immunostainned with LAP1 antibody. Overall, Figures III.8.B-C enabled the identification of LAP1 in the NE of in somatic cells namely, peritubular, Leydig, and Sertoli cells. Furthermore, germ cell distribution of LAP1 in the NE is restricted to spermatogonia and spermatocytes. Elongating spermatids are depicted in Figure III.8.B, showing LAP1 in the centriolar pole of the cell, which is concomitant with nuclear reshaping and chromatin condensation. In Figure III.8.C it is possible to determine that LAP1 is localized to the centriolar pole of completely elongated spermatids, due to the fact that maximum chromatin condensation is evident through darker staining by haematoxylin. These results reinforce the hypothesis proposed earlier that LAP1 might function as a cytoskeleton regulator of spermiogenesis and that simultaneously might be coordinating chromatin tethering and condensation in the process.

Assessment of LAP1 distribution in human spermatogenesis allowed us to conclude that LAP1 has an expression pattern quite similar to mouse spermatogenesis. This INM membrane protein rests in the NE of germ cells until meiotic division, but its localization shifts in spermiogenesis. Throughout elongation of spermatids there is a concentration of LAP1's signal in the centriolar pole (Figure III.9.C), however, later on it is rather difficult to determine if this signal is localized to the midpiece of developing sperm (Figure III.9.D) or if it is staining the surplus cytoplasm known as the residual body. Due to challenges in visualizing fully matured spermatids in human testis sections, ICC analysis was later performed to determine LAP1 localization in sperm.

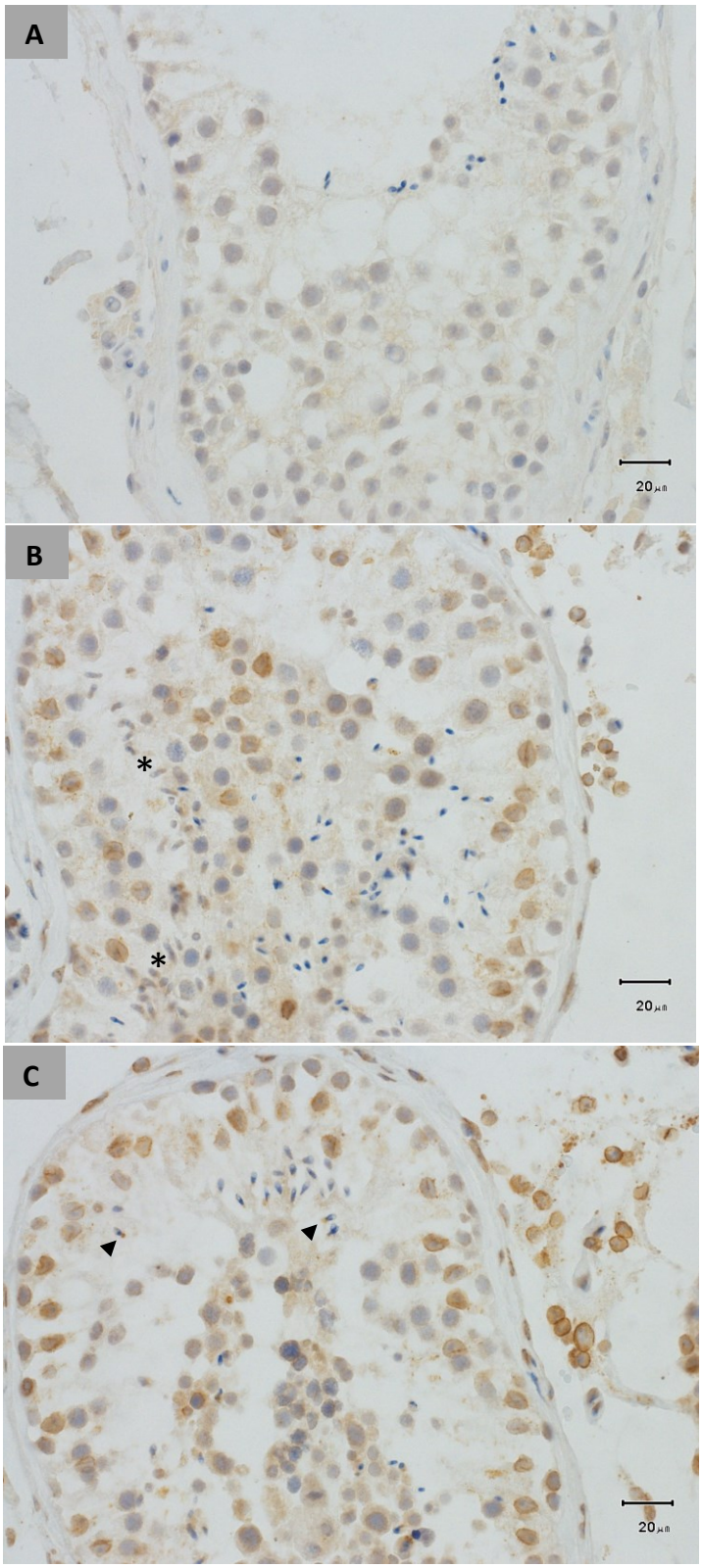

Figure III.8. Immunohistochemical localization of LAP1 in human testis sections fixated in 4% PFA. Positive immunostaining in brown colour, counterstaining with haematoxylin. **(A)** Negative controls showed very light staining. **(B, C)** LAP1 is present in the NE of peritubular, Leydig, and Sertoli cells, spermatogonia and spermatocytes. **(B)** LAP1 polarizes in elongating spermatids (asterisk) concomitant with nuclear reshaping and chromatin condensation. **(C)** LAP1 is also present in elongated spermatids at the centriolar pole (arrowhead).

Interestingly, there is one particular difference between LAP1 localization profile from mouse and human sections. As depicted in Figure III.9.B, LAP1 presents a doted feature in the cytoplasm of spermatocytes which is quite unusual for this membrane integrating protein. The reasons behind this specific localization are unknown but one might speculate if it is related with centrosome association. As previously reported[59], LAP1 colocalizes with γ-tubulin in centrosomes and LAP1 depletion leads to a decline in mitosis. Additionally, it was possible to determine that LAP1 is important for centrosome positioning near the NE. All these evidences might explain this peculiar localization of LAP1 prior to meiosis in spermatocytes. However, additional studies through IHC analysis of colocalization between LAP1 and γ-tubulin in human testis sections might clarify this rather erratic behaviour of LAP1.

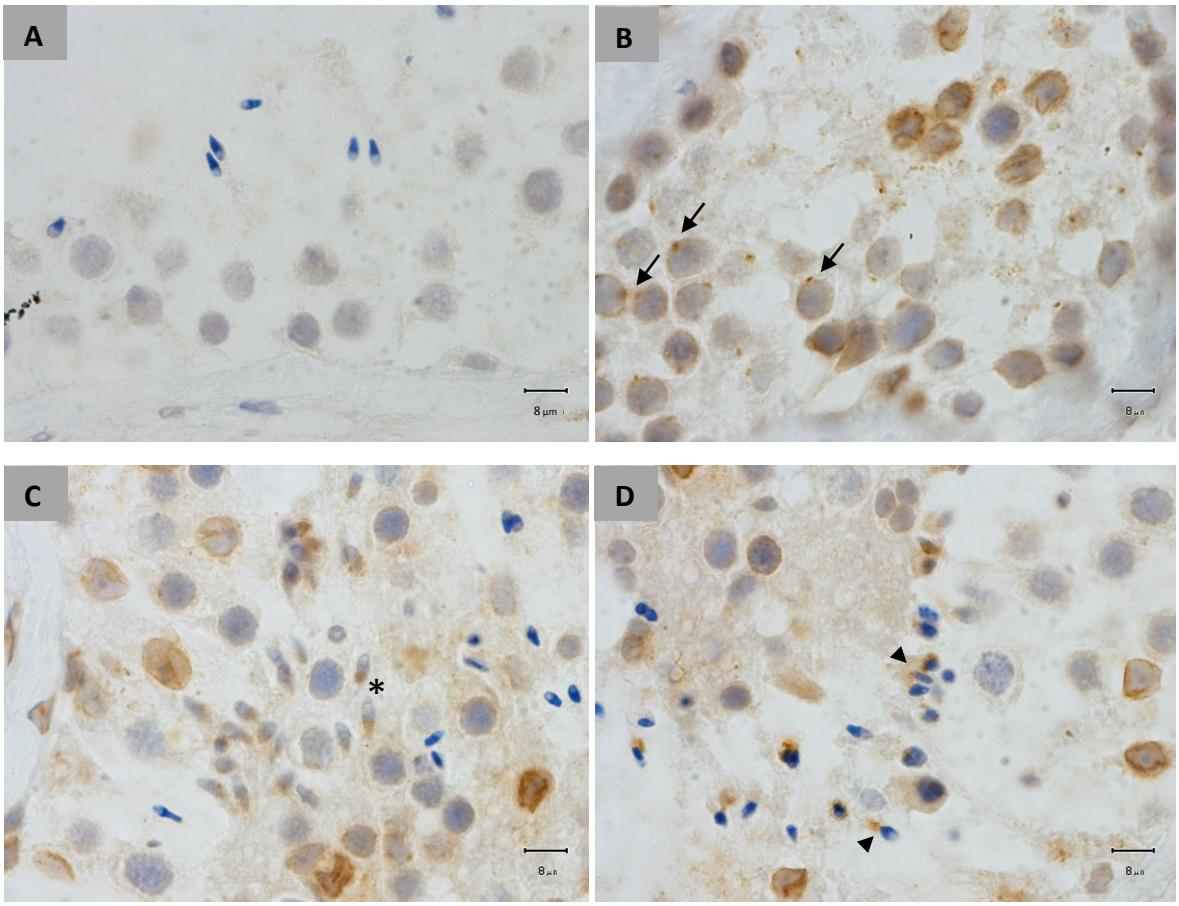

Figure III.9. Immunohistochemical localization of LAP1 in human testis sections fixated in 4% PFA. Positive immunostaining in brown colour, counterstaining with haematoxylin. **(A)** Negative controls showed no staining. **(B, C, D)** LAP1 is present in the NE of peritubular and Sertoli cells, spermatogonia, spermatocytes and round spermatids. **(B)** Accumulation of LAP1 in a cytoplasmic spot near the nucleus of round spermatids (arrows). **(C)** LAP1 polarizes in elongating spermatids (asterisk) concomitant with nuclear reshaping and chromatin condensation. **(D)** LAP1 is also present in elongated spermatids at the centriolar pole of totally elongated spermatids (arrowhead).

3.3.1.2 PP1 isoforms differential distribution in the testis

PP1 has four isoforms (α, β, γ1, γ2), two of which, PP1γ1 and PP1γ2, derive by alternative splicing of a single gene, *PPP1CC*. PP1γ2, expression is confined almost completely to spermatogenic cells, being the sole isoform found in mammalian sperm[188]. Although PP1γ1, the other *Ppp1cc* product, is expressed in many tissues including testis, the only phenotype resulting from deletion of *Ppp1cc* gene is male infertility[175]. However, it was recently determined that the isoform that is essential to infertility is PP1γ2 because the production of sperm capable of fertilization *in vivo* can take place in the complete absence of PP1γ1 expression[189]. Particularly, PP1α is a ubiquitously expressed protein that is functionally associated with mitosis (reviewed in [190]).

Using specific antibodies against PP1α, PP1γ and PP1γ2, a distinct differential distribution of these proteins in mouse testicular cells was investigated (Figure III.10). PP1α and PP1γ negative controls (Figures III.10.A and C) showed some staining in Leydig and peritubular cells which impaired the determination of positive staining in the respective antibodies. No staining was found in PP1γ2 negative control (Figure III.10.E). PP1α IHC results (Figure III.10.B) are in agreement with previous reports[188], as this isoform was found to be localized to the cytoplasm of Leydig and peritubular cells, spermatogonia, and pachytene spermatocytes. Concerning PP1γ immunostaining in mouse testis (Figure III.10.D), it is possible to determine that this isoform is present in Sertoli, Leydig and peritubular cells. In germ cells, it stains the cytoplasm of some spermatogonia and meiotic cells. In pachytene spermatocytes and round spermatids, PP1γ is present in the nucleus, shifting later onto the cytoplasm of elongating spermatids. Once more, due to the fact that the negative IgG control showed some staining in Leydig and peritubular cells, it is not possible to confirm the respective staining in sections incubated with PP1α or PP1γ, a fact that has been previously established for these somatic cells[188]. Finally, IHC analysis of PP1γ2 throughout mouse spermatogenesis (Figure III.10.F), delivered results which are in conformity with the previously reported localization of PP1γ2[175] and with the staining presented with PP1γ for both isoforms. PP1γ2 seems to be expressed in the nucleus of late pachytene spermatocytes before meiosis. During meiosis this isoform is distributed all over the cytoplasm, but afterwards localizes to both the nucleus and cytoplasm of round spermatids. Lastly, and most prominently, PP1γ2 is dispersed in the cytoplasm of elongating spermatids until excision of residual bodies in the end of spermiogenesis.

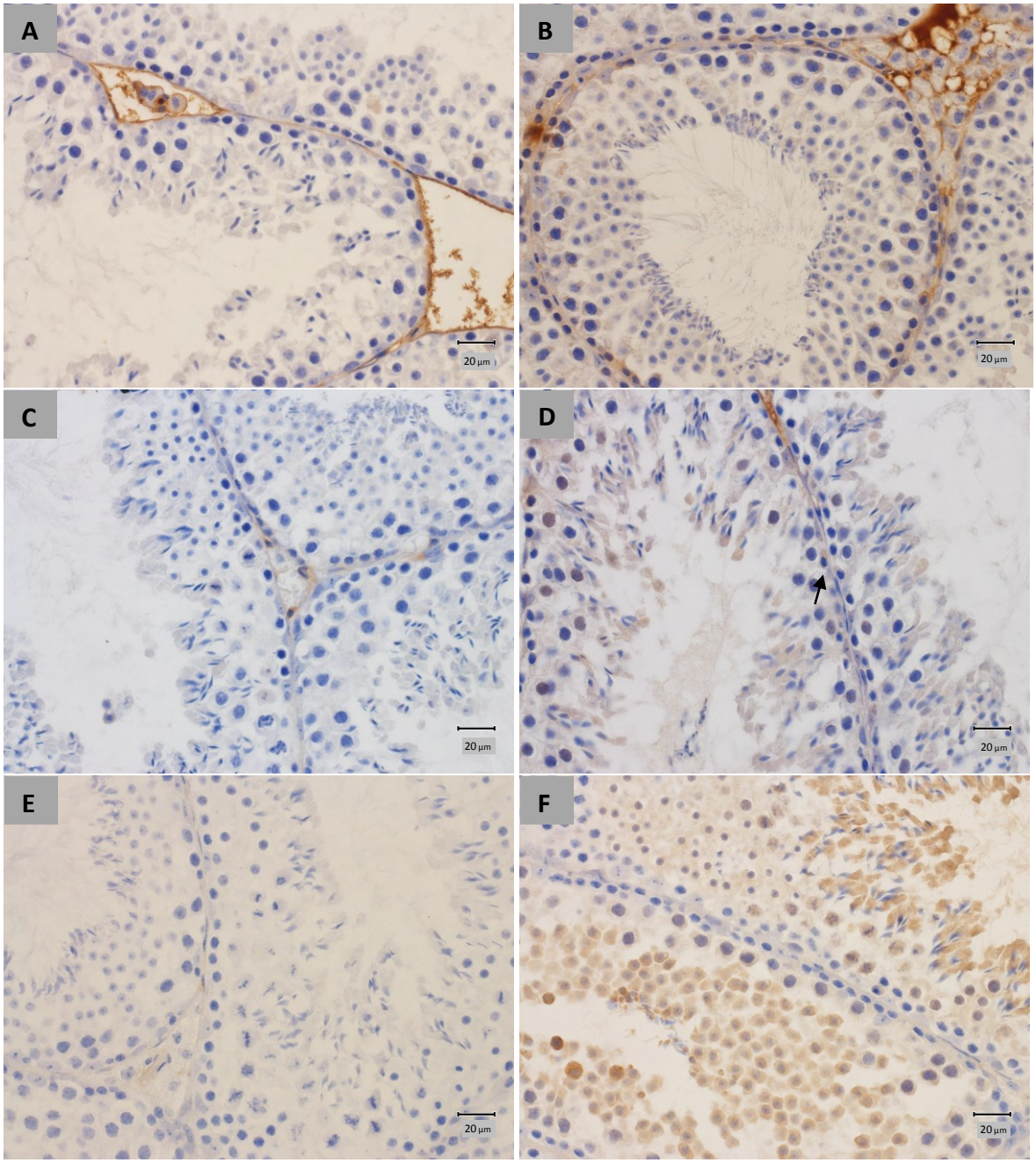

Figure III.10. Immunohistochemical localization of PP1 isoforms in mouse testis sections fixated in Bouin. Positive immunostaining in brown colour, counterstaining with haematoxylin. **(A, C, E)** Negative controls showed staining in peritubular cells. **(B)** PP1α showed strong expression in the cytoplasm of Leydig and peritubular cells, spermatogonia, and pachytene spermatocytes. **(D)** PP1γ staining is present in Sertoli, Leydig and peritubular cells. Additionally, it stains: the cytoplasm of some spermatogonia (arrow) and meiotic cells; the nucleus of pachytene spermatocytes and round spermatids; and the cytoplasm of elongating spermatids. **(F)** PP1γ2, concentrates: in the cytoplasm of late pachytene spermatocytes only before meiosis; during meiosis is distributed all over the cytoplasm; in the nucleus and cytoplasm of round spermatids; and most prominently in the cytoplasm of elongating spermatids.

Despite being thoroughly described in mouse testis, the differential distribution of PP1 isoforms in human spermatogenesis has not been investigated by IHC. Therefore, using the same antibodies that were used in mice, IHC analysis of PP1α, PP1γ and PP1γ2 in human testis was performed. No staining was found in all the negative controls for the different PP1 antibodies (Figure III.11.A, .C and .E). The IHC analyses of PP1α (Figure III.11.B) revealed an extremely light staining, preventing the characterization of this isoform throughout spermatogenesis. However, analysis of multiple sections identified PP1α in the nucleus of peritubular and Sertoli cells and pachytene spermatocytes. Further optimization is needed for the confirmation of these results. In the case of PP1γ (Figure III.11.D) staining is present in the nucleus of Sertoli, Leydig cells, pachytene spermatocytes and round spermatids. Lastly, PP1γ2 (Figure III.11.F) displays a much stronger signal when compared to the other isoforms analysed. This isoform concentrates in the nucleus of late pachytene spermatocytes immediately before meiosis. Later on, PP1γ2 shifts from the nucleus and cytoplasm of round spermatids to the centriolar pole of elongating spermatids (Figure III.11.F, right ROI) and completely elongated spermatids (Figure III.11.F, left ROI).

The implications of the distribution of PP1 isoforms have been previously described for mouse testis[175,176]. Considering the results obtained for PP1α in mouse testis (Figure III.10.B), it would be reasonable to speculate that the presence of this protein in the initial stages of spermatogenesis might be related to its prominent role in mitosis[174], as the most robust signal is conferred to spermatogonia. The expression pattern of PP1γ is quite similar between spermatogenic cells in mouse (Figure III.10.D) and human testis (Figure III.11.D). In both specimens, there is specific staining in somatic cells, namely Sertoli and Leydig cells. This is, partially, in accordance with previous reports that acknowledge that PP1γ1 staining in mice is evident in Sertoli cells[176]. Moreover, PP1γ is also present in some spermatogonia (Figure III.10.D, arrow), whereas this particular staining was absent in developing germ cells stained with PP1γ2 (Figure III.10.F). In fact, PP1γ2 expression in mice (Figure III.10.F) and human testis (Figure III.11.F) is detected in pachytene spermatocytes and in all subsequent stages of post-meiotic developing germ cells. Therefore it is reasonable to conclude that pre-meiotic and somatic staining might be conferred to PP1γ1. These staining patterns also confirm observations from earlier studies[175,176].

Due to these results, it is interesting to consider that impaired spermatogenesis and male infertility could be influenced by the combined loss of both PP1γ isoforms in testicular somatic cells (PP1γ1) and developing germ cells (PP1γ2).

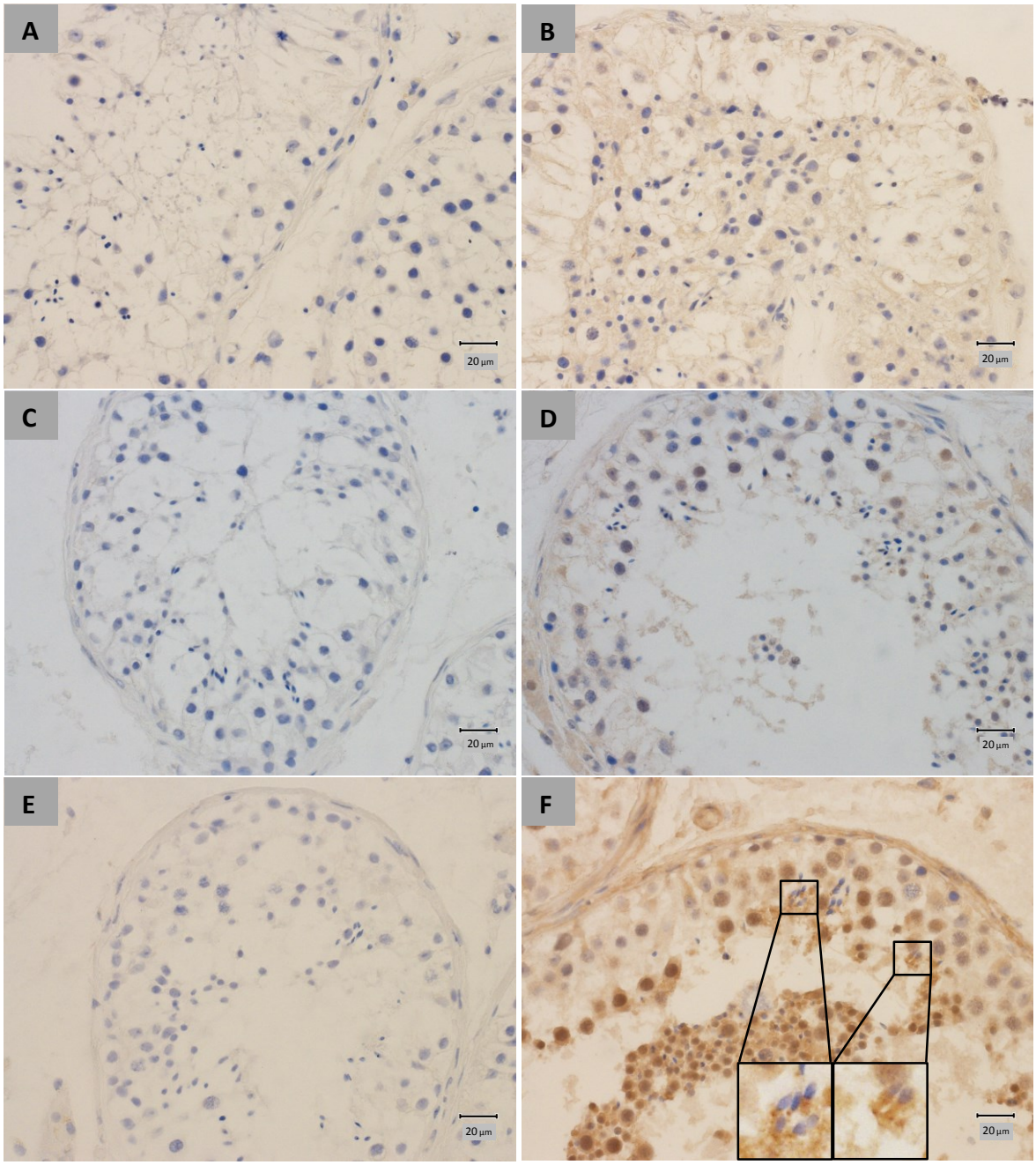

Figure III.11. Immunohistochemical localization of PP1 isoforms in human testis sections fixated in Bouin. Positive immunostaining in brown colour, counterstaining with haematoxylin. **(A, C, E)** Negative controls showed no staining. **(B)** Staining not clear. PP1α seems to be expressed in the nucleus of peritubular and Sertoli cells and pachytene spermatocytes. **(D)** PP1γ staining is present in the nucleus of Sertoli, Leydig cells, pachytene spermatocytes and round spermatids. **(F)** PP1γ2, concentrates in the nucleus of late pachytene spermatocytes, and of germ cells ranging from the nucleus and cytoplasm of round spermatids progressively shifting to the centriolar pole of elongating spermatids (right ROI) and mature spermatids (left ROI).

Global analysis regarding the distribution of PP1γ2 in mouse testis reveals a peculiar pattern, one that is similar to LAP1 throughout spermatogenesis. As depicted in Figure III.12.A, PP1γ2 signal in the cytoplasm appears quite noticeably in stage VIII round spermatids, which is also the case for LAP1. As elongation proceeds in stage IX, PP1γ2 relocates to the centriolar pole, still distributed through the cytoplasm but also evident in one half of the NE (Figure III.12.B, .C), concomitant with LAP1 staining. Later on, stage X spermatids (Figure III.12.D) present nuclear reshaping and cytoplasm elongation, which persistent with PP1γ2 immunostaining in the NE and cytoplasm, similar to LAP1. After complete narrowing of the nucleus into a needle like shape, PP1γ2 is only present in the extended cytoplasm of stage XI spermatids (Figure III.12.E). Finally, after meiosis, elongated spermatids remain stained with PP1γ2 only in the cytoplasm (Figure III.12.F). All the stages and respective staining described for PP1γ2 possibly colocalize with LAP1 as both proteins have an extraordinary similar expression pattern throughout spermiogenesis. This hypothesis can be easily clarified through future immunofluorescent colocalization of LAP1 and PP1γ2.

When exploring the putative interaction between LAP1 and PP1γ2 in spermiogenesis, functional perspectives arise. LAP1 has been previously identified as a PP1γ substrate[49,52]. Therefore, the overlapping localization of both proteins throughout spermiogenesis might be associated to the shifting of LAP1 from the NE to the cytoplasm, and its activity there. The phosphorylation status of LAP1 throughout mitosis has been shown to vary. In fact, LAP1 has been shown to be phosphorylated during both interphase and mitosis but appeared to be most highly phosphorylated during mitosis, consistent with previous reports for NE proteins[18,59]. Additionally, given that both proteins have important roles in the process of mitosis regarding MT dynamics[59,190], there is an additional putative significance to this association in the spermatid elongation process.

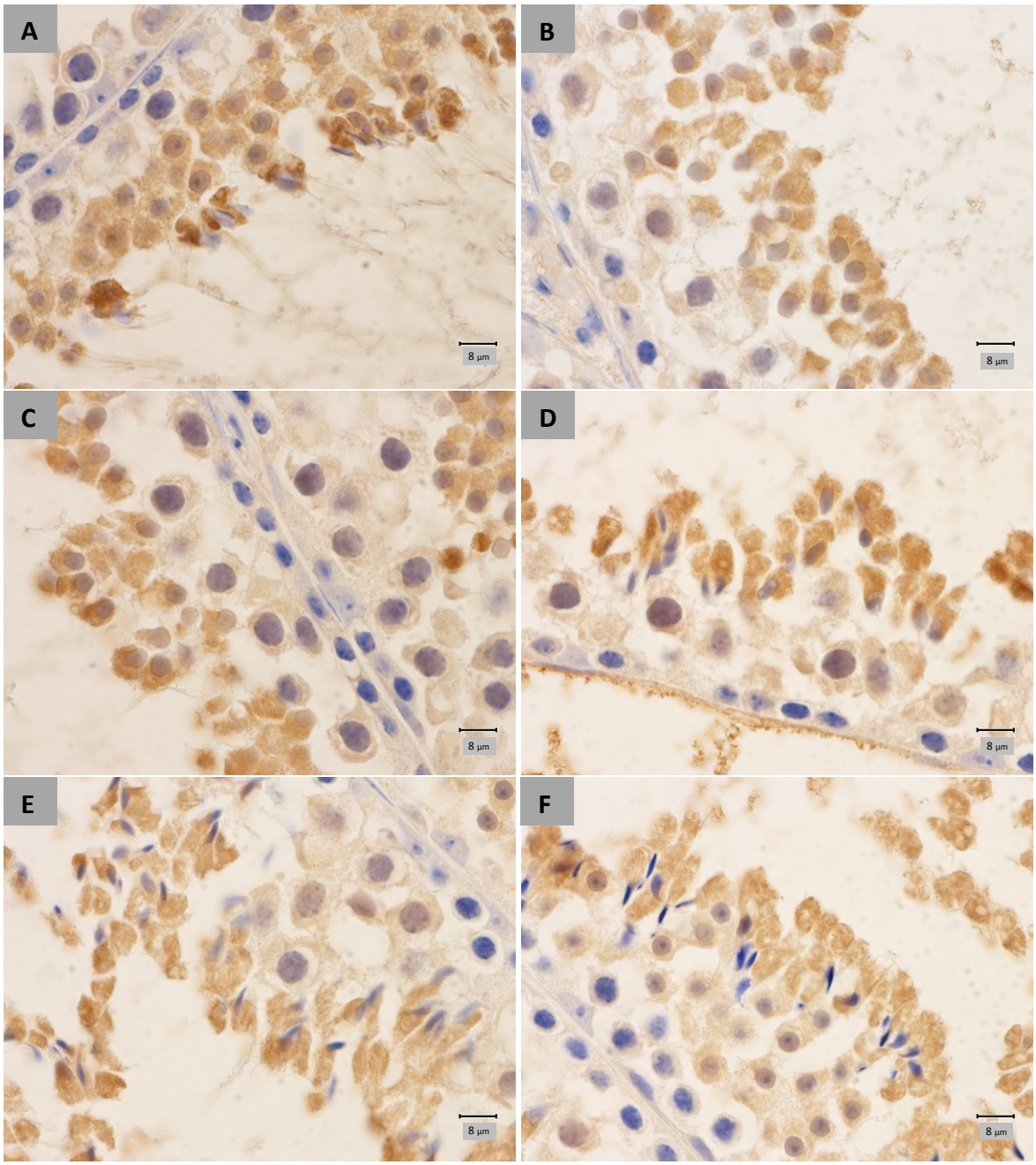

Figure III.12. Immunohistochemical localization of PP1γ2 in mouse testis sections fixated in Bouin. Positive immunostaining in brown colour, counterstaining with haematoxylin. PP1γ2, concentrates in the nucleus pachytene spermatocytes, and is prominently expressed in the cytoplasm of germ cells ranging from late pachytene spermatocytes, round spermatids to elongating spermatids and sperm. Depicted are stages concomitant with the expression, and possible colocalization, of LAP1. **(A)** Stage VIII round spermatids stain with PP1γ2. **(B, C)** High positive staining in the cytoplasm of stage IX spermatids**. (D)** In stage X nuclear reshaping occurs, accompanied by cytoplasmic extension and high positive staining of PP1γ2. **(E)** Prior to meiosis, in stage XI, PP1γ2 distinctively stains the nucleus of late spermatocytes and the cytoplasm of elongating spermatids. **(F)** In stage I, round spermatids are equally stained in the nucleus and cytoplasm while elongated spermatids remain stained only in the cytoplasm.

3.3.1.3 Lamin localization in the testis

Nuclear lamins are important structural protein components of the nuclear envelope. The composition and properties of the nuclear lamina of spermatogenic cells differ significantly from those of somatic cells in the same species. Alsheimer and colleagues have extensively investigated the expression of lamins and lamin-binding proteins throughout spermatogenesis[91–93,97,100,101,103,104]. Extensive study during the course of decades revealed that among somatic lamins, lamin B1 is the only one that is expressed during spermatogenesis, concluding that lamins A, C, and B2 are not present in any phase of this differentiation process. Instead, two short gametogenesis-specific lamins appear at different stages to become part of a therefore specifically modified lamina: A-type lamin C2 that is selectively expressed during meiotic prophase I[100] and lamin B3, a short lamin B2 isoform[24], whose expression is restricted to post-meiotic stages.

However, recent reports show that lamin A/C is expressed in the mouse testis during the different stages of spermatogenesis and in mature sperm[99], contrary to what was previously thought. Lamin A/C was found to be localized to the acrosome during spermiogenesis, from round spermatids until mature sperm, and that the decreased expression of lamin A/C caused a significant increase in sperm head abnormalities. Partially, our results seem to be in agreement with these observations, as lamin A/C is expressed most prominently in the acrosome of late spermatids (Figure III.13.B, .E, .F). Moreover, in the initial stages of spermatogenesis, spermatogonia (Figure III.13.F, arrow) do not seem to contain lamin A/C, as previously reported. A distinct result from the literature is the presence of lamin A/C in the NE of pachytene spermatocytes and Sertoli cells (Figure III.13.C, asterisk) and in the tail of elongated spermatids (Figure III.13.D). Additionally, staining is visible in the NE of Leydig and peritubular cells (Figure III.13.B).

Lamin B1 expression in mouse testis has been previously attributed to one half of the nuclear periphery of late round spermatids, which later became concentrated to a spot in the centriolar pole of elongated nuclei[98]. The results obtained after our IHC analysis show that lamin B1 (Figure III.14.B) is present in the NE of peritubular, Leydig and Sertoli cells, spermatogonia and round spermatids. As depicted in Figure III.14.C, lamin B1 also specifically stains the NE of pachytene spermatocytes. Lastly, lamin B1 seems to appear dispersed in the cytoplasm of meiotic cells (Figure III.14.D, arrowhead). Together, the results obtained in this work partially disagree with previous reports. No staining was obtained in germ cells after round spermatids, as it was described for lamin B1[98]. However, due to the fact that the localization of lamin B1 in spermiogenesis is constrained to a small part of the NE maybe it might only be detectable by immunofluorescence.

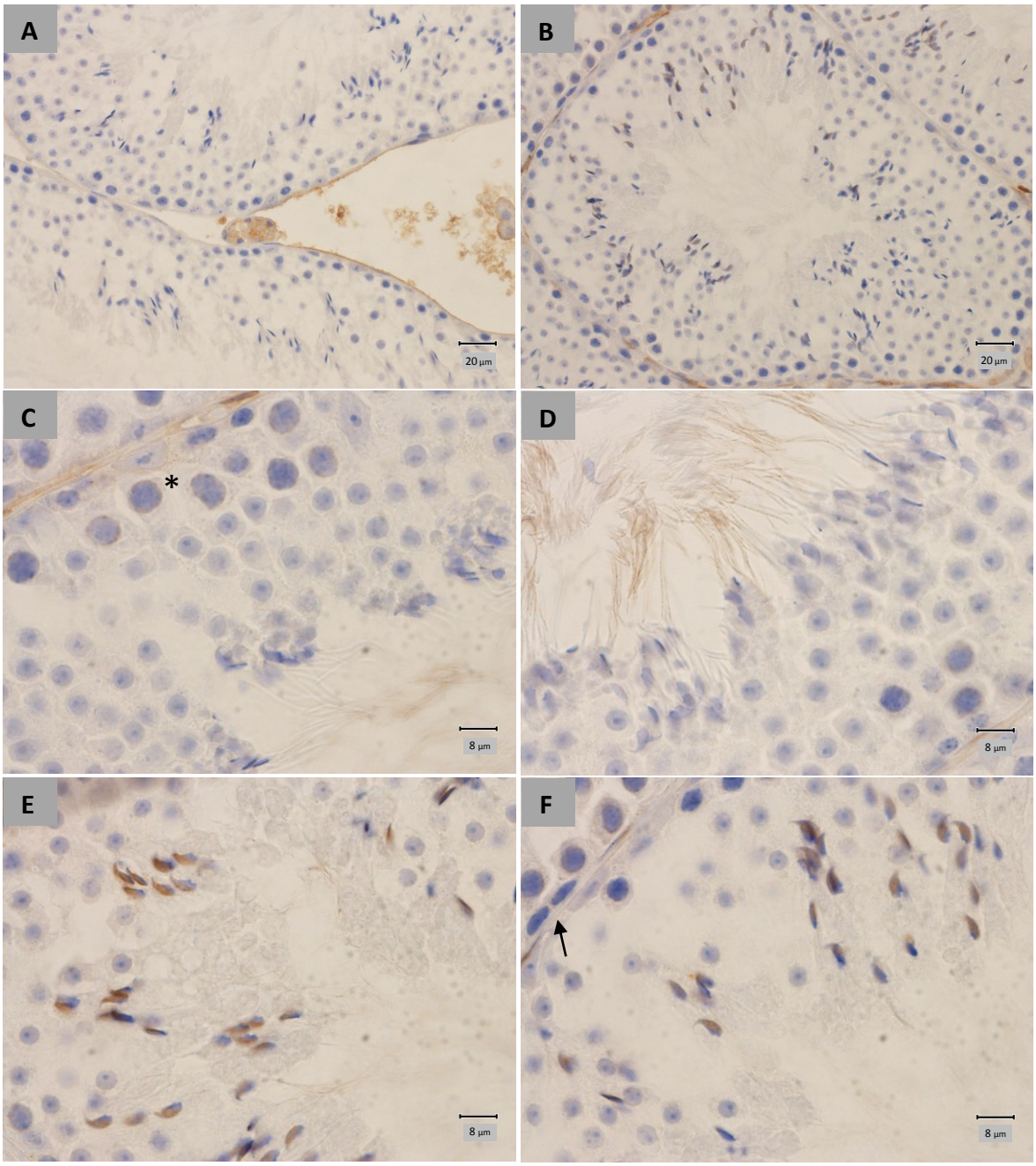

Figure III.13. Immunohistochemical localization of lamin A/C in mouse testis sections fixated in Bouin. Positive immunostaining in brown colour, counterstaining with haematoxylin. **(A)** Negative controls showed staining in the cytoplasm of interstitial tissue. **(B)** Tubule stained for lamin A/C showing concentration in the NE of peritubular and Leydig cells and most evidently mature spermatids acrosome. **(C)** Light staining of the NE of Sertoli cells and pachytene spermatocytes (asterisk). **(D)** Elongated spermatids show positive staining in the axoneme. **(E, F)** Specific coloration in the acrosome of elongated spermatids, **(F)** however spermatogonia appear to have no lamin A/C (arrow).

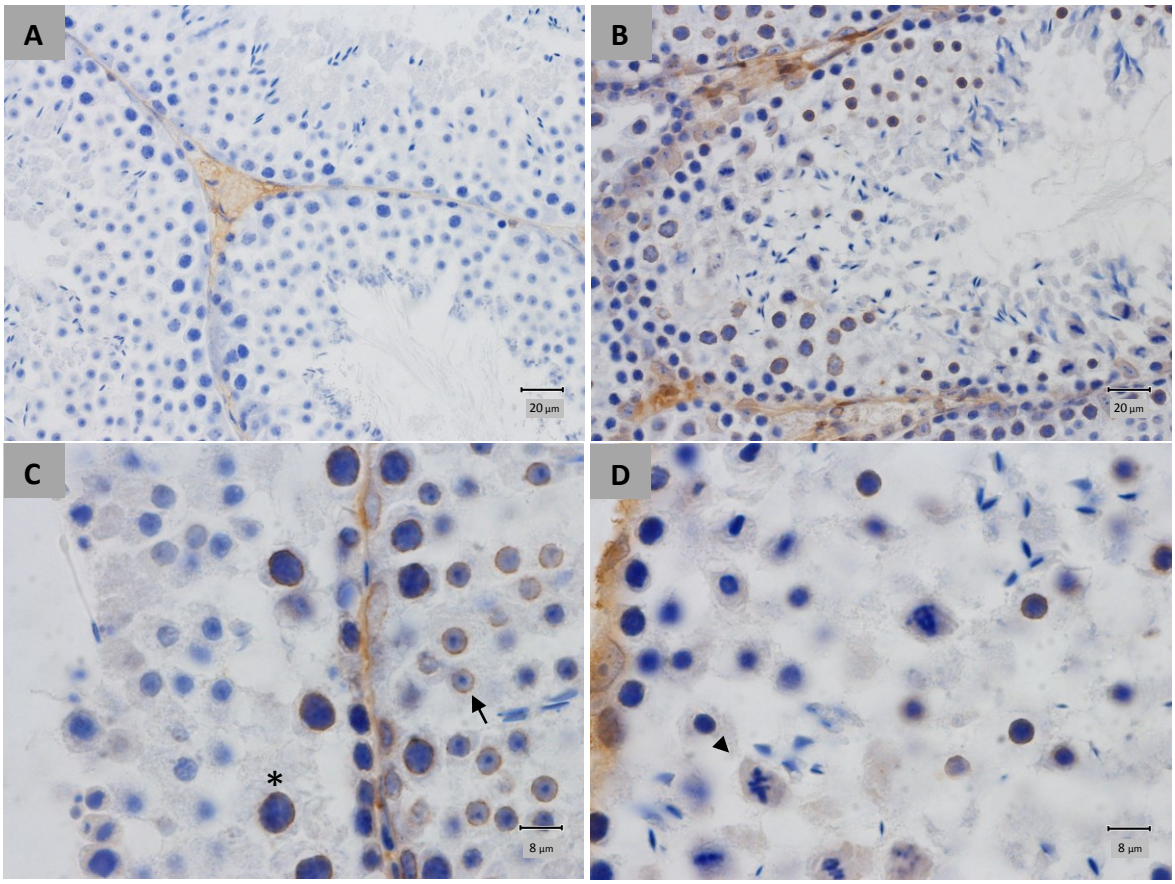

Figure III.14. Immunohistochemical localization of lamin B1 in mouse testis sections fixated in Bouin. Positive immunostaining in brown colour, counterstaining with haematoxylin. **(A)** Negative control showed staining in interstitial tissue. **(B)** Lamin B1 is present in the NE of peritubular, Leydig and Sertoli cells and spermatogonia. **(C)** Lamin B1 is clearly present in pachytene spermatocytes (asterisk) and round spermatids (arrow). **(D)** Meiotic cells (arrowhead) clearly present positive staining in the cytoplasm.

Throughout human spermatogenic cycle, the presence of lamin A/C has not been detected[191]. Our IHC results for lamin A/C (Figure III.14.B) demonstrate that lamin A/C is present in the NE of peritubular, Leydig and Sertoli cells, pachytene spermatocytes and round spermatids. Conversely, a previous study of lamin B1 in human testis[191] concluded that this isoform is present at the nuclear periphery of round spermatids, in the area that opposed to the acrosome. During spermatid maturation, lamin B1 progressively transfers to the posterior pole of the nucleus as the acrosome spreads. In elongated spermatids, lamin B1 is located at the posterior pole of the nuclei. This report is extremely similar to our results for lamin B1 in human testis. Lamin B1 (Figure III.14.D) is clearly expressed in the NE of peritubular, Leydig and Sertoli cells, late pachytene spermatocytes and round spermatids. Additionally, Lamin B1 staining in (Figure III.14.E) round and (Figure III.14.F) elongated spermatids at the centriolar pole is observed. Interestingly, when compared with the fixation in Bouin, human testis fixated in 4% PFA present lamin B1 staining more clearly in the centriolar pole of elongated spermatids, as depicted in the ROI (Figure III.14.H).

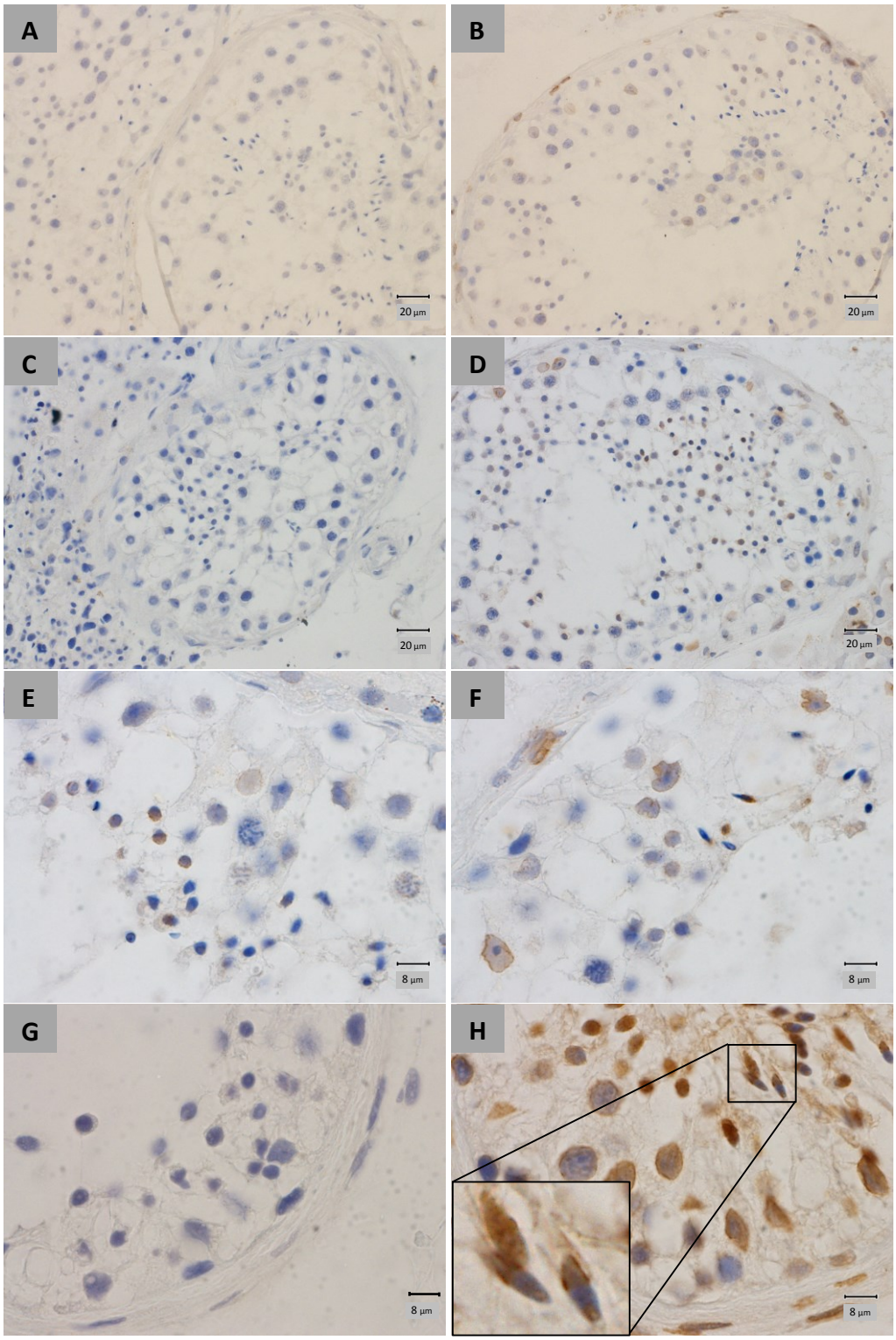

Figure III.15. Immunohistochemical localization of lamin A/C and lamin B1 in human testis sections fixated in Bouin and 4% PFA. Positive immunostaining in brown colour, counterstaining with haematoxylin. **(A, C, G)** Negative controls showed no staining. **(B)** In human testis fixated in Bouin, lamin A/C is present in the NE of peritubular, Leydig and Sertoli cells, pachytene spermatocytes and round spermatids. **(D)** In human testis fixated in Bouin, lamin B1 is clearly expressed in the NE of peritubular, Leydig and Sertoli cells, late pachytene spermatocytes and round spermatids. **(E, F)** Lamin B1 staining in **(E)** round and **(F)** elongated spermatids at the centriolar pole is observed. **(H)** When compared with the fixation in Bouin, in human testis fixated in 4% PFA lamin B1 is more clearly expressed in the centriolar pole of elongated spermatids, as depicted in the ROI.

There is mounting evidence that the nuclear lamina plays a crucial role in spermatid differentiation during spermiogenesis. With this work it was possible to conclude that lamin A/C retains a quite peculiar expression pattern in mouse testis, which is quite different from human. In mouse, lamin A/C is expressed most prominently in the acrosome and tail of late spermatids, additionally staining the NE of pachytene spermatocytes, Leydig, peritubular and Sertoli cells. In human, the same isoform seems to be present in the NE of peritubular, Leydig and Sertoli cells, pachytene spermatocytes and round spermatids.

Concerning lamin B1, our results, supplemented with similar literature, enable the conclusion that lamin B1 is continuously present throughout spermatogenesis. In pre-meiotic stages it seems to localize in the NE, during meiosis it is dispersed in the cytoplasm of meiotic cells, but afterwards concentrates to the centriolar pole of elongated nuclei[98]. In human, our results seem to agree with previous studies. Lamin B1 is clearly expressed in the NE of late pachytene spermatocytes and round spermatids. In post-meiotic cells, lamin B1 concentrates in the periphery of round spermatids, distributed opposed to the acrosome. During spermatid elongation, lamin B1 transfers to the posterior pole of the nucleus, finally localizing in the centriolar pole of elongated spermatids.

Taken together, these results seem to indicate that the role of nuclear lamina is to increase the flexibility of the nucleus in order to enable the intense nuclear remodelling that occurs during spermiogenesis, either in the acrosome cap (lamin A/C) or at the centriolar pole (lamin B1). Additionally, the presence at the centriolar pole of lamin B1 seems to be similar to LAP1 distribution in the NE, during mouse and human spermiogenesis. Once again, these results accentuate the putative role of LAP1 and lamins in the regulation of chromatin condensation and simultaneous nuclear reshaping, during the process of spermiogenesis.

3.3.1.4 γ-tubulin in spermatogenesis

Tubulin dimers are polymerized into microtubules at the microtubule organising centres (MTOCs). Physiological nucleation requires a nucleator that stabilizes a small microtubule seed composed of multiple heterodimers. The best known nucleator, γ-tubulin, localises to all known cellular MTOCs and forms a γ-tubulin ring complex (γ-TuRC), which is a highly efficient nucleation site. The most prominent and best known MTOC in cells is the centrosome, consisting of a pair of centrioles surrounded by pericentriolar material (PCM). In spermiogenesis, the spermatid nucleus polarizes to one side of the cell, as it begins the process of nuclear compaction and reshaping which is facilitated by the manchette. The manchette is a skirt-like structure of microtubules that project from a perinuclear ring, just below the acrosome, into the spermatid cytoplasm. The origin of the manchette microtubules is a matter of debate. It has been assumed that the perinuclear ring, from which the manchette microtubules emanate, is the MTOC. However, this hypothesis has not been proven yet[187].

The distribution of γ-tubulin in mouse has been previously described by immunofluorescence[192], making cell identification rather difficult, but sharing similarities with our results. As depicted in Figure III.16.B, γ-Tubulin stains peritubular and Leydig cells. Interestingly, in in the initial phases of the spermatogenic cycle, germ cells ranging from spermatogonia until late spermatocytes stain homogenously through the cytoplasm. However, from meiosis onwards, γ-tubulin concentrates in dots at the centriolar poles (Figure III.16.B, asterisk). In Figure III.16.C, cytoplasmic distribution of γ-tubulin in spermatogonia, leptotene and pachytene spermatocytes is evident. However, round spermatids present only one dot at the centriolar pole. When elongation proceeds, spermatids maintain a centriolar dot, near the nucleus facing the tubule lumen (Figure III.16.D). In completely elongated spermatids one dot is also present at the centriolar pole. Lastly, in dividing cells two dots are observed at the centriolar regions.

Throughout human spermatogenesis, γ-tubulin stains quite similar from mouse testis. As depicted in Figure III.17.B, γ-Tubulin stains centrioles in peritubular and Leydig cells. Additionally, in germ cells from initial phases of the spermatogenic cycle, ranging from spermatogonia until late spermatocytes, staining appears distributed through the cytoplasm. As depicted in arrows in Figures III.17.C and .D, after meiosis γ-tubulin concentrates in dots at the centriolar poles, while also being distributed homogenously through the cytoplasm of round spermatids. In completely elongated spermatids (Figure III.17.D), γ-tubulin concentrates in a dot at the centriolar pole.

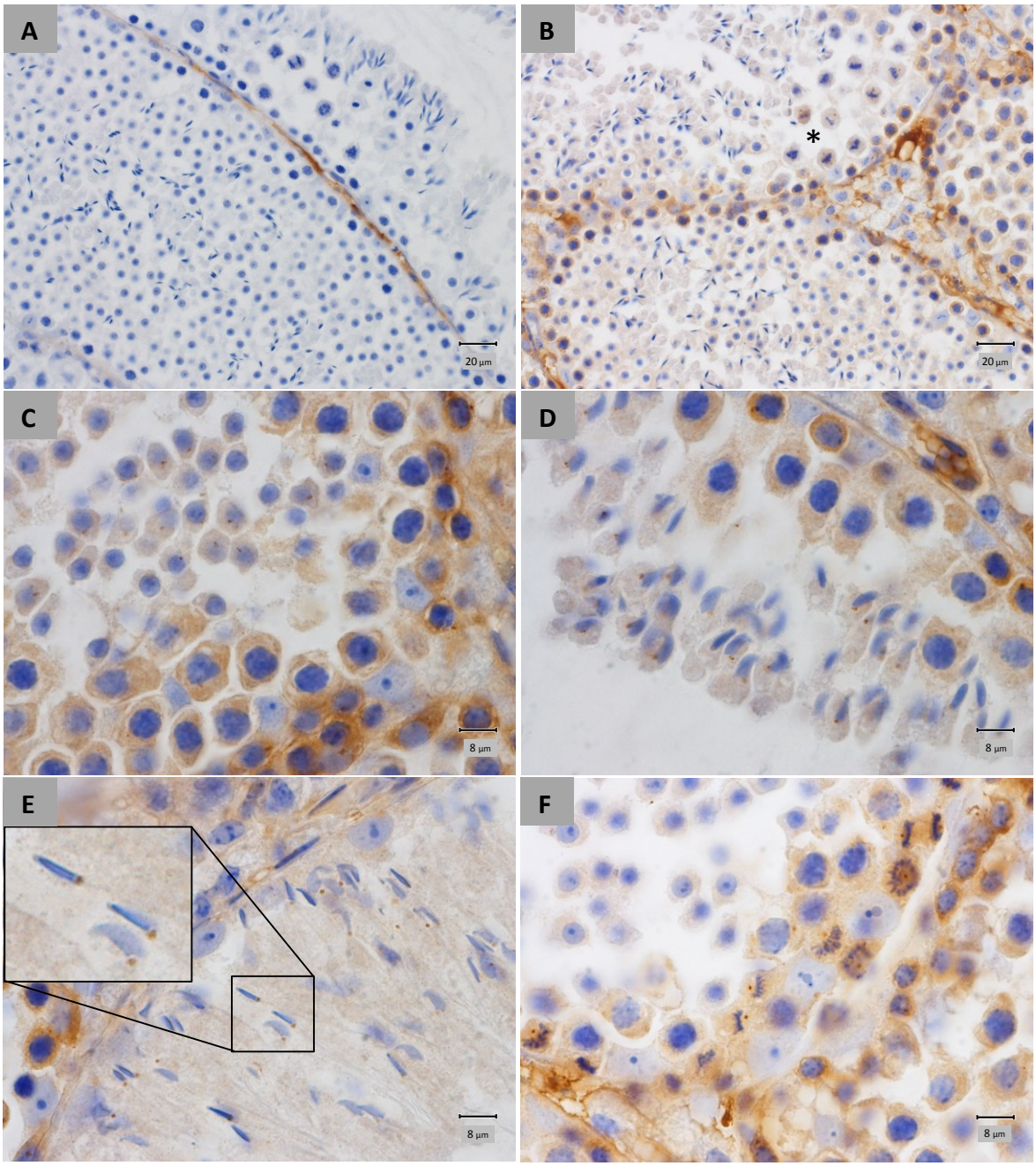

Figure III.16. Immunohistochemical localization of γ-tubulin in mouse testis sections fixated in Bouin. Positive immunostaining in brown colour, counterstaining with haematoxylin. **(A)** Negative control showed staining in peritubular cells. **(B)** γ-Tubulin stains peritubular and Leydig cells. Additionally, in germ cells from initial phases of the spermatogenic cycle, ranging from spermatogonia until late spermatocytes, staining appears distributed through the cytoplasm. From meiosis (asterik) onwards, γ-tubulin concentrates in dots at the centriolar poles. **(C)** Cytoplasmic distribution of γ-tubulin in spermatogonia, leptotene and pachytene spermatocytes is evident; in turn, round spermatids present one dot only at the centriolar pole. **(D)** In elongating spermatids a centriolar dot is clearly observed. **(E)** In completely elongated spermatids one dot is present at the centriolar pole. **(F)** Dividing cells confirm that the dots observed are the centriolar regions.

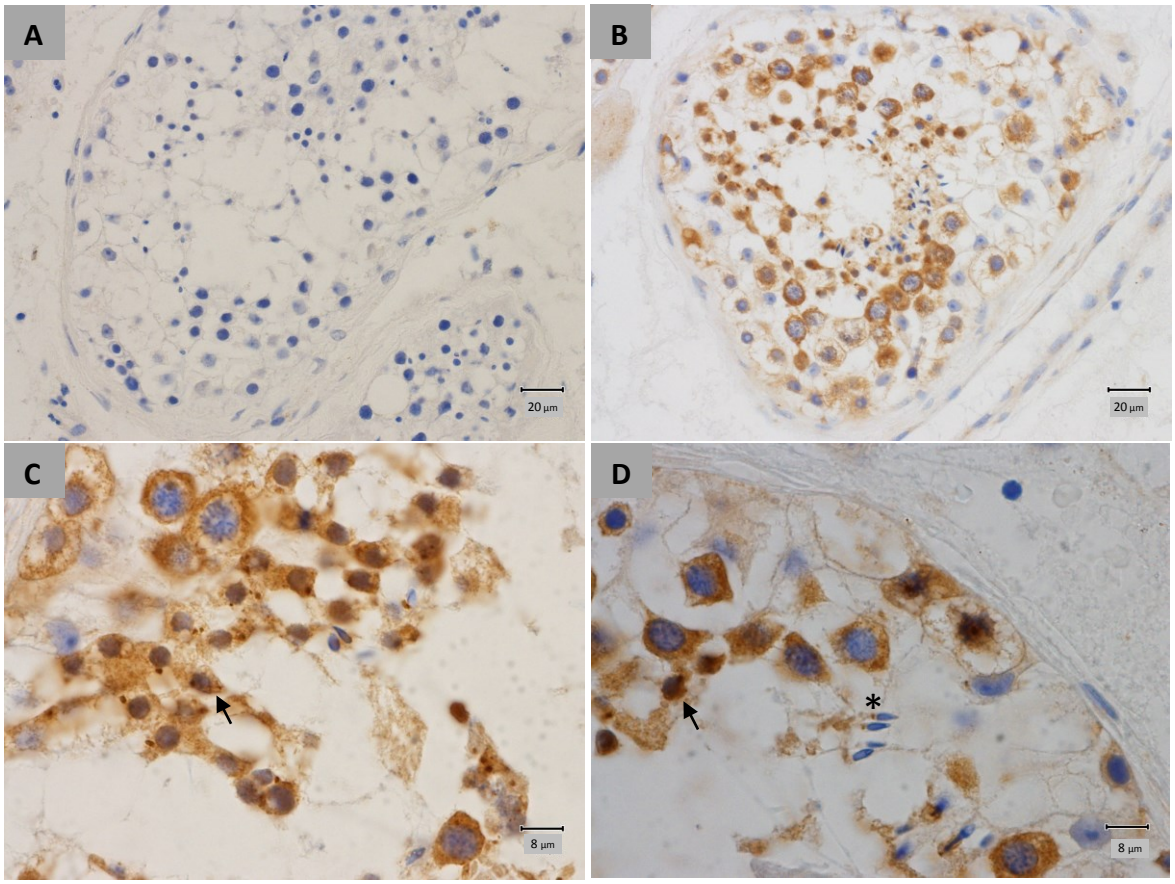

Figure III.17. Immunohistochemical localization of γ-tubulin in human testis sections fixated in Bouin. Positive immunostaining in brown colour, counterstaining with haematoxylin. **(A)** Negative control showed no staining. **(B)** γ-Tubulin stains centrioles in peritubular and Leydig cells. Additionally, in germ cells from initial phases of the spermatogenic cycle, ranging from spermatogonia until late spermatocytes, staining appears distributed through the cytoplasm. **(C, D)** After meiosis, γ-tubulin concentrates in dots at the centriolar poles, while it is also distributed homogenously through the cytoplasm of round spermatids (arrows). **(D)** In completely elongated spermatids γ-tubulin (asterisk) concentrates in a dot at the centriolar pole.

The comparative study of expression profiles of LAP1 and γ-tubulin, in human spermatogenesis, reveals an interesting association. The cytoplasmic distribution of γ-tubulin in round and elongating spermatids coincides with LAP1 localization in the same cells. Additionally, the cytoplasmic presence of γ-tubulin in elongating spermatids is not reproduced by γ-tubulin in the mouse testis, and has not been previously described. Additionally, in fully elongated spermatids the dotted pattern at the centriolar pole coincides between LAP1 and γ-tubulin staining in mouse and human testis. Further analysis of this association might clarify and reveal interesting functions for LAP1 regarding manchette organization. Moreover, future studies might contribute to the clarification of the present debate regarding the origin and organization of the manchette microtubules.

3.3.1.5 TorsinA localization in the testis

Torsin A is a chaperone protein that mediates conformational changes in target proteins. Interestingly, the torsin protein family has never been described in the spermatogenic cycle. General observation of the results obtained (Figure III.18.B) determined that torsinA presents a diffused expression in peritubular cells, Sertoli cells and early pachytene spermatocytes (Figure III.18.B, asterisk). Afterwards, torsinA concentrates in a cytoplasmic granule of mid and late pachytene spermatocytes (Figure III.18.B). In mid pachytene spermatocytes (Figure III.18.C, arrow) a highly concentrated staining is observed as granule in the cytoplasm, with no shape. Late pachytene spermatocytes (Figure III.18.D, ROI) have a less dense staining than mid pachytene spermatocytes, and the granule acquires a circular shape. The volume of this cytoplasmic granule seems to later decrease exponentially in round spermatids (Figure III.18.B, arrowheads).

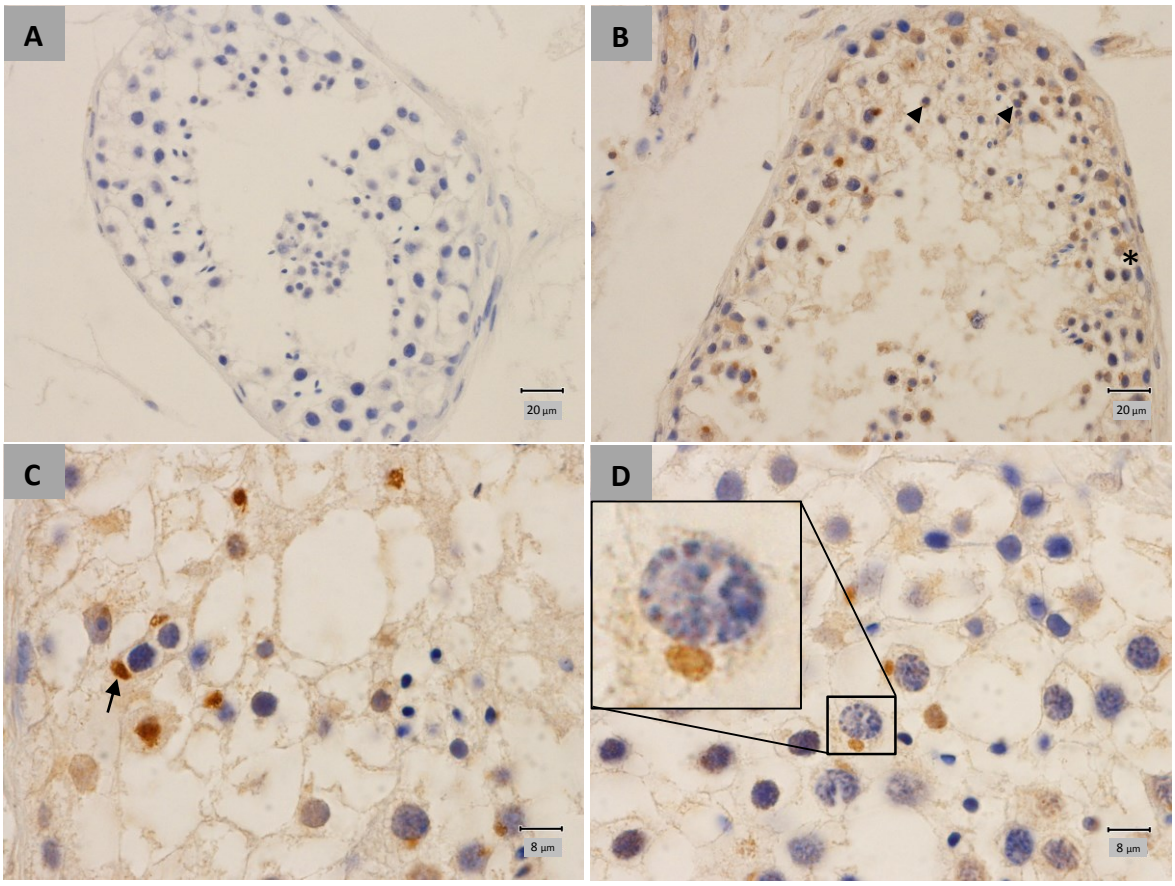

Figure III.18. Immunohistochemical localization of torsinA in human testis sections fixated in Bouin. Positive immunostaining in brown colour, counterstaining with haematoxylin. **(A)** Negative control showed no staining. **(B)** General observation determined that torsinA is expressed in peritubular cells, Sertoli cells and early pachytene spermatocytes (asterisk); posteriorly, it is concentrated in a cytoplasmic granule of mid and late pachytene spermatocytes and some round spermatids (arrowheads). **(C)** In mid pachytene spermatocytes (arrow) a highly concentrated staining is observed as granule in the cytoplasm, without shape. **(D)** Late pachytene spermatocytes (ROI) have inferior staining than mid pachytene spermatocytes, and the granule acquires a circular shape.

We propose that this granule is the Golgi apparatus. The Golgi apparatus is a subcellular organelle that functions in glycosylation, processing, and sorting of newly synthesized proteins being transported from the ER. Throughout spermatogenesis, the Golgi apparatus is highly important for the formation of the acrosome. In mammals, acrosome biogenesis begins with the fusion of proacrosomal granules synthesized by the Golgi apparatus in pachytene spermatocytes. In these cells, the Golgi apparatus forms an eccentric sphere surrounding the proacrosomal granules[193].

TorsinA is involved in several functions, including protein folding and degradation, membrane trafficking, DNA replication and repair, mitosis and cytoskeletal regulation. Typically, this protein resides in the NE, however, it seems that in pre-meiotic phases of spermatogenesis it localizes to the Golgi apparatus[177,194]. In order to determine the role of torsinA throughout spermatogenesis it would be interesting to confirm by immunofluorescence the colocalization of torsinA with a Golgi marker. Additionally, it would be interesting to study the localization of this protein during spermiogenesis using mouse testis. We attempted this final procedure, but due to antibody specificity the IHC results were not favourable and will not be presented.

3.3.2 LAP1 distribution in spermatogonia and sperm

LAP1 subcellular localization was investigated in spermatogonial cells through ICC. GC-1 spg is a mouse spermatogonial cell line that corresponds to a stage between spermatogonia type B and primary spermatocytes, based on its characteristics in phase contrast and electron microscopy[195].

In conformity with the IHC study of LAP1 in mouse spermatogenetic cells, overall ICC analysis determined the localization of LAP1 in the NE of spermatogonia type B and primary spermatocytes. Depicted in Figure III.19 is a typical phenotype described for commitant spermatogonia, in this case, B spermatogia. When a spermatogonium divides, telophase is incomplete, leaving an open area of cytoplasmic continuity called a cytoplasmic bridge. Bridges allow sharing of gene products between cells of a clone. If gene products in adjacent cells are shared, cellular activities become synchronized, resulting in a synchronized development[84].

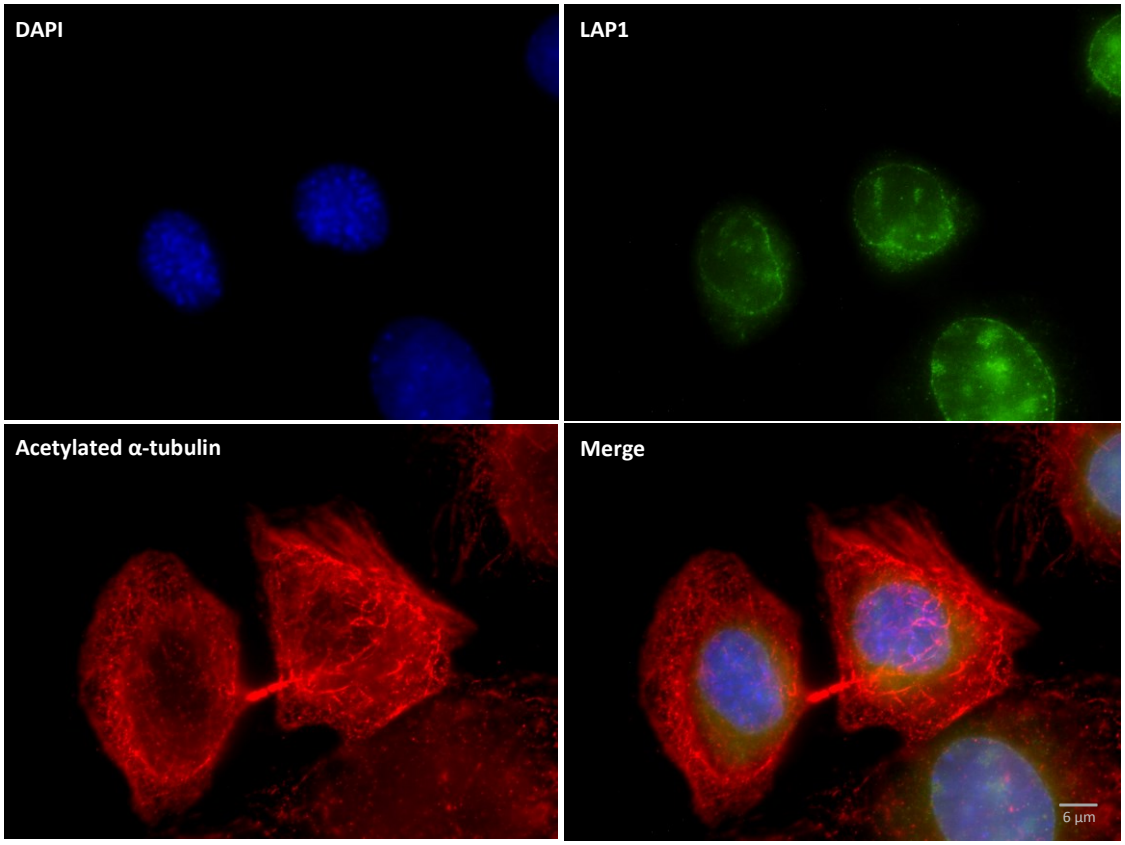

Figure III.19. Subcellular distribution of LAP1 in mouse spermatogonia. Immunocytochemistry in GC-1 spg cells was performed using specific antibodies to endogenous LAP1 (green) and acetylated α-tubulin (red). Photographs were acquired by epifluorescence microscopy. Negative control showed no staining (data not shown).

IHC analysis of human testis section in this work revealed that throughout the elongation of spermatids, LAP1 is concentrated at the centriolar pole. However, we found it difficult to determine if this signal is localized to the midpiece of developing sperm (Figure III.9.D) or if it was staining of the surplus cytoplasm known as the residual body. Consequently, we proceeded to investigate the localization of LAP1 in sperm (Figure III.20).

Subcellular localization of LAP1 in human sperm revealed differential staining prior to and after acrosome reaction. As depicted in Figure III.20, the acrosome of non-reacted sperm is stained with PSA-FITC. In this case, LAP1 is localized to the post-acrosomal region and the midpiece. After acrosome reaction, LAP1 is distributed along the post-acrosomal sheath and the midpiece. The significance of these results is most likely associated to motility purposes considering the distribution of LAP1 in the midpiece. During sperm movement, the adenosine triphosphate (ATP) needed to whip the flagellum and propel the sperm comes from rings of mitochondria located in the midpiece of sperm. In mammals, there is a layer of dense fibres interposed between the mitochondrial sheath and the axoneme that stiffens the sperm tail. Since the thickness of this layer decreases toward the tip, the fibres probably prevent the sperm head from being whipped around too suddenly[196]. Due to the continuity of LAP1 staining between the midpiece and the post-acrosomal region it is reasonable to deduce that LAP1 might be associated to the maintenance of these structures.

Considering the differential staining of LAP1 between non-reacted and acrosome-reacted sperm, it is interesting to consider the membrane interaction between sperm and the oocyte. In acrosome-reacted sperm, the forward part of the sperm head is covered only by the former inner membrane of the acrosome. The post-acrosomal region is crucial for sperm to bind to the oocyte[196]. Therefore, these ICC might reveal an unknown association between LAP1 and the fertilization process.

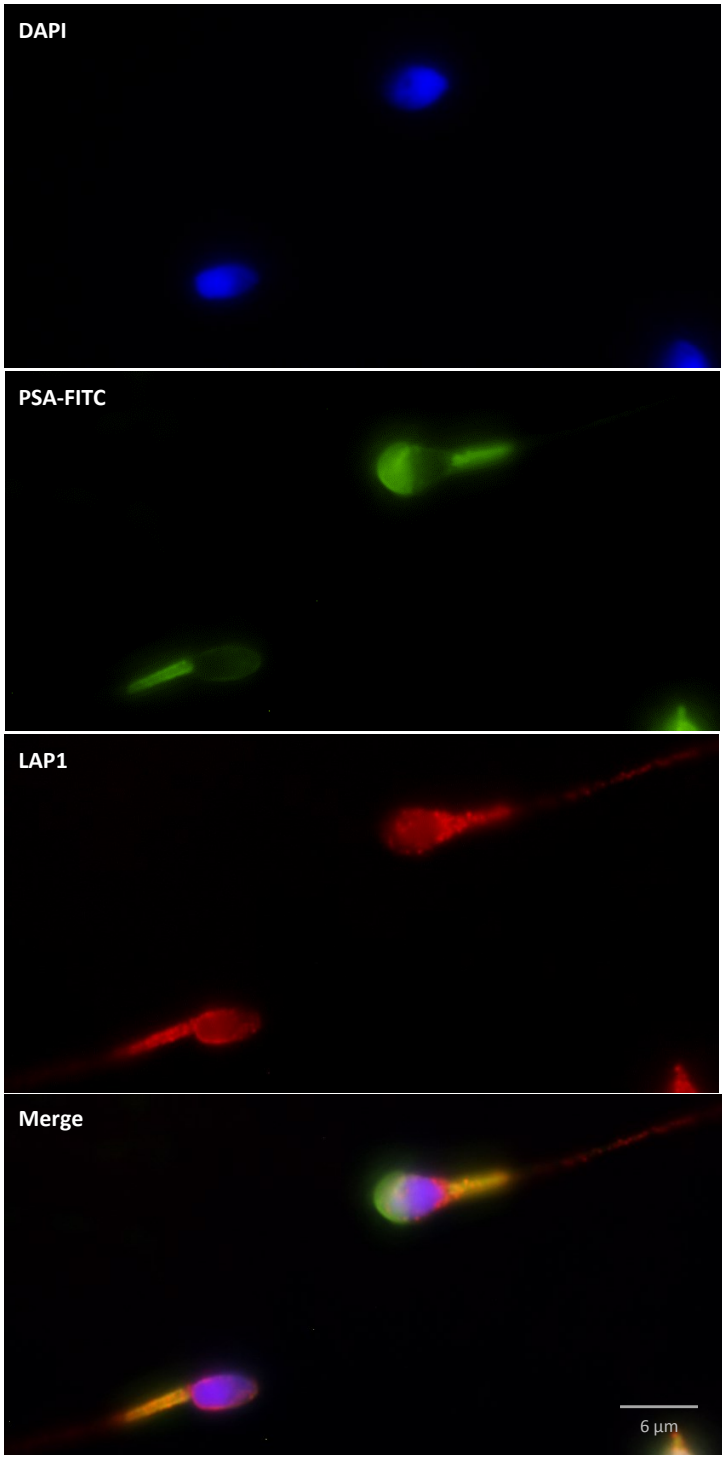

Figure III.20. Subcellular distribution of LAP1 in human sperm. Immunocytochemistry in human sperm cells was performed using a specific antibody to endogenous LAP1 (green). Photographs were acquired by epifluorescence microscopy. Negative control showed no staining (data not shown). Sperm cells with negative staining in the nucleus with PSA-FITC (green) were considered acrosome reacted.

Identification of LAP1 in the midpiece prompted the colocalization study between LAP1 and a midpiece marker, Cytochrome c oxidase IV (COX IV). It is well-established that mitochondria collect around the flagellum near the base of the nucleus and become incorporated into the midpiece of sperm[196]. COX IV is a known element of the mitochondrial respiratory chain. It is a multi-subunit enzyme complex that couples the transfer of electrons from cytochrome c to molecular oxygen and contributes to a proton electrochemical gradient across the inner mitochondrial membrane[197]. As depicted in Figure III.21 LAP1 shows colocalization with the midpiece. These results reinforce the hypothesis that LAP1 is associated with the structures responsible for motility in sperm, making it a worthy candidate for future studies regarding sperm development and activity.

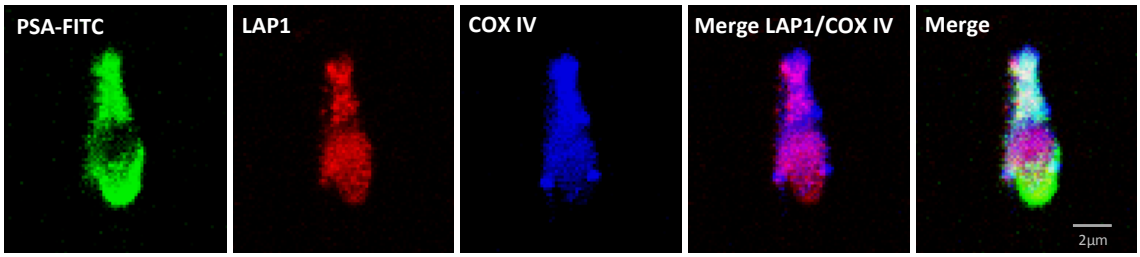

Figure III.21. Subcellular distribution of LAP1 and COX IV, in human sperm. Immunocytochemistry in human sperm cells was performed using specific antibodies to endogenous LAP1 (red) and COX IV (blue). Immunolocalization of LAP1 and COX IV is observed. Z-Projections of stack images were acquired by confocal microscopy. Negative control showed no staining (data not shown). Sperm cells with negative staining in the nucleus with PSA-FITC (green) were considered acrosome reacted.

Lastly, the possible regulation of LAP1 in sperm was investigated. Given the known regulatory role of PP1γ on LAP1[49,52] we inquired if these proteins possibly interact in sperm. This experiment (Figure III.22) revealed that acrosome-reacted sperm exhibit partial colocalization between LAP1 and PP1γ, which is apparent in the merged images of both proteins. PP1γ2 is the only isoform found in mammalian sperm[188] and it is known to regulate sperm motility[198]. Therefore it is safe to consider that this putative regulatory interaction occurs between PP1γ2 and LAP1. Additionally, the fact that both PP1γ2 and LAP1 are present in the equatorial and posterior (respectively) regions of the head, suggests a functional role of both proteins in the acrosome reaction. Hence, future studies regarding the functional role of this interaction in acrosome reaction and fertility should be pursued.

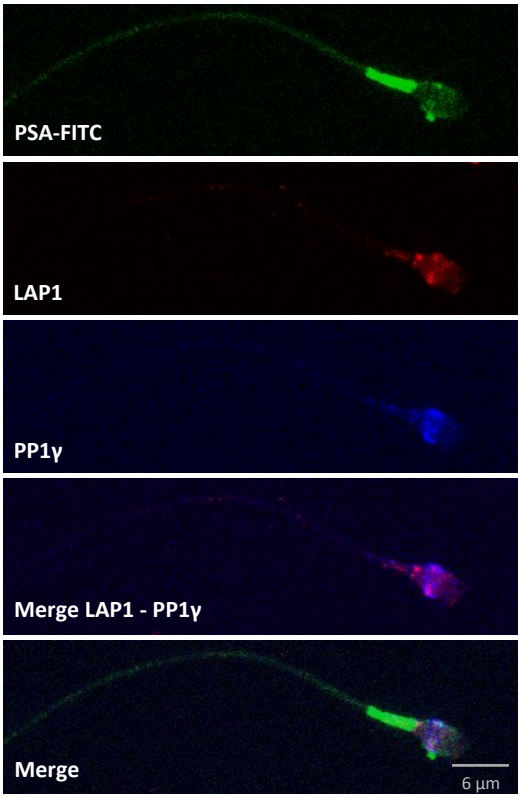

Figure III.22. Subcellular distribution of LAP1 and PP1γ, in human sperm. Immunocytochemistry in human sperm cells was performed using specific antibodies to endogenous LAP1 (red) and PP1γ (blue). Immunolocalization of LAP1 and PP1γ is observed. Z-Projections of stack images were acquired by confocal microscopy. Negative control showed no staining (data not shown). Sperm cells with negative staining in the nucleus with PSA-FITC (green) were considered acrosome reacted.

3.4 CONCLUSIONS

As portrayed in Figure III.23, the activity of LAP1 during the mouse spermatogenic cycle is most evident from stage VIII until the end of spermiogenesis, which is characteristic of manchette development. Concomitantly, some LAP1 interactors studied in this work share a similar localization, namely, PP1γ2 and Lamin B1. Interestingly, γ-tubulin in human testis also seems to localize to the cytoplasm of elongating spermatids, which might help to understand the morphologic changes promoted by manchette formation. Together these proteins might support spermiogenesis. Through moving to the posterior pole, the chromatin binding sites at the nuclear envelope would possibly contribute to the achievement of the non-random, sperm specific chromatin distribution and cellular reshaping. Additionally, LAP1 distribution in sperm might have unravelled novel functional properties of this protein. Throughout the years, researchers have established that the NE undergoes significant changes in the course of spermiogenesis. Thereby, the nuclear reshaping and condensation processes seem to have a highly significant role in the development of healthy sperm. Hopefully, this study has contributed to the understanding of LAP1's functional role during this differentiation process.

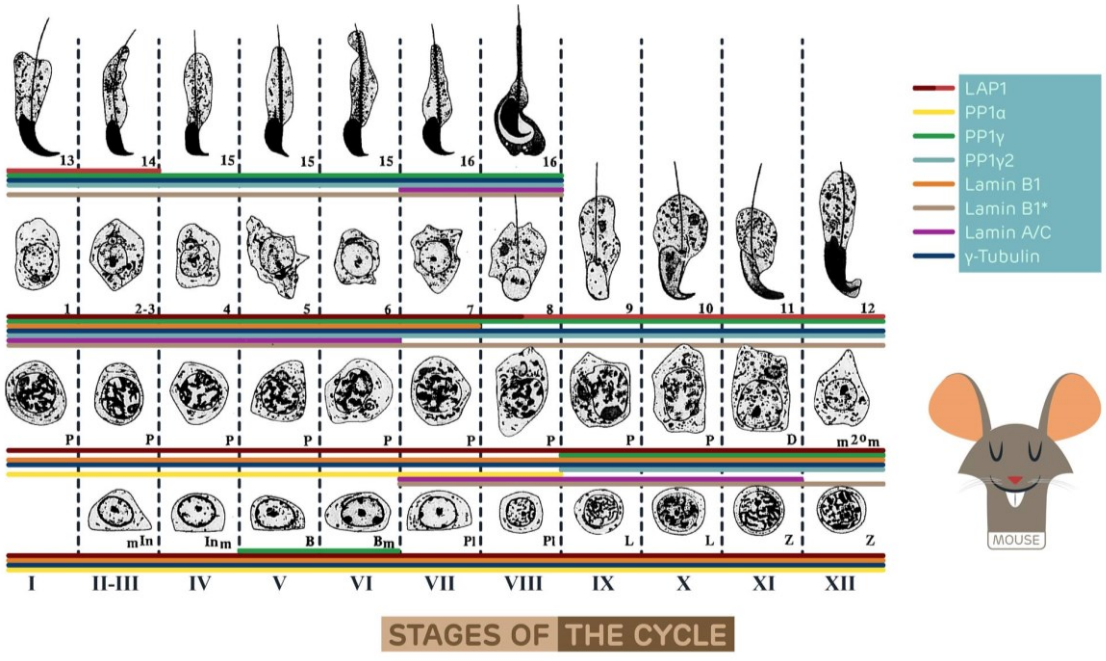

Figure III.23. LAP1 and its interactors expression throughout the cycle of spermatogenesis in the mouse. This schematic representation illustrates the stage-specific expression of LAP1 (dark red: LAP1 localized to the NE, light red: LAP1 in the centriolar pole), PP1α, PP1γ, PP1γ2, Lamin B1, Lamin B1* (lamin B1 localization taken from [91,98]) Lamin A/C and γ-Tubulin during spermatogenesis in mouse testis. There are twelve stages (designated with Roman numerals) in mouse spermatogenic cycle which are thoroughly depicted in the scheme. $_{m}$In, intermediate spermatogonium prior to mitosis; In$_{m}$, intermediate spermatogonium after to mitosis; B, B spermatogonium; Bm, B spermatogonium undergoing mitosis; Pl, preleptotene spermatocyte; L, leptotene spermatocyte; Z, zygotene spermatocyte; P, pachytene spermatocyte; D, diplotene spermatocytes; m^{2o}m, two meiotic divisions; 1–16, 16 steps of spermatid development. Adapted from [82].

CONCLUDING REMARKS & FUTURE PERSPECTIVES

The integrative results attained from this work allowed for the discovery of several prospective functions regarding the biological role of LAP1. The integration of multiple bioinformatic tools established novel functions to LAP1 such as DNA damage response and telomere association. In conjunction, bioinformatic results reinforced the association of LAP1 with mitosis and the already identified role of LAP1 in nuclear morphology. Furthermore, the study of LAP1 throughout different periods of the male reproductive system attributed potential new biological functions to LAP1. Thereby, this work can be the foundation of future studies regarding LAP1 and the regulation of multiple cellular processes and disease conditions.

Therefore, we propose the following complementary and future prespectives:

- Investigate the functional association of LAP1 with the shelterin complex and telomeres;
- Research the association of LAP1 with DNA damage responses, upon genotoxic insults;
- Confirm the expression of LAP1 in the testis and sperm with immunoblotting technics;
- Complement the present study with increasing the number of animals and patients, regarding IHC analysis;
- Immunofluorescent studies to determine the colocalization profiles of LAP1 with PP1γ2, lamin A/C, lamin B1, γ-tubulin, α-tubulin and torsinA, in mouse and human testis, and sperm samples;
- Investigate the integrity and morphology of LAP1 knockout mice testis and the distribution of LAP1 interactors throughout spermatogenesis;
- Study the localization and pattern of LAP1 in sperm with comprised morphology and motility.

BIBLIOGRAPHY

1. Gerace, L. & Burke, B. Functional organization of the nuclear envelope. *Annu Rev Cell Biol* **4,** 335–374 (1988).

2. Watson, M. L. The Nuclear Envelope. Its Structure and Relation to Cytoplasm Membranes. *J. Biophys. Biochem. Cytol.* **I,** 257–269 (1955).

3. Callan, H. G. & Tomlin, S. G. Experimental Studies on Amphibian Oocyte Nuclei. I. Investigation of the Structure of the Nuclear Membrane by Means of the Electron Microscope. *Proc. R. Soc. B Biol. Sci.* **137,** 367–378 (1950).

4. Aebi, U., Cohn, J., Buhle, L. & Gerace, L. The nuclear lamina is a meshwork of intermediate-type filaments. *Nature* **323,** 560–564 (1986).

5. Malik, P. *et al.* Cell-specific and lamin-dependent targeting of novel transmembrane proteins in the nuclear envelope. *Cell. Mol. Life Sci.* **67,** 1353–1369 (2010).

6. Rout, M. P. *et al.* The yeast nuclear pore complex: composition, architecture, and transport mechanism. *J. Cell Biol.* **148,** 635–651 (2000).

7. Schirmer, E. C., Florens, L., Guan, T., Yates, J. R. & Gerace, L. Nuclear membrane proteins with potential disease links found by subtractive proteomics. *Science* **301,** 1380–2 (2003).

8. Stuurman, N., Heins, S. & Aebi, U. Nuclear lamins: their structure, assembly, and interactions. *J. Struct. Biol.* **122,** 42–66 (1998).

9. Pathak, R. K., Luskey, K. L. & Anderson, R. G. Biogenesis of the crystalloid endoplasmic reticulum in UT-1 cells: evidence that newly formed endoplasmic reticulum emerges from the nuclear envelope. *J. Cell Biol.* **102,** 2158–2168 (1986).

10. Roux, K. J. *et al.* Nesprin 4 is an outer nuclear membrane protein that can induce kinesin-mediated cell polarization. *Proc. Natl. Acad. Sci. U. S. A.* **106,** 2194–2199 (2009).

11. Wilhelmsen, K. Nesprin-3, a novel outer nuclear membrane protein, associates with the cytoskeletal linker protein plectin. *J. Cell Biol.* **171,** 799–810 (2005).

12. Crisp, M. Coupling of the nucleus and cytoplasm: role of the LINC complex. *J. Cell Biol.* **172,** 41–53 (2006).

13. Minn, I., Rolls, M. M., Hanna-Rose, W. & Malone, C. J. SUN-1 and ZYG-12, Mediators of Centrosome-Nucleus Attachment, Are a Functional SUN/KASH Pair in Caenorhabditis elegans. *Mol. Biol. Cell* **20,** 4586–4595 (2009).

14. Wilson, K. L. & Berk, J. M. The nuclear envelope at a glance. *J. Cell Sci.* **123,** 1973–1978 (2010).

15. Pappas, G. D. The fine structure of the nuclear envelope of Amoeba proteus. *J. Biophys. Biochem. Cytol.* **2,** 431–4 (1956).

16. Fawcett, D. W. On the occurrence of a fibrous lamina on the inner aspect of the nuclear envelope in certain cells of vertebrates. *Am. J. Anat.* **119,** 129–45 (1966).

17. Dwyer, N. NANCY DWYER and GISNTER BLOBEL From The Rockefeller University, New York 10021. **70,** 581–591 (1976).

18. Fisher, D. Z., Chaudhary, N. & Blobel, G. cDNA sequencing of nuclear lamins A and C reveals primary and secondary structural homology to intermediate filament proteins. *Proc. Natl. Acad. Sci. U. S. A.* **83,** 6450–6454 (1986).

19. McKeon, F. D., Kirschner, M. W. & Caput, D. Homologies in both primary and secondary structure between nuclear envelope and intermediate filament proteins. *Nature* **319,** 463–8 (1986).

20. Furukawa, K., Inagaki, H. & Hotta, Y. Identification and cloning of an mRNA coding for a germ cell-specific A-type lamin in mice. *Experimental cell research* **212,** 426–30 (1994).

21. Machiels, B. M. *et al.* An alternative splicing product of the lamin A/C gene lacks exon 10. *J. Biol. Chem.* **271,** 9249–9253 (1996).

22. Pollard, K. M. *et al.* In vitro posttranslational modification of lamin B cloned from a human T-cell line. *Mol. Cell. Biol.* **10,** 2164–2175 (1990).

23. Höger, T. H., Zatloukal, K., Waizenegger, I. & Krohne, G. Characterization of a second highly conserved B-type lamin present in cells previously thought to contain only a single B-type lamin. *Chromosoma* **99,** 379–90 (1990).

24. Furukawa, K. & Hotta, Y. cDNA cloning of a germ cell specific lamin B3 from mouse

spermatocytes and analysis of its function by ectopic expression in somatic cells. *EMBO J.* **12,** 97–106 (1993).

25. Lin, F. & Worman, H. J. Structural Organization of the Human Gene (LMNB1) Enconding Nuclear Lamina B1. *Genomics* **27,** 230–236 (1995).

26. Stewart, C. & Burke, B. Teratocarcinoma stem cells and early mouse embryos contain only a single major lamin polypeptide closely resembling lamin B. *Cell* **51,** 383–92 (1987).

27. Kapinos, L. E. *et al.* Characterization of the Head-to-Tail Overlap Complexes Formed by Human Lamin A, B1 and B2 'Half-minilamin' Dimers. *J. Mol. Biol.* **396,** 719–731 (2010).

28. Goldberg, M. W., Huttenlauch, I., Hutchison, C. J. & Stick, R. Filaments made from A- and B-type lamins differ in structure and organization. *J. Cell Sci.* **121,** 215–225 (2008).

29. Burke, B. & Stewart, C. L. The nuclear lamins: flexibility in function. *Nat. Rev. Mol. Cell Biol.* **14,** 13–24 (2012).

30. Gerace, L. & Blobel, G. The nuclear envelope lamina is reversibly depolymerized during mitosis. *Cell* **19,** 277–287 (1980).

31. Song, M. H. & Adolph, K. W. Received August 16, 1983. **115,** 938–945 (1983).

32. Zhang, Y.-Q. & Sarge, K. D. Sumoylation regulates lamin A function and is lost in lamin A mutants associated with familial cardiomyopathies. *J. Cell Biol.* **182,** 35–39 (2008).

33. Schirmer, E. C. & Gerace, L. The nuclear membrane proteome: extending the envelope. *Trends Biochem. Sci.* **30,** 551–558 (2005).

34. Schirmer, E. C. & Foisner, R. Proteins that associate with lamins: Many faces, many functions. *Exp. Cell Res.* **313,** 2167–2179 (2007).

35. Gruenbaum, Y. & Foisner, R. Lamins: Nuclear Intermediate Filament Proteins with Fundamental Functions in Nuclear Mechanics and Genome Regulation. *Annu. Rev. Biochem.* **84,** 131–164 (2015).

36. Hoffmann, K. *et al.* Mutations in the gene encoding the lamin B receptor produce an

altered nuclear morphology in granulocytes (Pelger–Huët anomaly). *Nat. Genet.* **31,** 410–414 (2002).

37. Hoffmann, K., Sperling, K., Olins, A. L. & Olins, D. E. The granulocyte nucleus and lamin B receptor: Avoiding the ovoid. *Chromosoma* **116,** 227–235 (2007).

38. Ye, Q. & Worman, H. J. Interaction between an integral protein of the nuclear envelope inner membrane and human chromodomain proteins homologous to Drosophila HP1. *J. Biol. Chem.* **271,** 14653–14656 (1996).

39. Foisner, R. & Gerace, L. Integral membrane proteins of the nuclear envelope interact with lamins and chromosomes, and binding is modulated by mitotic phosphorylation. *Cell* **73,** 1267–1279 (1993).

40. Senior, a & Gerace, L. Integral membrane proteins specific to the inner nuclear membrane and associated with the nuclear lamina. *J. Cell Biol.* **107,** 2029–36 (1988).

41. Martin, L., Crimaudo, C. & Gerace, L. cDNA cloning and characterization of lamina-associated polypeptide 1C (LAP1C), an integral protein of the inner nuclear membrane. *The Journal of biological chemistry* **270,** 8822–8828 (1995).

42. Dechat, T. *et al.* Lamina-associated polypeptide 2alpha binds intranuclear A-type lamins. *J. Cell Sci.* **113 Pt 19,** 3473–3484 (2000).

43. Margalit, A., Brachner, A., Gotzmann, J., Foisner, R. & Gruenbaum, Y. Barrier-to-autointegration factor - a BAFfling little protein. *Trends Cell Biol.* **17,** 202–208 (2007).

44. Bione, S. *et al.* Identification of a novel X-linked gene responsible for Emery-Dreifuss muscular dystrophy. *Nat. Genet.* **8,** 323–327 (1994).

45. Burke, B. & Roux, K. J. Nuclei take a position: managing nuclear location. *Dev. Cell* **17,** 587–97 (2009).

46. Salpingidou, G., Smertenko, A., Hausmanowa-Petrucewicz, I., Hussey, P. J. & Hutchison, C. J. A novel role for the nuclear membrane protein emerin in association of the centrosome to the outer nuclear membrane. *J. Cell Biol.* **178,** 897–904 (2007).

47. Buch, C. *et al.* An integral protein of the inner nuclear membrane localizes to the mitotic spindle in mammalian cells. *J. Cell Sci.* **122,** 2100–2107 (2009).

48. Kondo, Y. *et al.* Molecular cloning of one isotype of human lamina-associated polypeptide 1s and a topological analysis using its deletion mutants. *Biochem. Biophys. Res. Commun.* **294,** 770–8 (2002).

49. Santos, M. *et al.* Identification of a Novel Human LAP1 Isoform That Is Regulated by Protein Phosphorylation. *PLoS One* **9,** e113732 (2014).

50. Kayman-Kurekci, G. *et al.* Mutation in TOR1AIP1 encoding LAP1B in a form of muscular dystrophy: a novel gene related to nuclear envelopathies. *Neuromuscul. Disord.* **24,** 624–33 (2014).

51. Barford, D., Das, a K. & Egloff, M. P. The structure and mechanism of protein phosphatases: insights into catalysis and regulation. *Annu. Rev. Biophys. Biomol. Struct.* **27,** 133–164 (1998).

52. Santos, M. *et al.* The nuclear envelope protein, LAP1B, is a novel protein phosphatase 1 substrate. *PLoS One* **8,** e76788 (2013).

53. Webster, M., Witkin, K. L. & Cohen-Fix, O. Sizing up the nucleus: nuclear shape, size and nuclear-envelope assembly. *J. Cell Sci.* **122,** 1477–1486 (2009).

54. Gerace, L. & Foisner, R. Integral membrane proteins and dynamic organization of the nuclear envelope. *Trends Cell Biol.* **4,** 127–131 (1994).

55. Neumann, B. *et al.* Phenotypic profiling of the human genome by time-lapse microscopy reveals cell division genes. *Nature* **464,** 721–7 (2010).

56. Olsen, J. V *et al.* Quantitative phosphoproteomics reveals widespread full phosphorylation site occupancy during mitosis. *Sci. Signal.* **3,** ra3 (2010).

57. Dephoure N Ville´ J, Beausoleil S A, Bakalarski C E, Stephen Elledge J, Gygi S P, Z. C. A Quantitive Atlas of Mitotic Phosphorylation. *Proc Natl Acad Sci U S A* **105,** 10762–10767 (2008).

58. Bollen, M., Gerlich, D. W. & Lesage, B. Mitotic phosphatases: from entry guards to exit guides. *Trends Cell Biol.* **19,** 531–541 (2009).

59. Santos, M. *et al.* LAP1 is a crucial protein for the maintenance of the nuclear envelope structure and cell cycle progression. *Mol. Cell. Biochem.* **399,** 143–53 (2015).

60. Haraguchi, T. *et al.* Live fluorescence imaging reveals early recruitment of emerin, LBR, RanBP2, and Nup153 to reforming functional nuclear envelopes. *J. Cell Sci.* **113 (Pt 5,** 779–794 (2000).

61. Graça, M. S. M. Characterization of novel LAP1 complexes and their relevance in DYT1 dystonia. (Universidade de Aveiro, 2014).

62. Hendzel, M. J. *et al.* Mitosis-specific phosphorylation of histone H3 initiates primarily within pericentromeric heterochromatin during G2 and spreads in an ordered fashion coincident with mitotic chromosome condensation. *Chromosoma* **106,** 348–360 (1997).

63. Thompson, L. J., Bollen, M. & Fields, A. P. Identification of Protein Phosphatase 1 as a Mitotic Lamin Phosphatase. *J. Biol. Chem.* **272,** 29693–29697 (1997).

64. Kuga, T., Nozaki, N., Matsushita, K., Nomura, F. & Tomonaga, T. Phosphorylation statuses at different residues of lamin B2, B1, and A/C dynamically and independently change throughout the cell cycle. *Exp. Cell Res.* **316,** 2301–12 (2010).

65. Steen, R. L., Martins, S. B., Taskén, K. & Collas, P. Recruitment of protein phosphatase 1 to the nuclear envelope by A-kinase anchoring protein AKAP149 is a prerequisite for nuclear lamina assembly. *J. Cell Biol.* **150,** 1251–1261 (2000).

66. Maison, C., Pyrpasopoulou, a, Theodoropoulos, P. a & Georgatos, S. D. The inner nuclear membrane protein LAP1 forms a native complex with B-type lamins and partitions with spindle-associated mitotic vesicles. *EMBO J.* **16,** 4839–50 (1997).

67. Kim, C. E., Perez, A., Perkins, G., Ellisman, M. H. & Dauer, W. T. A molecular mechanism underlying the neural-specific defect in torsinA mutant mice. *Proc. Natl. Acad. Sci.* **107,** 9861–9866 (2010).

68. Worman, H. J., Ostlund, C. & Wang, Y. Diseases of the nuclear envelope. *Cold Spring Harb. Perspect. Biol.* **2,** 1–18 (2010).

69. Goodchild, R. E. & Dauer, W. T. The AAA+ protein torsinA interacts with a conserved domain present in LAP1 and a novel ER protein. *J. Cell Biol.* **168,** 855–62 (2005).

70. Shin, J. *et al.* Lamina-associated Polypeptide-1 Interacts with the Muscular Dystrophy Protein Emerin and is Essential for Skeletal Muscle Maintenance. **26,** 591–

603 (2014).

71. Ozelius, L. J. *et al.* The early-onset torsion dystonia gene (DYT1) encodes an ATP-binding protein. *Nat. Genet.* **17,** 40–48 (1997).

72. Shin, J. Y. *et al.* Lamina-associated polypeptide-1 interacts with the muscular dystrophy protein emerin and is essential for skeletal muscle maintenance. *Dev. Cell* **26,** 591–603 (2013).

73. Rebelo, S., Edgar, F. & Odete, A. B. Mutation Research / Reviews in Mutation Research Genetic mutations strengthen functional association of LAP1 with DYT1 dystonia and muscular dystrophy. *Mutat. Res. Mutat. Res.* 2–7 (2015). doi:10.1016/j.mrrev.2015.07.004

74. Goodchild, R. E., Kim, C. E. & Dauer, W. T. Loss of the Dystonia-Associated Protein TorsinA Selectively Disrupts the Neuronal Nuclear Envelope. *Neuron* **48,** 923–932 (2005).

75. Hermo, L., Pelletier, R. M., Cyr, D. G. & Smith, C. E. Surfing the wave, cycle, life history, and genes/proteins expressed by testicular germ cells. Part 1: Background to spermatogenesis, spermatogonia, and spermatocytes. *Microsc. Res. Tech.* **73,** 241–278 (2010).

76. Ježek, D., Kozina, V. & Vukasović, A. in *Atlas on the Human Testis* (ed. Ježek, D.) 77–97 (Springer London, 2013). doi:10.1007/978-1-4471-2763-5_7

77. Weinbauer, G. F., Luetjens, C. M., Simoni, M. & Nieschlag, E. in *Andrology* 11–59 (Springer Berlin Heidelberg, 2010). doi:10.1007/978-3-540-78355-8_2

78. Roosen-Runge, E. the Process of Spermatogenesis in Mammals*. *Biol. Rev.* **37,** 343–377 (1962).

79. Hess, R. a & Franca, L. R. De. in *Molecular Mechanisms in Spermatogenesis* (ed. Cheng, C. Y.) 1–15 (Landes Bioscience and Springer Science+Business Media, 2008).

80. Amann, R. P. The Cycle of the Seminiferous Epithelium in Humans: A Need to Revisit? *J. Androl.* **29,** 469–487 (2008).

81. Guraya, S. S. *Biology of Spermatogenesis and Spermatozoa in Mammals*. *Animal Reproduction Science* **20,** (Springer Berlin Heidelberg, 1987).

82. Russell, L. D., Ettlin, R. A., Hikim, A. P. S. & Clegg, E. D. Histological and histopathological evaluation of the testis. *Int. J. Androl.* **16,** 83 (1990).

83. Timmons, P. M., Rigby, P. W. J. & Poirier, F. The murine seminiferous epithelial cycle is pre-figured in the Sertoli cells of the embryonic testis. *Development* **129,** 635–647 (2002).

84. De Rooij, D. G. & Russell, L. D. All you wanted to know about spermatogonia but were afraid to ask. *J. Androl.* **6512,** 776–798 (2000).

85. Chiarini-Garcia, H. & Russell, L. D. High-resolution light microscopic characterization of mouse spermatogonia. *Biol. Reprod.* **65,** 1170–8 (2001).

86. Russell, L. Movement of spermatocytes from the basal to the adluminal compartment of the rat testis. *Am. J. Anat.* **148,** 313–28 (1977).

87. Bellvé, A. R. *et al.* Spermatogenic cells of the prepuberal mouse. Isolation and morphological characterization. *J. Cell Biol.* **74,** 68–85 (1977).

88. Junqueira, L. C. & Carneiro, J. *Histologia Básica*. (Guanabara Koogan, 2013).

89. Muciaccia, B. *et al.* Novel Stage Classification of Human Spermatogenesis Based on Acrosome Development. *Biol. Reprod.* **89,** 60–60 (2013).

90. Chemes, H. E., Fawcett, D. W. & Dym, M. Unusual Features of the Nuclear Envelope in Human Spermatogenic Cells. *Anat. Rec.* **192,** 493–512 (1978).

91. Alsheimer, M., Fecher, E. & Benavente, R. Nuclear envelope remodelling during rat spermiogenesis : distribution and expression pattern of LAP2 / thymopoietins. **2234,** 2227–2234 (1998).

92. Alsheimer, M., Glasenapp, E. Von, Hock, R. & Benavente, R. Architecture of the Nuclear Periphery of Rat Pachytene Spermatocytes : Distribution of Nuclear Envelope Proteins in Relation to Synaptonemal Complex Attachment Sites. **10,** 1235–1245 (1999).

93. Alsheimer, M., Jahn, D., Schramm, S. & Benavente, R. in *Epigenetics and Human Reproduction* (eds. Rousseaux, S. & Khochbin, S.) **2148,** 279–288 (Springer Berlin Heidelberg, 2011).

94. Dernburg, A. F. Pushing the (nuclear) envelope into meiosis. *Genome Biol.* **14,** 110 (2013).

95. Link, J. *et al.* Analysis of Meiosis in SUN1 Deficient Mice Reveals a Distinct Role of SUN2 in Mammalian Meiotic LINC Complex Formation and Function. **10,** 14–21 (2014).

96. Mylonis, I. Temporal Association of Protamine 1 with the Inner Nuclear Membrane Protein Lamin B Receptor during Spermiogenesis. *J. Biol. Chem.* **279,** 11626–11631 (2004).

97. Schmitt, J., Benavente, R. & Alsheimer, M. Mammalian Sperm Head Formation Involves Different Polarization of Two Novel LINC Complexes. **5,** (2010).

98. Vester, B., Smith, a, Krohne, G. & Benavente, R. Presence of a nuclear lamina in pachytene spermatocytes of the rat. *J. Cell Sci.* **104 (Pt 2,** 557–63 (1993).

99. Shen, J. *et al.* Lamin A/C proteins in the spermatid acroplaxome are essential in mouse spermiogenesis. *Reproduction* **148,** 479–487 (2014).

100. Alsheimer, M. & Benavente, R. Change of karyoskeleton during mammalian spermatogenesis: expression pattern of nuclear lamin C2 and its regulation. *Exp. Cell Res.* **228,** 181–8 (1996).

101. Schütz, W., Alsheimer, M., Ollinger, R. & Benavente, R. Nuclear envelope remodeling during mouse spermiogenesis: postmeiotic expression and redistribution of germline lamin B3. *Exp. Cell Res.* **307,** 285–91 (2005).

102. Barthès, P., Buard, J. & de Massy, B. Epigenetics and Human Reproduction. *Epigenetics Hum. Heal.* **2148,** 119–156 (2011).

103. Alsheimer, M. *et al.* Disruption of spermatogenesis in mice lacking A-type lamins. *J. Cell Sci.* **117,** 1173–8 (2004).

104. Link, J. *et al.* The meiotic nuclear lamina regulates chromosome dynamics and promotes efficient homologous recombination in the mouse. *PLoS Genet.* **9,** e1003261 (2013).

105. Tzur, Y. B., Wilson, K. L. & Gruenbaum, Y. SUN-domain proteins: 'Velcro' that links

the nucleoskeleton to the cytoskeleton. *Nat. Rev. Mol. Cell Biol.* **7,** 782–788 (2006).

106. Dauer, W. T. & Worman, H. J. The Nuclear Envelope as a Signaling Node in Development and Disease. *Dev. Cell* **17,** 626–638 (2009).

107. Gruenbaum, Y., Margalit, A., Goldman, R. D., Shumaker, D. K. & Wilson, K. L. The nuclear lamina comes of age. *Nat. Rev. Mol. Cell Biol.* **6,** 21–31 (2005).

108. Burke, B. & Stewart, C. L. *Functional architecture of the cell's nucleus in development, aging, and disease*. *Current Topics in Developmental Biology* **109,** (Elsevier Inc., 2014).

109. Gerace, L. & Huber, M. D. Nuclear lamina at the crossroads of the cytoplasm and nucleus. *J. Struct. Biol.* **177,** 24–31 (2012).

110. Gonzalez-Alegre, P. Aberrant Cellular Behavior of Mutant TorsinA Implicates Nuclear Envelope Dysfunction in DYT1 Dystonia. *J. Neurosci.* **24,** 2593–2601 (2004).

111. Goodchild, R. E. & Dauer, W. T. Mislocalization to the nuclear envelope: an effect of the dystonia-causing torsinA mutation. *Proc. Natl. Acad. Sci. U. S. A.* **101,** 847–852 (2004).

112. Kayman-Kurekci, G. *et al.* Mutation in TOR1AIP1 encoding LAP1B in a form of muscular dystrophy: a novel gene related to nuclear envelopathies. *Neuromuscul. Disord.* **24,** 624–33 (2014).

113. Dorboz, I. *et al.* Severe dystonia, cerebellar atrophy, and cardiomyopathy likely caused by a missense mutation in TOR1AIP1. *Orphanet J. Rare Dis.* **9,** 174 (2014).

114. Stark, C. BioGRID: a general repository for interaction datasets. *Nucleic Acids Res.* **34,** D535–D539 (2006).

115. Orchard, S. *et al.* The MIntAct project - IntAct as a common curation platform for 11 molecular interaction databases. *Nucleic Acids Res.* **42,** 358–363 (2014).

116. Calderone, A., Castagnoli, L. & Cesareni, G. Mentha: a Resource for Browsing Integrated Protein-Interaction Networks. *Nat. Methods* **10,** 690–691 (2013).

117. Brown, K. R. & Jurisica, I. Online Predicted Human Interaction Database. *Bioinformatics* **21,** 2076–2082 (2005).

118. Prieto, C. & De Las Rivas, J. APID: Agile Protein Interaction DataAnalyzer. *Nucleic Acids Res.* **34,** W298–W302 (2006).

119. Schaefer, M. H. *et al.* Hippie: Integrating protein interaction networks with experiment based quality scores. *PLoS One* **7,** 1–8 (2012).

120. Maglott, D., Ostell, J., Pruitt, K. D. & Tatusova, T. Entrez Gene: gene-centered information at NCBI. *Nucleic Acids Res.* **35,** D26–D31 (2007).

121. del-Toro, N. *et al.* A new reference implementation of the PSICQUIC web service. *Nucleic Acids Res.* **41,** W601–W606 (2013).

122. Ashburner, M. *et al.* Gene ontology: tool for the unification of biology. *Nat. Genet.* **25,** 25–29 (2000).

123. Mi, H., Muruganujan, A. & Thomas, P. D. PANTHER in 2013: modeling the evolution of gene function, and other gene attributes, in the context of phylogenetic trees. *Nucleic Acids Res.* **41,** D377–D386 (2013).

124. Gene, T., Consortium, O., Gene, T. & Go, O. Gene Ontology Consortium: going forward. *Nucleic Acids Res.* **43,** D1049–D1056 (2015).

125. Shannon, P. *et al.* Cytoscape : A Software Environment for Integrated Models of Biomolecular Interaction Networks. 2498–2504 (2003). doi:10.1101/gr.1239303.metabolite

126. Montojo, J. *et al.* GeneMANIA Cytoscape plugin: fast gene function predictions on the desktop. *Bioinformatics* **26,** 2927–2928 (2010).

127. Warde-Farley, D. *et al.* The GeneMANIA prediction server: biological network integration for gene prioritization and predicting gene function. *Nucleic Acids Res.* **38,** W214–W220 (2010).

128. Maere, S., Heymans, K. & Kuiper, M. BiNGO: a Cytoscape plugin to assess overrepresentation of gene ontology categories in biological networks. *Bioinformatics* **21,** 3448–9 (2005).

129. Abdelmohsen, K. *et al.* Ubiquitin-mediated proteolysis of HuR by heat shock. *EMBO J.* **28,** 1271–1282 (2009).

130. Chu, L. *et al.* Multiple myeloma-associated chromosomal translocation activates orphan snoRNA ACA11 to suppress oxidative stress. *J. Clin. Invest.* **122,** 2793–806 (2012).

131. Gautier, V. W. *et al.* In vitro nuclear interactome of the HIV-1 Tat protein. *Retrovirology* **6,** 47 (2009).

132. Wu, W. *et al.* The Interactome of the Human Respiratory Syncytial Virus NS1 Protein Highlights Multiple Effects on Host Cell Biology. *J. Virol.* **86,** 7777–7789 (2012).

133. Lynch, D. T., Zimmerman, J. S. & Rowe, D. T. Epstein-Barr virus latent membrane protein 2B (LMP2B) co-localizes with LMP2A in perinuclear regions in transiently transfected cells. *J. Gen. Virol.* **83,** 1025–35 (2002).

134. Cohen, S., Etingov, I. & Pante, N. *Effect of Viral Infection on the Nuclear Envelope and Nuclear Pore Complex*. *International Review of Cell and Molecular Biology, Vol 299* **299,** (Elsevier, 2012).

135. Huttlin, E. L. *et al.* High-Throughput Proteomic Mapping of Human Interaction Networks via Affinity-Purification Mass Spectrometry (Pre-Publication). *Pre-Publication Dataset* (2014). at <http://thebiogrid.org/166968/publication/high-throughput-proteomic-mapping-of-human-interaction-networks-via-affinity-purification-mass-spectrometry.html>

136. Matsuoka, S. *et al.* ATM and ATR Substrate Analysis Reveals Extensive Protein Networks Responsive to DNA Damage. *Science (80-.).* **316,** 1160–1166 (2007).

137. Pestov, N. B. *et al.* Evolution of Na,K-ATPase beta m-subunit into a coregulator of transcription in placental mammals. *Proc. Natl. Acad. Sci. U. S. A.* **104,** 11215–11220 (2007).

138. Huttlin, E. L. *et al.* The BioPlex Network: A Systematic Exploration of the Human Interactome. *Cell* **162,** 425–440 (2015).

139. Hutchins, J. R. a *et al.* Systematic Characterization of Human Protein Complexes Identifies Chromosome Segregation Proteins. *Science (80-.).* **328,** 593–599 (2010).

140. Hanson, D., Stevens, A., Murray, P. G., Black, G. C. M. & Clayton, P. E. Identifying biological pathways that underlie primordial short stature using network analysis. *J.*

Mol. Endocrinol. **52,** 333–344 (2014).

141. Tong, J., Taylor, P. & Moran, M. F. Proteomic Analysis of the Epidermal Growth Factor Receptor (EGFR) Interactome and Post-translational Modifications Associated with Receptor Endocytosis in Response to EGF and Stress. *Mol. Cell. Proteomics* **13,** 1644–1658 (2014).

142. Havugimana, P. C. *et al.* A Census of Human Soluble Protein Complexes. *Cell* **150,** 1068–1081 (2012).

143. Kubben, N. *et al.* Identification of differential protein interactors of lamin A and progerin. *Nucleus* **1,** 513–525 (2010).

144. Zhong, N., Radu, G., Ju, W. & Brown, W. T. Novel progerin-interactive partner proteins hnRNP E1, EGF, Mel 18, and UBC9 interact with lamin A/C. *Biochem. Biophys. Res. Commun.* **338,** 855–861 (2005).

145. Roux, K. J., Kim, D. I., Raida, M. & Burke, B. A promiscuous biotin ligase fusion protein identifies proximal and interacting proteins in mammalian cells. *J. Cell Biol.* **196,** 801–810 (2012).

146. Rozenblatt-Rosen, O. *et al.* Interpreting cancer genomes using systematic host network perturbations by tumour virus proteins. *Nature* **487,** 491–5 (2012).

147. Martin, I. *et al.* Ribosomal protein s15 phosphorylation mediates LRRK2 neurodegeneration in Parkinson's disease. *Cell* **157,** 472–85 (2014).

148. Nicholson, J. *et al.* A systems wide mass spectrometric based linear motif screen to identify dominant in-vivo interacting proteins for the ubiquitin ligase MDM2. *Cell. Signal.* **26,** 1243–1257 (2014).

149. Emdal, K. B. *et al.* Temporal proteomics of NGF-TrkA signaling identifies an inhibitory role for the E3 ligase Cbl-b in neuroblastoma cell differentiation. *Sci. Signal.* **8,** ra40–ra40 (2015).

150. Santos, M. Characterization of novel LAP1 complexes and their relevance in DYT1 dystonia. (Universidade de Aveiro, 2014).

151. Esteves, S. L., Domingues, S. C., da Cruz e Silva, O. A., Fardilha, M. & da Cruz e Silva, E. F. Protein phosphatase 1alpha interacting proteins in the human brain. *Omics* **16,**

3–17 (2012).

152. Esteves, S. L. C. *et al.* Protein phosphatase 1γ isoforms linked interactions in the brain. *J. Mol. Neurosci.* **50,** 179–197 (2013).

153. Lee, O.-H. *et al.* Genome-wide YFP fluorescence complementation screen identifies new regulators for telomere signaling in human cells. *Mol. Cell. Proteomics* **10,** M110.001628 (2011).

154. Zhu, L., Millen, L., Mendoza, J. L. & Thomas, P. J. A unique redox-sensing sensor II motif in TorsinA plays a critical role in nucleotide and partner binding. *J. Biol. Chem.* **285,** 37271–80 (2010).

155. Naismith, T. V, Dalal, S. & Hanson, P. I. Interaction of torsinA with its major binding partners is impaired by the dystonia-associated DeltaGAG deletion. *J. Biol. Chem.* **284,** 27866–74 (2009).

156. Zhao, C. & et. al. Regulation of Torsin ATPases by LAP1 and LULL1. *Proc. Natl. Acad. Sci. U. S. A.* **110,** E1545–54 (2013).

157. Brown, R. S. H., Zhao, C., Chase, A. R., Wang, J. & Schlieker, C. The mechanism of Torsin ATPase activation. *Proc. Natl. Acad. Sci.* **111,** E4822–E4831 (2014).

158. Danielsen, J. M. R. *et al.* Mass spectrometric analysis of lysine ubiquitylation reveals promiscuity at site level. *Mol. Cell. Proteomics* **10,** M110.003590 (2011).

159. Wagner, S. a. *et al.* A Proteome-wide, Quantitative Survey of In Vivo Ubiquitylation Sites Reveals Widespread Regulatory Roles. *Mol. Cell. Proteomics* **10,** M111.013284–M111.013284 (2011).

160. Kim, W. *et al.* Systematic and Quantitative Assessment of the Ubiquitin-Modified Proteome. *Mol. Cell* **44,** 325–340 (2011).

161. Emanuele, M. J. *et al.* Global identification of modular cullin-RING ligase substrates. *Cell* **147,** 459–474 (2011).

162. Povlsen, L. K. *et al.* Systems-wide analysis of ubiquitylation dynamics reveals a key role for PAF15 ubiquitylation in DNA-damage bypass. *Nat. Cell Biol.* **14,** 1089–1098 (2012).

163. Stes, E. *et al.* A COFRADIC protocol to study protein ubiquitination. *J. Proteome Res.* **13,** 3107–3113 (2014).

164. Hewett, J. W., Zeng, J., Niland, B. P., Bragg, D. C. & Breakefield, X. O. Dystonia-causing mutant torsinA inhibits cell adhesion and neurite extension through interference with cytoskeletal dynamics. *Neurobiol. Dis.* **22,** 98–111 (2006).

165. Yang, M. *et al.* p31comet blocks Mad2 activation through structural mimicry. *Cell* **131,** 744–55 (2007).

166. Chao, W. C. H., Kulkarni, K., Zhang, Z., Kong, E. H. & Barford, D. Structure of the mitotic checkpoint complex. *Nature* **484,** 208–213 (2012).

167. Chi, Y. *et al.* Identification of CDK2 substrates in human cell lysates. *Genome Biol.* **9,** R149 (2008).

168. Blethrow, J. D., Glavy, J. S., Morgan, D. O. & Shokat, K. M. Covalent capture of kinase-specific phosphopeptides reveals Cdk1-cyclin B substrates. *Proc. Natl. Acad. Sci. U. S. A.* **105,** 1442–1447 (2008).

169. Xu, Y., Shao, Y., Voorhees, J. J. & Fisher, G. J. Ultraviolet Irradiation-Induces Epidermal Growth Factor Receptor (EGFR) Nuclear Translocation in Human Keratinocytes. *J. Cell. Biochem.* **107,** 873–880 (2009).

170. Lange, T. De. Shelterin : the protein complex that shapes and safeguards human telomeres. 2100–2110 (2005). doi:10.1101/gad.1346005.quence

171. Silverman, J., Takai, H., Buonomo, S. B. C., Eisenhaber, F. & de Lange, T. Human Rif1, ortholog of a yeast telomeric protein, is regulated by ATM and 53BP1 and functions in the S-phase checkpoint. *Genes Dev.* **18,** 2108–19 (2004).

172. Santos, M., Rebelo, S., da Cruz e Silva, E. F. & da Cruz e Silva, O. A. B. DYT1 dystonia-associated mutant affects cytoskeletal dynamics. *Microsc. Microanal.* **21,** 26–27 (2015).

173. Darszon, A., Nishigaki, T., Beltran, C. & Trevino, C. L. Calcium Channels in the Development, Maturation, and Function of Spermatozoa. *Physiol. Rev.* **91,** 1305–1355 (2011).

174. Rebelo, S., Santos, M., Martins, F., da Cruz e Silva, E. F. & da Cruz e Silva, O. A. B.

Protein phosphatase 1 is a key player in nuclear events. *Cellular Signalling* (Elsevier B.V., 2015). doi:10.1016/j.cellsig.2015.08.007

175. Chakrabarti, R. *et al.* Analysis of Ppp1cc-null mice suggests a role for PP1gamma2 in sperm morphogenesis. *Biol. Reprod.* **76,** 992–1001 (2007).

176. Sinha, N., Puri, P., Nairn, A. C. & Vijayaraghavan, S. Selective ablation of Ppp1cc gene in testicular germ cells causes oligo-teratozoospermia and infertility in mice. *Biol. Reprod.* **89,** 128 (2013).

177. Neuwald, A. F., Aravind, L., Spouge, J. L. & Koonin, E. V. AAA+: A class of chaperone-like ATPases associated with the assembly, operation, and disassembly of protein complexes. *Genome Res.* **9,** 27–43 (1999).

178. Organization, W. H. *WHO laboratory manual for the examination and processing of human semen*. (WHO Press, 2010).

179. da Cruz e Silva, E. F. *et al.* Differential expression of protein phosphatase 1 isoforms in mammalian brain. *J. Neurosci.* **15,** 3375–89 (1995).

180. Smith, G. D. *et al.* Primate sperm contain protein phosphatase 1, a biochemical mediator of motility. *Biol. Reprod.* **54,** 719–727 (1996).

181. BIORAD. Detection Methods | Applications & Technologies | Bio-Rad. at <http://www.bio-rad.com/en-us/applications-technologies/detection-methods>

182. Hogarth, C. A. & Griswold, M. D. in **927,** 309–320 (2013).

183. Burry, R. W. *Immunocytochemistry, A Practical Guide for Biomedical Research*. **XXXIII,** (Springer New York, 2010).

184. Tu, L., Yu, L. & Zhang, H. Morphology of rat testis preserved in three different fixatives. *J. Huazhong Univ. Sci. Technolog. Med. Sci.* **31,** 178–80 (2011).

185. Howat, W. J. & Wilson, B. A. Tissue fixation and the effect of molecular fixatives on downstream staining procedures. *Methods* **70,** 12–19 (2014).

186. Jan, S. Z. *et al.* Molecular control of rodent spermatogenesis. *Biochim. Biophys. Acta - Mol. Basis Dis.* **1822,** 1838–1850 (2012).

187. O'Donnell, L. & O'Bryan, M. K. Microtubules and spermatogenesis. *Semin. Cell Dev. Biol.* **30,** 45–54 (2014).

188. Chakrabarti, R., Cheng, L., Puri, P., Soler, D. & Vijayaraghavan, S. Protein phosphatase PP1γ2 in sperm morphogenesis and epididymal initiation of sperm motility. *Asian J. Androl.* **9,** 445–452 (2007).

189. Sinha, N., Pilder, S. & Vijayaraghavan, S. Significant Expression Levels of Transgenic PPP1CC2 in Testis and Sperm are required to Overcome the Male Infertility Phenotype of Ppp1cc Null Mice. *PLoS One* **7,** e47623 (2012).

190. Korrodi-Gregório, L., Esteves, S. L. C. & Fardilha, M. Protein phosphatase 1 catalytic isoforms: specificity toward interacting proteins. *Transl. Res.* **164,** 366–391 (2014).

191. Elkhatib, R. *et al.* Nuclear envelope remodelling during human spermiogenesis involves somatic B-type lamins and a spermatid-specific B3 lamin isoform. *Mol. Hum. Reprod.* **21,** 225–236 (2015).

192. Fouquet, J. P., Kann, M. L., Combeau, C. & Melki, R. Gamma-tubulin during the differentiation of spermatozoa in various mammals and man. *Mol. Hum. Reprod.* **4,** 1122–9 (1998).

193. Moreno, R. D. Vesicular Traffic and Golgi Apparatus Dynamics During Mammalian Spermatogenesis: Implications for Acrosome Architecture. *Biol. Reprod.* **63,** 89–98 (2000).

194. Granata, A. & Warner, T. T. The role of torsinA in dystonia. *Eur. J. Neurol.* **17,** 81–87 (2010).

195. Hofmann, M. C., Narisawa, S., Hess, R. a & Millán, J. L. Immortalization of germ cells and somatic testicular cells using the SV40 large T antigen. *Exp. Cell Res.* **201,** 417–435 (1992).

196. Jonge, C. J. De & Barratt, C. L. R. The Sperm Cell. Production, Maturation, Fertilization, Regeneration. 384 (2006).

197. Li, Y., Park, J.-S., Deng, J.-H. & Bai, Y. Cytochrome c oxidase subunit IV is essential for assembly and respiratory function of the enzyme complex. *J. Bioenerg. Biomembr.* **38,** 283–91 (2006).

198. Vijayaraghavan, S. *et al.* Sperm motility development in the epididymis is associated with decreased glycogen synthase kinase-3 and protein phosphatase 1 activity. *Biol. Reprod.* **54,** 709–718 (1996).

APPENDIX

Cell Culture Solutions

PBS (1x)

For a final volume of 500 mL, dissolve one pack of BupH Modified Dulbecco's Phosphate Buffered Saline Pack (Pierce) in deionised H_2O. Final composition:

- 8 mM Sodium Phosphate
- 2 mM Potassium Phosphate
- 140 mM Sodium Chloride
- 10 mM Potassium Chloride

Sterilize by filtering through a 0.2 µm filter and store at 4°C.

10% FBS DMEM

- 13,4 g DMEM
- 3,7 g NaHCO3
- 10 mL Streptomycin/Penicillin/Amphotericin solution (AAs)
- 100 mL 10% FBS

Dissolve in deionised H_2O. Adjust the pH to 7.3. Adjust the volume to 1 L with deionised H_2O.

Earl's balance solution (Sebss)

- 1.8 mM CaCl2
- 5.4 mM KCl 1.8 mM CaCl2
- 5.4 mM KCl, 0.81 mM MgSO4
- 25.0 mM NaHCO3
- 1.0 mM NaH2PO4, 116.4 mM NaCl
- 5.5 mM D-glucose, 2.5 mM Na–pyruvate
- 41.8 mM Na–lactate
- 0.3% BSA

Immunohistocheminal and Immunofluorescence Solutions

4% Paraformaldehyde

For a final volume of 100 mL, add 4 g of paraformaldehyde to 25 mL deionised H_2O. Dissolve by heating the mixture at 58°C while stirring. Add 1-2 drops of 1 M NaOH to clarify the solution and filter through a 0.2 µm filter. Add 50 mL of PBS 2x and adjust the volume to 100 mL with deionised H_2O.

Bouin's Solution

- 75 mL Picric acid solution
- 25 mL Formalin
- 5 mL Glacial Acetic acid

Alternatively, combine the saturated picric acid with the formalin, and the glacial acetic acid. Store at 4°C.

Sodium Citrate Buffer

- **0.1 M Citric Acid Solution (1 L):** add 21.01 g of Citric Acid Monohydrate ($C_6H_8O_7.H_2O$) to deionized H_2O, for a final volume of 1 L. Store at 4°C.

- **0.1 M Sodium Citrate Solution (1 L):** add 26.41 g Trisodium Citrate Dihydrate ($C_6H_5Na_3O_7.2H_2O$) to deionized H_2O, for a final volume of 1 L. Store at 4°C.

- **0.1 M Sodium Citrate Buffer (500 mL), pH 6.0:** add 9 mL of Citric Acid Solution (0.1M stock solution), and 41 mL of Sodium Citrate Solution for a final volume of 500 mL. Adjust the pH to 6.0 and store at 4°C.

Ethanol solutions (1 L)

- **Ethanol 96%:** add 960 mL of Ethanol Absolute and 40 mL of deionized H_2O.
- **Ethanol 70%:** add 700 mL of Ethanol Absolute and 300 mL of deionized H_2O.

Mayer's Haematoxylin

- 25 g Aluminium potassium sulphate
- 0.5 g Haematoxylin
- 0.1 g Sodium iodate
- 10 mL Glacial Acetic Acid
- 500 mL Demi-water

Dissolve aluminium potassium sulphate in demi-water. When it is completely dissolved, add hematoxylin. When hematoxylin is completely dissolved, add sodium iodate and acetic acid. Bring to boil (5 min) and cool. Filter if necessary.

Blocking solutions

- **3% BSA:** To 10 mL of PBS 1x add 0.3 g of Bovine Serum Albumine (BSA).
- **5% BSA:** To 10 mL of PBS 1x add 0.5 g of BSA.
- **5% BSA + 0,01% BSA-C:** To 10 mL of PBS 1x add 0.5 g of BSA and 1 µL of acetylated BSA.